INFORMATION TO USERS

This manuscript has been reproduced from the microfilm master. UMI films the text directly from the original or copy submitted. Thus, some thesis and dissertation copies are in typewriter face, while others may be from any type of computer printer.

The quality of this reproduction is dependent upon the quality of the copy submitted. Broken or indistinct print, colored or poor quality illustrations and photographs, print bleedthrough, substandard margins, and improper alignment can adversely affect reproduction.

In the unlikely event that the author did not send UMI a complete manuscript and there are missing pages, these will be noted. Also, if unauthorized copyright material had to be removed, a note will indicate the deletion.

Oversize materials (e.g., maps, drawings, charts) are reproduced by sectioning the original, beginning at the upper left-hand corner and continuing from left to right in equal sections with small overlaps.

ProQuest Information and Learning
300 North Zeeb Road, Ann Arbor, MI 48106-1346 USA
800-521-0600

Durability of Fiberglass Composite Sheet Piles in Water

by

Kouassi Serge P. Kouadio

May 2001

Department of Civil Engineering and Applied Mechanics

McGill University

Montréal, Canada

A thesis submitted to the faculty of Graduate Studies
and Research in partial fulfillment of the requirements
for the degree of Master of Engineering

Durability of Fiberglass Composite Sheet Piles in Water

Abstract

With the advance of composite materials in the past 50 years, fiber-reinforced polymer sheet piles are becoming increasingly popular in the marine and waterfront applications. While these materials possess high strength-to-weight ratio and are corrosion resistant, their durability in water has been not well studied due to the lack of historical data for these fairly new materials.

The purpose of this research is to establish the absorption characteristics of a pultruded fiberglass-reinforced polyester composite for a sheet pile wall and quantify the effect of water on long term mechanical properties. The tests conducted were water absorption, tensile strength, flexural strength, and freeze/thaw cycling. An analytical model was developed to establish the nature of the absorption process and prediction of the change in mechanical properties.

The results indicated that the water absorption process of the material followed a combination of Fickian diffusion and polymeric relaxation. The moisture saturation was 1.72% for the flange and 3.11% for web. The absorption process modeling indicated that saturation would be reached in 4.5 years for flange and 7 years for web in tap water, at room temperature. The coefficients of diffusion calculated were 4.2 10^{-6} mm^2/s and 3.0 10^{-6} mm^2/s respectively. During the water absorption test at 70°C and in boiling water, a mass loss of the material occurred. Tensile strength was found to decrease with the increase in percentage of water absorbed with no further degradation seen after saturation was reached. There was a decrease of 60% in the tensile strength at saturation. On the other hand, there was no noticeable change in the tensile modulus of elasticity during the water-ageing period. The freeze/thaw cycling test revealed that there were no significant changes in the tensile strength and the modulus after 564 cycles from 4.4°C to -17.8°C.

La Durabilité des Palplanches de Composites de Fibres de Verre dans l'eau

Résumé

Avec l'avancement des composites dans les dernières 50 années. les palplanches de polymères renforcés de fibres sont de plus en plus populaires dans les applications maritimes et en bordure des eaux. Tandis que ces matériaux possèdent un facteur resistance-masse élévé et sont résistants à la corrosion. leur durabilité n'est pas très bien connue dûe au manque de données historiques pour ces nouveaux materiaux.

L'objectif de cette recherche est d'établir les charactéristiques d'absorption d'un mur de palplanches tirées de polyestère renforcé de fibres de verre et quantifier les effets à long term de l'eau sur les propriétés mechaniques. Les expériences entreprises étaient l'absorption de l'eau. résistances à la traction. à la flexion. et au gel et à la rosée. Des models analytiques ont été développés pour établir la nature du proccédé d'absorption et la prédiction du changement des propriétés mechaniques.

Les résultats indiquent que le proccédé d'absorption était une combinaison de la diffusion Fickienne et la relaxation polymérique. Le taux de saturation était de 1.72% pour le rebord et 3.11% pour la palmure. Ces taux seront respectivement atteints à 4.5 ans et 7 ans. dans l'eau de robinet à la température ambiente. Les coéfficients de diffusion caculés étaient respectivement 4.2 10^{-6} mm^2/s et 3.0 10^{-6} mm^2/s. Pendant l'absorption de l'eau à 70°C et dans l'eau bouillante. une perte de masse s'était produite. La résistance à la traction dimunuait avec l'augmentation du taux d'absorption. avec aucune perte après le temps de saturation. Les pertes s'élévaient à 60% au temps de saturation. Il n'yavait pas de changement notable du module d'élasticité durant la période d'absorption. L'expérience de gel et de rosée a montré aucun changement notable de resistance à la traction et du module d'élasticité après 564 cycles. de 4.4°C à 17.8°C.

Acknowledgements

The author would like to thank Professor Y. Shao for his continued encouragement, support, and knowledgeable advice throughout the research program. Furthermore, the author would like to thank Pultronex Corporation, Nisku, AB, for supplying the composite for this research. The author would especially like to thank Mr. Michael Yeats of Pultronex for his assistance and valuable comments regarding this research.

All the research was carried out in the Materials Laboratory at McGill University. The author would like to thank Ron Sheppard, John Bartczak, Damon Kiperchuk, and Marek Pryskorski for their assistance in the laboratory. The author would also like to thank Shylesh Moras, Cindy Giroux, and Liying Jiang for their help in the laboratory when I needed it.

Finally, the author would like to send specials thank to his family and friends for their selfless support and making this endeavor possible.

Table of Contents

Abstract.....i

Resumé.....ii

Acknowledgements.....iii

Table of Contents.....iv

List of Figures.....vii

List of Tables.....ix

List of Symbols.....x

Chapter 1 Introduction.....1

1.1 Traditional Sheet Pile Systems.....1
1.2 Composites in Marine and Waterfront Applications.....3
1.3 Challenge for Composites in Water.....4

Chapter 2 Literature Review.....6

2.1 Water Absorption of Composites.....6
2.2 Effect of Water-Ageing on Mechanical Properties of Composites.....8

Chapter 3 Objectives.....10

3.1 Objectives of the Research.....10
3.2 Structure of the Thesis.....12

Chapter 4 Material and Experimental Program.....14

4.1 Material Characteristics.....14
4.2 Water Absorption Tests.....18
4.3 Mass Loss Correction Test for Absorption at 23°C and 70°C.....22
4.4 Boiling Distilled Water Tests for Saturation.....24
4.5 Test of Water Absorption under Load.....24
4.6 Tensile Tests for Mechanical Properties.....27
4.7 Freeze/Thaw Test.....29
4.8 Specimen Designation.....30

Chapter 5 Absorption Theory 31

5.1 Theory 31
5.2 Prediction of Absorption by Curve Fitting 36

Chapter 6 Experimental Results 39

6.1 Water Absorption Tests 39
6.1.1 Absorption Test in Tap and Salted Waters at 23°C, 40°C and 70°C 39
6.1.2 Mass Loss Correction of Tap Water absorption at 70°C 45
6.1.3 Boiling Water Absorption Test for Saturation 47
6.1.4 Water Absorption under Three-Point Flexural Load 49
6.1.5 Comparison of Water Absorption Rate 52
6.1.6 ASTM D 570 2-Hour and 24-Hour Water Absorption 53
6.2 Loss of Mechanical Properties 54
6.3 Effect of Freeze/Thaw Cycling on Tensile Properties 60
6.3.1 Effect of ageing Path 60
6.3.2 Effect of Freeze/Thaw Cycling 63

Chapter 7 Prediction of Water Absorption and Mechanical Properties 65

7.1 Water Absorption Modeling 65
7.2 Prediction of Mechanical Properties 67
7.2.1 Tensile Strength 67
7.2.2 Tensile Modulus of Elasticity 74

Chapter 8 Discussion 77

8.1 Water Absorption 77
8.2 Tensile Properties 80

Chapter 9 Conclusion 84

References 87

Appendix A Reference 3-Point Flexural Strength Curves 89

Appendix B All Tensile Strength Curves.....91

Appendix C Boiling Distilled Water Absorption Data.....103

List of Figures

Chapter 1

1.1 Composite Sheet Pile Wall in Residential Area..... 1

Chapter 4

4.1 Cross-Section of Composite Sheet Pile Wall Panel..... 15
4.2 Schematic Diagram of Pultrusion Process..... 16
4.3 Specimen Arrangement for Water Absorption..... 20
4.4 Setup for Water Absorption Test at High Temperature..... 20
4.5 Flexural Strength Test Setup..... 25
4.6 Water Absorption under Load Setup..... 26
4.7 Tensile Strength Test Setup..... 28
4.8 Freeze/Thaw Chamber Setup..... 29

Chapter 5

5.1 Moisture Diffusion through a Plate..... 32
5.2 Theoretical Absorption Curves Due to Fickian Diffusion and Polymeric Relaxation..... 35
5.3 Theoretical Curves of Absorption Model..... 38

Chapter 6

6.1 Absorption Curves in Tap and Salted Waters at 23°C..... 40
6.2 Absorption Curves in Tap and Salted Waters at 40°C..... 41
6.3 Absorption Curves in Tap and Salted Waters at 70°C..... 42
6.4 Absorption Curves in Tap Water of Coated and Uncoated Web Specimens at 70°C..... 43
6.5 Absorption Curves in Tap Water of Coated and Uncoated Specimens at 23°C..... 44
6.6 Absorption Curves in Tap Water of Coated and Uncoated Specimens at 40°C..... 44
6.7 Mass Loss Correction for Tap Water Absorption at 70°C..... 46
6.8 Boiling Distilled Water Absorption of Flange..... 48
6.9 Boiling Distilled Water Absorption of Web..... 48
6.10 Load-Deflection Curves for Dry Composite Beams as Reference..... 49
6.11 Tap Water Absorption under Load at 23°C..... 51
6.12 Tap Water Absorption under Load at 70°C..... 51
6.13 Tensile Stress-Strain Curves for Reference Dry composite..... 55
6.14 Tensile Stress-strain Curves for Tap Water-Aged Flange..... 56
6.15 Tensile Stress-strain Curves for Tap Water-Aged Web..... 57
6.16 Tensile Stress-strain Curves for Tap Water-Aged in Boiling Water..... 58
6.17 Effect of Ageing Path on Tensile Properties..... 62
6.18 Effect of Freeze/Thaw Cycling on Tensile Properties..... 64

Chapter 7

7.1 Absorption Modeling of T23F and T23W..... 66
7.2 Tensile Strength vs. Absorption of Water-Aged Flange..... 68

7.3 Tensile Strength vs. Absorption of Water-Aged Web..... 69
7.4 Prediction of Tensile Strength of Flange with Time.....71
7.5 Prediction of Tensile Strength of Web with Time.....71
7.6 Tensile Modulus vs. Time of Water-Aged Specimens..... 74
7.7 Tensile Modulus vs. Absorption of Water-Aged Specimens..... 76

Chapter 8
8.1 Color Change of Specimens in different Ageing Conditions..... 79
8.2 Web and Flange Dog-Bone Coupons after Tensile Tests.....80
8.3 Schematic Diagram of failed Flanged Coupon.....81
8.4 Schematic Diagram of failed Web Coupon.....81

List of Tables

Chapter 4

4.1 Isophthalic Polyester Mechanical Properties..... 14
4.2 Properties of E-Glass and E-CR Glass Fibers..... 15
4.3 Composition of Sheet Pile Wall Panel Segments..... 17

Chapter 6

6.1 Mass Loss Corrected for Specimens in Water Absorption Test at 70°C..... 45
6.2 Loads Used in Loaded Absorption Tests..... 50
6.3 Initial Slopes of Absorption Curves..... 53
6.4 2-Hour and 24-Hour Distilled Water Absorption..... 54
6.5 Water Absorption Tensile Test..... 59
6.6 Freeze/Thaw and Effect of Ageing Path..... 61
6.7 Effect of Freeze/Thaw Cycling..... 63

Chapter 7

7.1 Parameters for Curve Fitting of Tap Water Absorption with Time..... 66
7.2 Comparison of D_z Values from Different Methods..... 67
7.3 Parameters from Curve Fitting of Tensile Strength with Time..... 73
7.4 Prediction of Tensile Strength with Time..... 73
7.5 Comparison of the Tensile Modulus of Elasticity..... 75

List of Symbols

c = moisture concentration in composite

c_i = the initial moisture concentration

c_m = the maximum moisture concentration at the surface of the material. (c_m is related to moisture content of the environment, c_a (Figure 5.1))

D_z = mass diffusivity along z direction

G = moisture weight gain as a function of time

h = normal thickness, in the direction of diffusion

k = relaxation rate constant

M_{cond} = conditioned mass (initial dry mass), g

M_{cond} = conditioned mass (initial dry mass), g

M_{cond2} = new conditioned mass (after reconditioning), g

M_{wet} = wet mass after immersion in water at a certain age, g

$\%M$ = percentage of water absorbed by weight

$\%M_i$ = initial weight percentage of moisture in the material, %

$\%M_{Loss}$ = percentage mass loss

$\%M_m$ = maximum weight percentage of moisture absorbed (at saturation), %

$\%M_{t,F}$ = Fickian absorption at time t

$\%M_{t,R}$ = absorption due to relaxation at time t, %

$\%M_{\infty,F}$ = maximum Fickian absorption at saturation, %

$\%M_{\infty,R}$ = maximum absorption due to relaxation, %

t = time

Chapter 1

Introduction

1.1 TRADITIONAL SHEET PILE SYSTEMS

Sheet pile walls are being used increasingly in the water environment as people are closely interacting with oceans, lakes, rivers and any body of water, as shown in an example in Figure 1.1. Whether the application is residential or industrial the water environment has been proven to be severe on this type of structure. This harshness has been a main factor in the decreased durability of the materials that have been traditionally used for this application. Wood, steel and concrete have been the materials of choice used in the piling industry in the past. But through the years, designers have come to realize that, although there are certain advantages in using these materials, the drawbacks they present may be serious enough to outweigh the positive aspects.

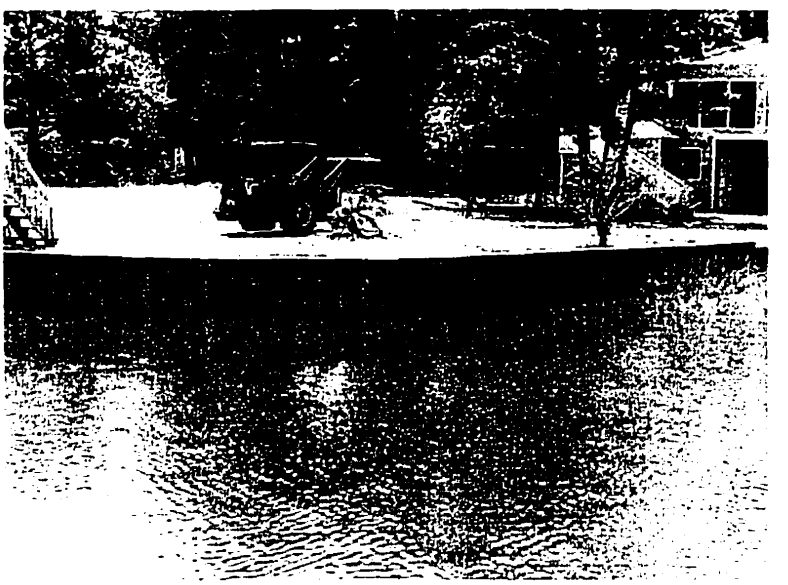

Figure 1.1 Composite Sheet Pile Wall in Residential Area [Pultronex Corporation]

Wood represents a versatile material with high strength-to-weight ratio. Products made from it can be easily handled and installed. But when timber sheet piles are immersed in brackish or saline water, they have to contend with molluscan or crustacean borers [Tomlinson 1994]. The action of these organisms can be quite destructive. In many instances, these borers have decomposed the wood to the extent that large voids appeared in the material. As a result, the structure can no longer withstand the loading capacity it was designed for and failure is imminent. Damages of this nature can only be remedied by the total replacement of the deteriorated member. Timber piling manufacturers have resorted to chemical treatment, such as treatment with creosote, in an attempt to extend the service life of their products, which is the most popular wood treatment adopted in the industry. This chemical compound presents a growing environmental disposal problem and is listed as a toxin by the Environmental Protection Agency. These chemicals may also pose a health risk to installation workers and a threat to marine life, particularly when used in large quantities. [Iskander et al., 1998]

The concrete sheet pile may not offer the flexibility encountered in the timber product but it does have the advantage of strength. But its installation is more costly as concrete has a low strength-to-weight ratio and requires more labor and machinery for installation. In the marine environment, the disintegration of the reinforced concrete does occur and is most severe in the splash zone. The expansive action created by the crystallization of salts and the freezing of water in the pores of the concrete can cause spalling. [Tomlinson 1994] This spalling will in turn lead to the exposure of steel in case of reinforced concrete. The direct actions of water, oxygen, carbon dioxide and chloride ions will help accelerate the corrosion process. The devastating nature of corrosion will lead to expansive rust being produced, leading to bursting pressure that may cause spalling of the cover in some areas.

The mechanical superiority of steel over the other two materials is well known. Also well documented is the corrosion phenomenon of steel in the water environment. Using weathering or galvanized steel or other special treated steel is epensive. Coating may pose a danger to marine life and the pollution of the water.

Overall, it is estimated that the deterioration of wood, concrete, and steel piling systems costs the U.S. military and civilian marine and waterfront communities is of the

order of $1 billion annually [USACERL 123 1998]. For economical and environmental reasons there has been a need to find an alternative material to the traditional ones for piling systems.

1.2 COMPOSITES IN MARINE AND WATERFRONT APPLICATIONS

The use of composite materials dates back more than 50 years. Throughout the years these materials have demonstrated superior capabilities to traditional materials and have been implemented slowly in different domains. There are a variety of composite materials but the ones used in the domain of engineering structures are polymeric matrix reinforced with fibers. Glass fibers would be the most common choice of reinforcement. They have been used in many areas with marine applications increasingly gaining popularity. The affinity for these materials stem from the fact that they have a high strength-to-weight ratio and most of all, their corrosion resistance is superior to that of the traditional materials.

Marine application of composites is extensive and ranges from transportation, aircraft to special military uses. The current specific marine applications of composites are: [Davies 1996]

- Surface vessels
- Offshore structures
- Underwater applications

The surface vessels relate to the boat industry, whether it is for pleasure boating, passenger transport, or military uses. The high specific compression properties make composites attractive for submersibles and submarines structures. Underwater applications are some of the most demanding for materials, and proving reliability is central to the adoption of new concepts. The existing and potential applications in offshore structures include: [Davies 1996]

- Walkways, flooring and ladders
- Tanks and storage vessels
- Shutdown valve protection, blast panels
- Accommodation modules

Composite piling products have been used to a limited degree, or experimentally, in the United States and Canada for waterfront barriers, fender piles, and bearing piles for light structures. A composite fender pile was first used in April 1987 in the Port of Los Angeles. It was a segmented recycled plastic with steel pipe core. Over the following few years, several vendors produced a variety of fender piling products made with virgin, recycled, or hybrid composites. The majority of the piles produced by the industry today have comparable properties to wood products. Most composite piling products are made of fiberglass or HDPE with fiberglass reinforcement and additives to improve their mechanical properties, durability, and ultraviolet protection. [Iskander et al., 1998]

1.3 CHALLENGE FOR COMPOSITES IN WATER

In marine and waterfront applications, water represents the main aggressive agent that regulates the life of any structure in these environments. Although composites have been used in these conditions, they are fairly new materials compared to the traditional ones. For this reason, their long-term performance in water, as it relates to durability, has not been truly established. Data have been collected for high performance aerospace composites, generally from exposure to varied relative humidities rather than immersion in water [Davies 1996]. A large database has also been collected for naval applications, with over 20 years of immersion in some cases [Gutierrez et al., 1992]. The problem that is encountered in trying to establish broad base evaluation criteria of composites is that there are always variations between composites. Composites with different mechanical and absorption properties could be created from the same components depending on the manufacturing process, reinforcement used, and the method of incorporation of fibers.

For this reason, almost every new composite developed needs to be tested to establish a more accurate database.

Chapter 2

Literature Review

2.1 WATER ABSORPTION OF COMPOSITES

Water absorption of fiber composite in humid environment or submerged in water has been extensively studied over the past two decades, mainly for aerospace industry, military vessels and surface boat industry. Almost all of the studies are carried out on laminate composites because of the special applications. Efforts have been made to improve the understanding of the absorption behavior of composites and the durability of these materials.

The composite can be divided in three phases: the polymer resin, the fiber reinforcement and the fiber-matrix interface. The physical process of water absorption in composites does not follow the same process as in the neat resin. Glass fiber reinforcements are hydrophobic in nature. The moisture mainly diffuses into the composite through the resin and the interface. The water absorption of the neat resin can usually be modeled by Fickian diffusion, while the composite often lends itself to a more complex absorption process. The interface is often responsible for a large portion of the moisture absorption in the composite. [Choqueuse et al., 1997, Grant et al., 1994, Gellert, et al., 1999] The Fickian diffusion is characterized by an exponential function, where the percentage of absorption at time t depends on the specimen thickness, the diffusion coefficient and the maximum percentage of absorption.

A study conducted by Choqueuse et al. [1997] on the aging of composites in water investigated five laminates immersed in distilled water at temperatures ranging from 5°C to 60°C. The different resins used were isophthalic polyester, vinyl ester, epoxy and PEEK, with fiber contents of 50% to 61% by weight. After 2 years, saturation

was not reached under any condition. It was found that the modeling of the absorption phenomena for marine composite materials by a single law is not possible.

Seawater immersion ageing of laminates for marine applications was studied by Gellert and Turley [1999]. The water uptake behavior of an isophthalic polyester, a phenolic and two vinylester GRP systems. The corresponding neat resin castings were also studied. The water absorption of the polyester and vinylester laminates appeared to be affected initially by the suppression from fiber barrier effects. At a later age, enhancement from the interface effects governed the absorption process.

The water absorption under load was also tested by means of flexural action. The application of 4 point-bending test on the absorption specimens does not have much effect on the maximum percentage water absorption at saturation [Geller et al., 1999, Kasturiarachchi et al., 1983]. However the diffusion coefficient did not follow the same trend. For polyester, phenolic and two kinds of vinylester GRPs in loaded absorption tests, the diffusion coefficient of the polyester and phenolic GRPs increased during the absorption under mechanical load while that of the two vinylester decreased [Gellert et al., 1999].

High temperature is commonly used to accelerate the absorption tests. The temperatures used are in the range from 40°C to 100°C. A study by Gutierrez et al. [1992] indicated that 1000 hours of accelerated ageing at 70°C caused a loss in flexural properties similar to that in 15 years under natural conditions. This is one of very few examples for which the effect of accelerated ageing has been examined. However, hot water acceleration also introduces mass loss by leaching simultaneously with water absorption in some material systems.

The mass loss is characterized by an absorption curve with a softening type of response. On the plot of percentage water absorbed vs. time, there appears to be a decrease in the percentage of water absorbed after an initial water uptake. A study carried out by Bonniau and Bunsell [1981] showed that mass loss occurred in E-glass reinforced bisphenol an epoxy resin with anhydride hardener at 40°C, 60°C and 90°C. The same resin with other types of hardeners exhibited a normal Fickian plateau. Isophthalic polyester resin was also recognized for its mass loss at high temperature. The physical and mechanical processes were described as water uptake, leaching of non-

bound substances and leaching of hydrolysis products [Abeysinghe et al., 1982]. A similar behavior was observed in the water absorption of the isophthalic resin at 90°C, in another study [Apicella et al., 1983]. The weight loss was likely caused by the autocatalytic hydrolysis of the ester groups in the resin.

The type of absorption curves of isophthalic polyester resin and composite at high temperature does not readily lend itself to a fit by any absorption model because of the softening type of response. The ASTM D 570, which is the standard that deals with the water absorption of plastics, allows a correction of the percentage water absorbed when the mass loss is suspected. The mass loss is the difference between the original dry mass and the dry mass of the aged specimen.

2.2 EFFECT OF WATER-AGEING ON MECHANICAL PROPERTIES OF COMPOSITES

As the composite is being used in a moist environment, the aggressive action of water affects the mechanical properties. The mechanical tests that have been performed to investigate this process range from tension to flexural to shear tests. In general the strength of the water-aged composite is lower compared to the strength of the unaged composite. Although the degradation of mechanical properties may occur at different rates, the extent of degradation is a function of the water absorbed. When water saturation is reached, no further degradation can occur [Geller et al., 1999, Pritchard et al., 1987]. Furthermore, many absorption tests are conducted at different temperatures, either to simulate the environment of the material or to perform an accelerated absorption test. The extent of degradation of mechanical properties does not depend on the temperature of testing but only on the amount of water absorbed by the material. The temperature may only regulate how fast the water is being absorbed, as expressed by the diffusion coefficient [Pritchard et al., 1987]. However, another study showed that high temperature acceleration could also generate strength loss by forming disc shaped crack, fiber debonding and delamination [Apicella et al., 1983].

A study was conducted on the use of water absorption data to predict the laminate property changes after water aging. The composite was a glass-fiber reinforced isophthalic polyester laminate prepared using the hand lay-up method. The study investigated the tensile strength and modulus and the shear strength of different laminate lay-ups. Appropriate equations to predict the strength with time, knowing the saturation moisture content, were developed. [Pritchard et al., 1987]

The freeze/thaw resistance of saturated composites is a major concern whenever structures have to be built in cold climate. The saturated materials are likely to be more vulnerable to freeze/thaw damages, especially if they possess a microstructure that allows the absorbed water to freeze. In composites, this microstructure relates to the matrix and the fiber/matrix interface. These are locations of probable cracks. The cracks that are small at first may grow due to various external forces. When these cracks form beyond a certain critical size and density, they coalesce to form macroscopic matrix cracks which tends to increase the diffusion of water in the system. In these larger openings, water may be able to freeze. The expansion created, as water freezes to form ice, would lead to further crack propagation. [Dutta et al., 1988]

The effect of freeze/thaw cycling on the mechanical properties of a material could be severe and the implication may be costly or even disastrous. Very limited studies have been conducted in this area. There is no standard test method specially designed for polymer matrix composites. The currently used test method is based on ASTM C 666 developed for concrete, where the temperature is cycled from -17.8°C to 4.4°C. It was found that the flexural strength and modulus were reduced in specimens of isophthalic polyester and vinylester glass reinforced composites after 300 freeze/thaw cycles in 2% salted water solution [Gomez et al., 1996]. But there was no significant reduction in tensile strength or modulus of elasticity in vinylester and epoxy glass reinforced composites after 300 cycles. The degradation that existed after saturation of the composite, prior to the start of freeze/thaw test, did not propagate after 300 cycles [Haramis et al., 2000].

Chapter 3

Objectives

Water absorption of composites once immersed in water degrades the matrix-dominated properties of these materials. Few long-term data are available on this degradation and the existing studies have concentrated mainly on laminated composites for aerospace industry and for ships and submarine applications. These materials are different from those considered for the sheet pile wall structural application both by their fabrication techniques (pultrusion vs. laminate molding), their constituents (material systems) and their service conditions (long-term vs. short-term immersion), therefore, the available data are not directly transferable all composites. Furthermore, none of the studies was done with the pultruded shapes, since the commercially available pultruded products are not designed for immersion applications. Nevertheless, it is recognized that polymeric composites undergo a slow degradation process when subjected to physical and chemical aging due to the moisture uptake. Increased temperatures can accelerate this process.

3.1 OBJECTIVES OF THE RESEARCH

The objectives of the research reported in this thesis are to study the water absorption of a pultruded fiberglass polyester composite designed and manufactured for sheet pile walls in the marine and waterfront applications, to evaluate the corresponding mechanical property changes, and to predict the long term performance based on short term experimental data.

Study of Water Absorption

The objective of the water absorption tests conducted was to characterize the moisture diffusion of the new material to be used in the wet environment. The parameters sought in this evaluation were the saturation moisture content of the composite, the diffusion coefficient and the time at which moisture saturation occurred.

Study of Freeze/Thaw Cycling

The objective of this study was to investigate the effect of freeze/thaw cycles on the mechanical properties of the proposed composite. This directly relates to the durability of the sheet pile wall made from it.

Prediction of Mechanical Properties

The prediction analysis undertaken on the proposed composite will help assess the evolution of the degradation of its mechanical properties in the water environment and the long-term performance of the composite.

Tests to be Conducted

The experiments that were undertaken are: (i) water absorption, (ii) freeze/thaw cycling, and (iii) strength loss due to water absorption and temperature cycling test. All experiments were performed to help evaluate the behavior of the composite at ambient conditions.

The water absorption test will help establish the saturation moisture content of the composite and the diffusion coefficient. This test was performed in both accelerated and

normal conditions. The latter will give a true picture of the water absorption of the composites under normal conditions. The accelerated water absorption test will be used to make long-term prediction of the changes in the mechanical properties of the water-aged material. Since the water absorption depends on the immersion solution, tap water, salted water and distilled water will be tested. The effect of flexural action on the absorption characteristics will be investigated.

Freeze/thaw test will assess the effect of temperature cycling on the mechanical properties by establishing the effect of ageing path with and without temperature cycles, on the properties. Moreover, the influence of the number of temperature cycles on these properties was also studied. The test was conducted by immersion in tap water environment in a freeze/thaw cycling chamber.

The prediction of changes in tensile properties was based on the monitoring the maximum tensile strength and the modulus of elasticity during the tap water absorption ageing and the freeze/thaw cycling. Statistical tools for curve fitting were used in order to make extrapolation of results. A relationship will be established between the normal water absorption and the one in accelerated conditions. The tensile properties of the composite after a number of years from now will be established. On the other hand the temperature cycles was correlated to the change of tensile properties occurring in the freeze/thaw test.

All experiments were focused on the ageing in the tap water, which is a moderate environment between the two extremes: salted water at the low end and distilled water at the higher end. This choice was made to conduct a more conservative study on the composite as the performance of the material in salted, which simulated the seawater environment, would be satisfied by the results obtained from tap water.

3.2 STRUCTURE OF THE THESIS

The structure of this thesis is organized as follows:

- Chapter 1 is an introduction to traditional sheet piling systems in the water environment and composites

- Chapter 2 presents the summary of the literature survey.
- Chapter 3 lays out the objectives of the research and a brief overview of the tests to be conducted.
- Chapter 4 presents the experimental program that was followed, including a description of the proposed composite material for this research.
- Chapter 5 depicts the moisture diffusion theory that was used in this research to profile the absorption process in the composite.
- Chapter 6 presents the results obtained for the tests conducted in the experimental program, with a preliminary analysis of the results .
- Chapter 7 focuses on the prediction of the mechanical properties in the long term.
- Chapter 8 encompasses discussions of the test results, observations and analysis procedures.
- Chapter 9 presents the concluding remarks that emanate from this research program.

Chapter 4

Material and Experimental Program

4.1 MATERIAL CHARACTERISTICS

The composite being investigated through this research is a glass-fiber reinforced polyester resin. The resin used in the composite system was an isophthalic polyester resin. Isophthalic polyester resin is produced from the reaction of isophthalic acid with propylene glycol. This type of polyester resin is characterized by greater strength, heat resistance, toughness and flexibility than their ortho cousins. In isophthalic acids, the acid groups are separated by one carbon of the benzene ring which increases the opportunity to produce polymers with greater linearity and higher molecular weight. [Peters 1998] The typical properties of the isophthalic polyester used are given in Table 4.1.

Table 4.1 Isophthalic Polyester Mechanical Properties [Peters 1998]

Properties	
Tensile Strength, MPa	48.3
Tensile modulus, GPa	3.6
Tensile elongation, %	1.5
Flexural strength, MPa	104.8
Flexural modulus, GPa	4.27

For the reinforcement, E-glass and E-CR glass were used. The rovings are composed of E-CR glass fibers and all mats are of E-glass. Some properties of the glass fibers used are given in Table 4.2.

Table 4.2 Properties of E-Glass and E-CR Glass Fibers [Peters 1998]

Properties	**E-Glass**	**E-CR Glass**
Tensile strength at 23°C, MPa	3100 - 3500	3300 - 3800
Modulus of elasticity at 23°C, GPa	76 - 78	80 - 81
Elongation at break, %	4.4 - 4.5	4.5 - 4.9
Softening point, °C	830 - 860	880

The glass fiber reinforced polyester composite sheet piles used in this study were designed and manufactured by Pultronex Corporation in Nisku, Alberta. A cross-section of the sheet pile is shown in Figure 4.1.

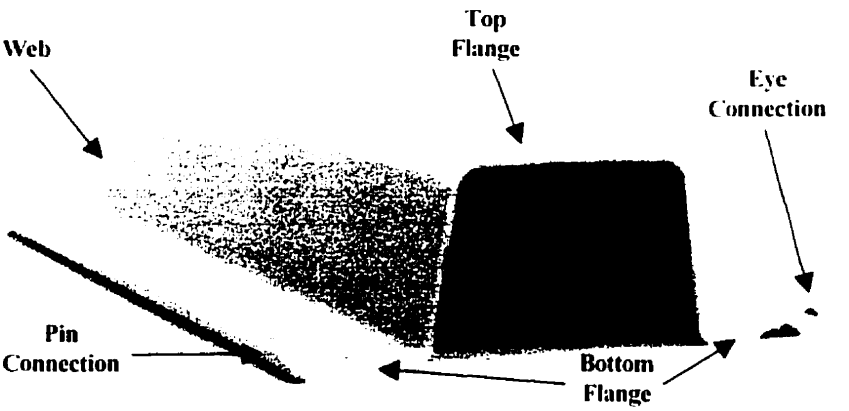

Figure 4.1 Cross-section of Composite Sheet Pile Wall Panel

The sheet pile panels have an interlocking mechanism to allow for the formation of the wall. The sheet pile panel was fabricated by the pultrusion process as shown in Figure 4.2. There is a resin tank, which contains a resin bath, between the material guides. The fibers that are initially wound on drums are pulled through the resin bath, which already contains a catalyst to help the cure when heat is later applied. The wetted fibers then pass through a long heated die whose cross-section is that of the final product. The heat applied to the die helps the fast curing of the resin as the wetted fibers are slowly pulled through it. By the time the fiber/resin comes out at the other end of the die complete curing has already taken place. At the other end of the die, the product can either be pulled by the friction action of a conveyor belt or by a mechanism of hydraulic rams. A moving saw is then used to cut the specimen at the desired length.

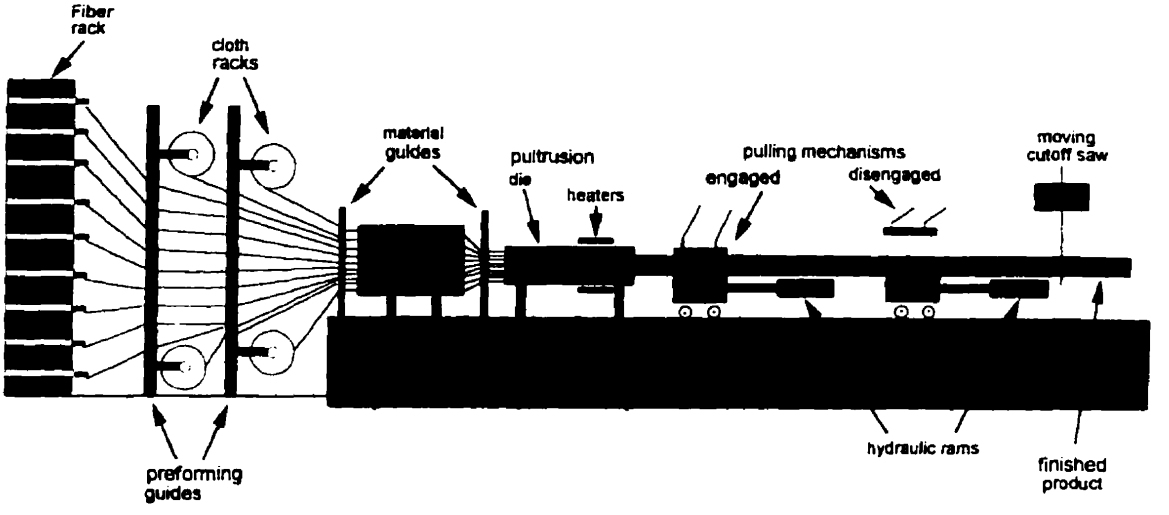

Figure 4.2 Schematic Diagram of Pultrusion Process [Peters 1998].

Three parts of the composite sheet pile can be distinguished from the cross-section of the panel shown in Figure 4.1: the top flange, the bottom flange and the two webs. The layer structure and the fiber volume ratio of the main segments are given in Table 4.3. The bottom flange and the web have the same thickness of 3.176 mm, while

the top flange has a thickness of 4.699 mm. The composition of these three parts follows a different order. The bottom flange and the top flange have the same type of reinforcement but in different percentages. The web also contains an additional layer of continuous filament mat (CFM) for the shear resistance. RCM stands for random chopped mat.

Table 4.3 Composition of Sheet Pile Wall Panel Segments

Segment	Layers	Layer Thickness (mm)	Layer Fiber/ Volume Ratio	Avg. Fiber/ Volume Ratio
Top Flange (4.699 mm)	RCM	0.459	0.257	0.487
	Transverse fibers	0.323	0.450	
	Rovings	3.135	0.562	
	Transverse fibers	0.323	0.450	
	RCM	0.459	0.257	
Bottom Flange (3.176 mm)	RCM	0.427	0.277	0.317
	Transverse fibers	0.341	0.426	
	Rovings	1.640	0.293	
	Transverse fibers	0.341	0.426	
	RCM	0.427	0.277	
Web (3.176 mm)	RCM	0.333	0.355	0.337
	Transverse fibers	0.343	0.424	
	Rovings	0.738	0.491	
	CFM	1.086	0.166	
	Transverse fibers	0.343	0.423	
	RCM	0.333	0.355	

The absorption and mechanical tests were performed only on coupons of segments of the sheet pile panel due to the difficulty in handling the full size panel in water. The tests were conducted only on the web and the top flange. Although the

bottom and the top flange do not have the same thickness, they have similar layout in terms of glass fiber reinforcement. The absorption characteristics of the bottom flange and the top flange are assumed to be similar, as the interface a very similar. Therefore, whenever the word flange is encountered in the following chapters, it refers to the top flange.

Two types of specimens were used in this study. One was the dog-bone coupon and the other straight beam specimen. The dog-bone specimens (150x10 mm) were specified by ASTM D 638M for the test of tensile properties of composites at normal and accelerated conditions. The straight beam specimens were prepared for ASTM D 570 absorption test and ASTM D 790M flexural test. The dimension of 10x200 mm was chosen for the beam specimens according to the ASTM D 790M instead of 24.4x76.2 mm according to ASTM D 570 absorption test. The reason for this choice is that, if the same size specimens were used in both loaded and unloaded absorption, the size effect could be minimized in comparison. In addition, the surface areas exposed in water in both specimens differed only by 3%. All specimens were cut along the longitudinal direction of the sheet pile panel as shown in Figure 4.1.

4.2 WATER ABSORPTION TESTS

The basic water absorption tests were carried out at room temperature (23°C ± 2°C) without the influence of external mechanical load. The absorption performance of the composite was evaluated in tap water and salted water at 23°C. The former was to simulate waterfront applications, while the latter the marine environment. Accelerated absorption tests were performed at higher temperatures to help correlate the water absorption at the standard temperature to that at accelerated conditions to predict the long-term performance.

The absorption tests were performed at the following three temperatures:

- 23° ± 2°C , room temperature
- 40°C, medium accelerated temperature
- 70°C, rapid accelerated temperature

For each temperature, absorption in tap water and salted water for both flange and web specimens was investigated. Three beam specimens for each were used in individual test condition to obtain the average. The tap water came directly from the tap. The salted water was made by a solution of reagent grade sodium chloride obtained by dissolving sodium chloride pellets in distilled water at a concentration of 35 per thousand. This was to simulate the normal seawater in the Pacific Ocean. It is a simplified solution compared to the actual seawater, which contains about 3% chemicals and organic substances. As sodium chloride is the most dominant chemical compound, this simplification is reasonable for all purposes.

The sample preparation was done by coating all the cut edges of the specimens with a two-part Flexolith epoxy resin. This procedure would eliminate the edge effect on absorption. The two faces of each specimen were first covered with tape to avoid any epoxy glue residues on the surfaces. The two-part epoxy was then mixed and a first coat was applied to the edges of the specimens. The beam strips were allowed to dry in the air for 24 hours and a second epoxy coating was then applied. After another 24 hours of drying in the air, the tape was removed from the faces of the specimens. A paper towel dipped in a little bit of acetone was used to remove any remaining tape residue on the surfaces of the specimen. The specimens were then ready to be conditioned.

The water absorption test followed the procedures specified by ASTM D 570 standard. The initial conditioning was in an oven for 24 hours at 50°C ± 3°C. The specimens were then cooled in a desiccator, and immediately weighed to the nearest 0.001 g. This was the initial dry mass, as the reference for the following absorption tests. The specimens were then put in their respective test environments, which have already been stabilized prior to the immersion of the specimen. A rectangular microwave plastic container with a sealing top lid was assigned to each group of specimens at different test conditions. While the samples were being conditioned in the solutions, they were already put in the containers at the respective temperatures. The specimens were placed on racks such as the one shown in Figure 4.3. They were arranged in the microwave plastic containers in such a way that the absorption faces were free and not touching the sides of the plastic containers. Figure 4.4 shows the set-up in the oven for high temperature tests.

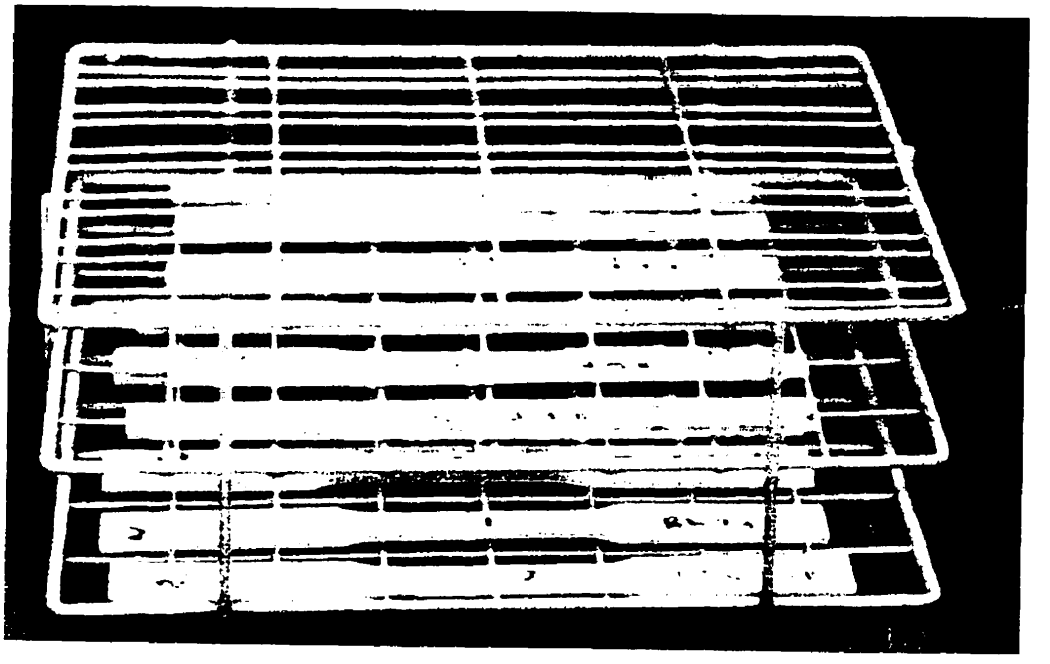

Figure 4.3 Specimen Arrangement for Water Absorption Test

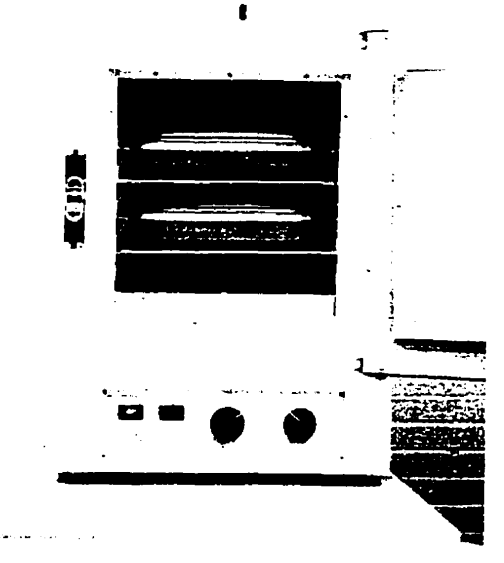

Figure 4.4 Set-up for Water Absorption Test at High Temperature

The procedure adopted to take readings was as following: a specimen was pulled out of its test environment. For test at 23°C, the specimen was surface-dried by a paper towel on each side and weighed within 15 seconds. The specimen was then replaced in its test environment. For tests at 40°C and 70°C, the specimens were taken from the oven and then placed in water at 23°C to allow them to cool down for 15 minutes. After surface drying, the wet mass was measured. The readings were taken at different time intervals, daily at the beginning of the test, to every two weeks or longer at the end of the test. The percentage water absorbed was calculated according to the following equation:

$$\%M = \frac{100(M_{wet} - M_{cond})}{M_{cond}} \tag{4.1}$$

where

$\%M$ = percentage water absorbed

M_{wet} = wet mass after immersion in water at a certain age, g

M_{cond} = conditioned mass (initial dry mass), g

Another set of short-term water absorption test was also performed to determine the absorption of the composite in distilled water after 2 hours and 24 hours. This is specified by the ASTM standard D 570. These values are commonly presented as a comparison of absorption capacity for different polymeric materials. The test was performed again on the flange and web specimens with a size of 76mm by 25mm at 23°C and boiling distilled water. The specimens were coated and conditioned as was done before. For the test at 23°C three specimens of each top flange and the web were placed on a rack and immersed in the water container as before. For the boiling test, six specimens of each flange and web were placed on a rack and then placed in a vessel on a hot plate to keep the distilled water boiling. For the absorption readings after 2 hours, three specimens of each were taken from the boiling water and cooled for 15 minutes in distilled water at room temperature before weighing. These specimens were not returned to the boiling water. Another set of new specimens was used for the absorption reading at 24 hours. For the water absorption at 23°C, the procedure followed for the reading did not involve a waiting period of 15 minutes.

4.3 MASS LOSS CORRECTION TEST FOR ABSORPTION AT 23°C AND 70°C

As was reported in some previous studies, polyester has the tendency to exhibit mass loss during water absorption tests at high temperature [Choqueuse et al., 1997, Apicella et al., 1983]. Although the polyester matrix composite sheet pile is not developed for high temperature applications, it is still important to know if saturation has occurred in the accelerated tests, despite a decline of the percentage of water absorbed with respect to time. Therefore, it is necessary to carry out the mass loss correction tests.

ASTM D 570 has a provision for the correction of the mass loss. The specimen suspected of water-soluble ingredients shall be reconditioned for the same time and at the same temperature as used in the original conditioning. The difference between the reconditioned and conditioned weight shall be considered as water-soluble matter lost during the immersion test. The water absorption shall be calculated as the sum of the increase in weight and the weight of the water-soluble matter. For the water absorption test at 70°C with clear sign of mass loss, correction of the mass loss was made only at the time when tension tests were conducted so that strength loss, if any, could be related to the water absorption in an accelerated test. Notice that the mass loss correction was only made for specimens in tap water at 70°C.

For mass loss correction, 24 beam specimens of 200mm by 10mm dimensions were used. Of these specimens, 12 were cut from the web and the 12 from the top flange. Three beams of each web and top flange were used to determine the mass loss every time a tension test was performed to evaluate the aged materials.

The specimens were edge-coated and conditioned the same way as described in the water absorption test. They were immersed in tap water at 70°C together with the specimens for the mechanical tests. At selected dates, the specimens were removed from the oven and weighed to obtain the wet mass, M_{wet}. The same specimens were then oven-dried for 24 hours at 50 ± 3°C for reconditioning them. The mass of the reconditioned dry specimens, or the new conditioned mass, M_{cond2}, was measured after the specimens were cooled down in a desiccator. The mass loss was calculated according to the following equation:

$$\%M_{Loss} = \frac{100 * (M_{cond2} - M_{cond})}{M_{cond}} \quad \textbf{(4.2)}$$

where

$\%M_{Loss}$ = percentage mass loss

M_{cond} = conditioned mass (initial dry mass), g

M_{cond2} = new conditioned mass (after reconditioning), g

If the reconditioned mass, M_{cond2}, is smaller than the initial dry mass, M_{cond}, the $\%M_{Loss}$ will be negative, indicating a loss has occurred. If there is no mass loss, $\%M_{Loss}$ will be equal to zero. The corrected percentage water absorbed, $\%M_C$, is given by equation 4.3.

$$\begin{aligned} \%M_C &= \frac{100(M_{wet} + (M_{cond} - M_{cond2}) - M_{cond})}{M_{cond}} \\ &= 100\frac{(M_{wet} - M_{cond})}{M_{cond}} - 100\frac{(M_{cond2} - M_{cond})}{M_{cond}} \\ &= \%M - \%M_{Loss} \end{aligned} \quad \textbf{(4.3)}$$

The same mass loss correction was also performed on the absorption for 2-hour and 24-hour boiling water tests.

4.4 BOILING DISTILLED WATER TESTS FOR SATURATION

The boiling distilled water tests were performed to examine the moisture saturation and the corresponding maximum percentage of absorption at saturation. The test was based on the ASTM Standard D 570.

The dimensions of the specimens were 76mm by 25 mm. The sample preparation and procedure for taking reading was the same as that described in Section 4.2 for the short-term boiling water test except that the specimens were not coated to allow fast absorption. Three specimens for each flange and web were used to measure the percentage of absorption in boiling distilled water. Every 3 to 4 days, together with the percent absorption measurements, correction for mass loss was undertaken. Twenty-four extra specimens of the same dimensions for each flange and web were immersed in the same boiling water. Eight corrections were performed with three samples, averaged for one reading. The ASTM Standard D 570 criterion was followed to determine the saturation. If the increase in weight using three consecutive weigh averages is less than 1% of the total increase in weight or 5mg, whichever is greater, the specimen shall be considered substantially saturated.

Six tension specimens, three for each flange and web, were also immersed in boiling water, at the same time, the process was accelerated for saturation. These six specimens had already been in hot water at 70°C for 73 days. They were used for the mechanical property tests at saturation to examine if the strength loss of the composite stopped after specimen saturation was attained.

4.5 TEST OF WATER ABSORPTION UNDER LOAD

The water absorption test under load was designed to investigate the absorption characteristics of the material under the action of external mechanical load. Three-point bending tests were adopted according to the ASTM Standard D 790M.

To evaluate the flexural strength of the polyester/glass composites in the dry condition as reference, beams of section 200mm by 10mm were tested in a three-point bending setup (Figure 4.5) with a span of 160 mm to assure a span to depth ratio (L/d) of 32 or larger. The tests were carried out using an MTS machine with a 150-kN capacity, with an LVDT to measure the deflection at mid-point. Five beams were tested for each flange and web.

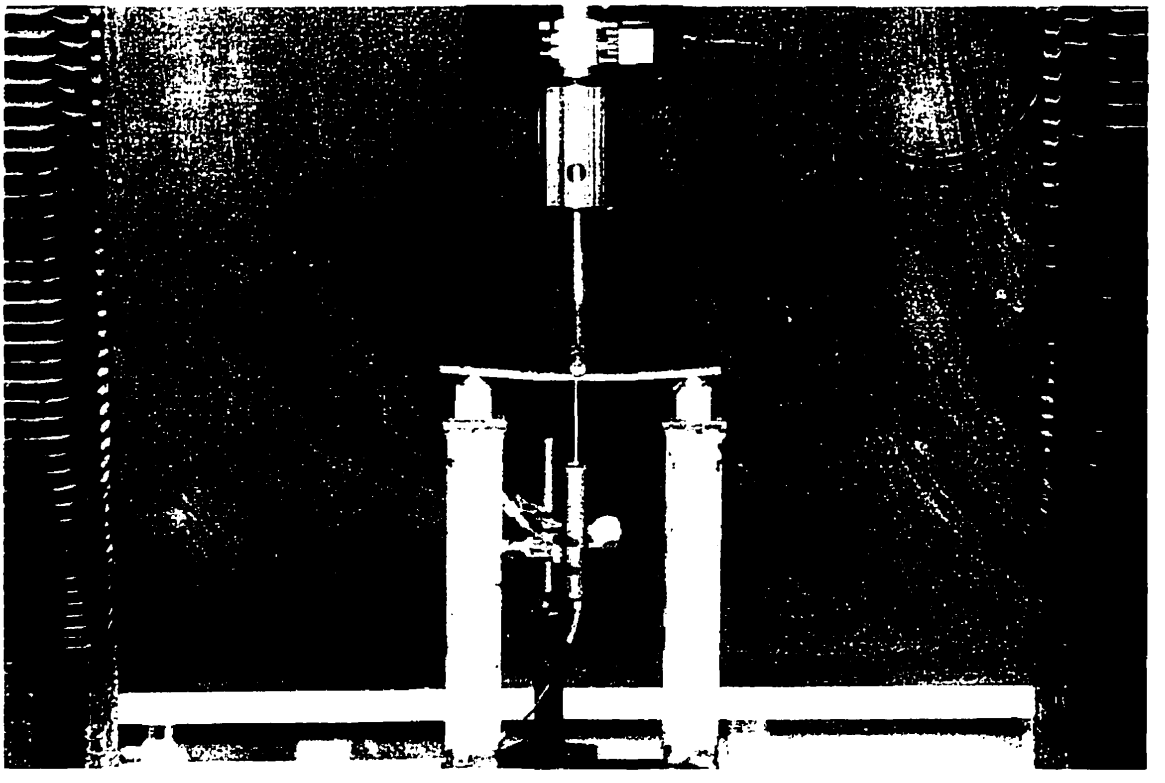

Figure 4.5 Flexural Strength Test Setup

The values of the flexural strength were used to determine the load at 25% of the ultimate flexural strength to be applied to the water absorption tests under load. Twenty-five percent was chosen because it is the design load in the current sheet pile wall design.

Six beam specimens of 200mm by 10mm section were prepared from both the web and the flange. The specimens were placed under the following conditions:

- 3 web beams in tap water at 23°C
- 3web beams in tap water at 70°C
- 3 flange beams in tap water at 23°C
- 3 flange beams in tap water at 70°C

Four sets of testing setups were fabricated to perform the loaded absorption test at the same time. The setup is shown in Figure 4.6. The size and geometry of the specimens for loaded absorption tests are the same as that used in the water absorption without load so that the comparison can be made without any size effect being involved.

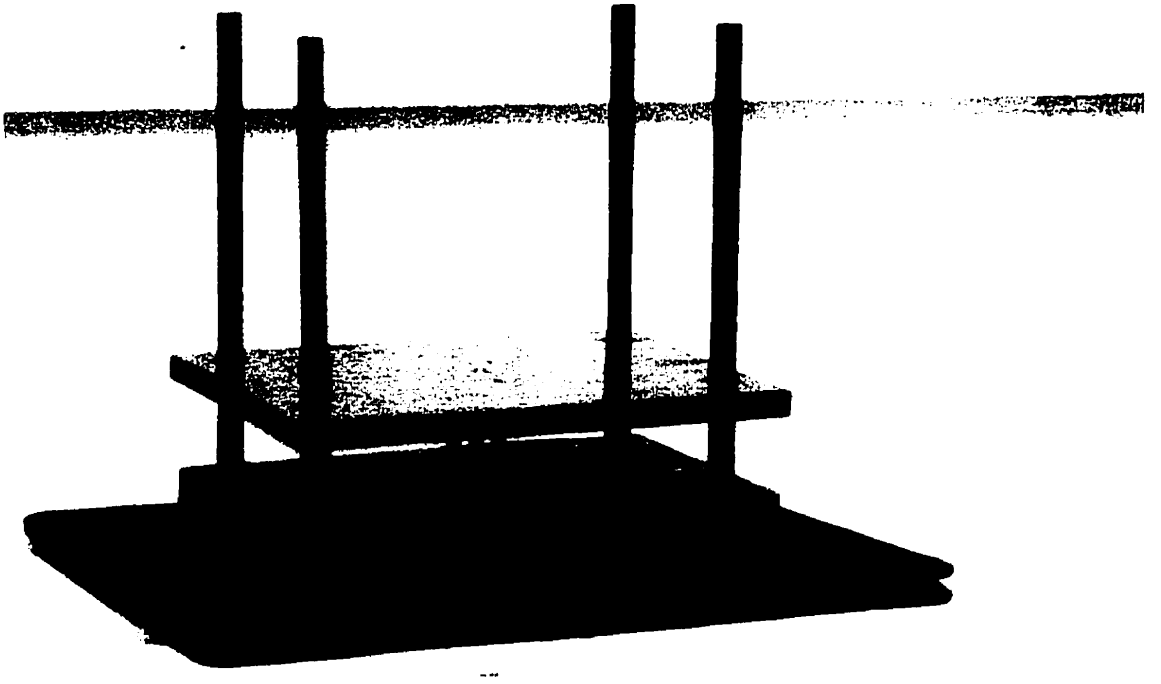

Figure 4.6 Water Absorption under Load Setup

The apparatus was made out of steel. The clear span in the specimen slot was 160mm. The setup was coated with an anti-rust paint to provide some protection against corrosion of the steel in the water environment. Grease was applied to the guiding rods to minimize the friction between the loading plates and the rods. This ensured that the full transfer of load to the specimens took place. When needed, weight was added to the loading plates to satisfy the 25% ultimate capacity load requirement.

The specimens were initially conditioned as described in Section 4.2. They were then placed in the specimen slots of the setups while separating the web beams from the flange beams as required by the different test conditions. Once the specimens were in place, the loading plate was positioned while ensuring that the loading noses are perfectly level and perpendicular to the specimens longitudinal direction. The loading plate had three separate loading noses, for each specimen in the slot, that could be adjusted in terms of height and angle. The setups were then placed in two strong plastic containers, one for room temperature and the other for 70°C experiments. Water was poured into the container to a level above the loading noses but below the base of the loading plate. For the test at 70°C, the water added was preheated to 70°C. Readings of water absorption were performed in the same way as was done for the water absorption without load.

4.6 TENSILE TESTS FOR MECHANICAL PROPERTIES

Tensile tests were performed to evaluate the tensile properties of the composite materials in different environments at different ageing stages. This evaluation examines the effect of environmental exposure on the ultimate tensile strength and the tensile modulus of the composite.

The reference tensile tests were conducted on the composites as received at room temperature and in dry condition. Five tests were averaged for each web and flange. For the aged specimens, each test was performed with three specimens for typical exposure condition. All tensile specimens were cut in the longitudinal direction of the sheet pile and the dog-bone shape was machined according to the ASTM Standard D 638.

The tensile tests of aged specimens were conducted only for the absorption in tap water at both 23°C and 70°C. The specimens were immersed in water at the same time as the other specimens for absorption tests.

The test was performed using the MTS machine, with a loading rate of 1.75 mm/min. An extensiometer with a gage length of 25.4 mm was used to measure the elongation and the strain. Figure 4.7 shows the set up for the tensile test. The test procedure was as following: the coupons were removed from the water, surface-dried, weighed to find the percentage of water absorption, and tested immediately as wet sample, to simulate the field condition. For coupons immersed in water at 70°C, the mass loss was corrected in the same day of tensile tests.

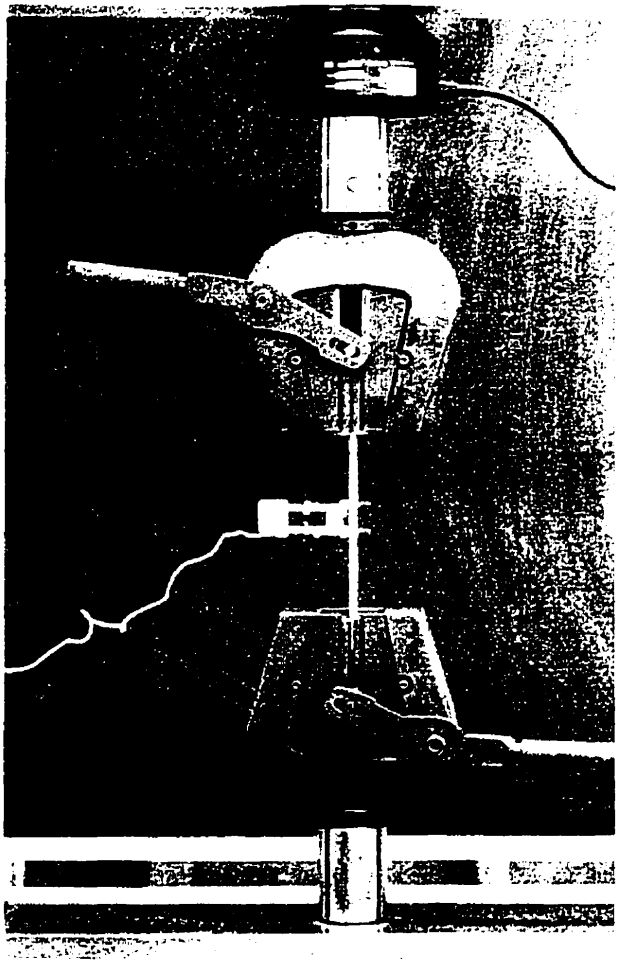

Figure 4.7 Tensile Strength Test Setup

4.7 FREEZE/THAW TEST

The specimens used for the freeze/thaw test were originally immersed in tap water at 70°C in an attempt to achieve saturation. The dog-bone specimens were machined according to the ASTM Standard D 638, and would be used later for tensile tests to investigate the freeze/thaw resistance of the saturated composites. Six specimens of each web and flange were used in the freeze/thaw test.

With the mass loss corrected and the point of saturation on absorption curves determined, the specimens were cooled down in water at 23°C and then placed in the freeze/thaw chamber as shown in Figure 4.8.

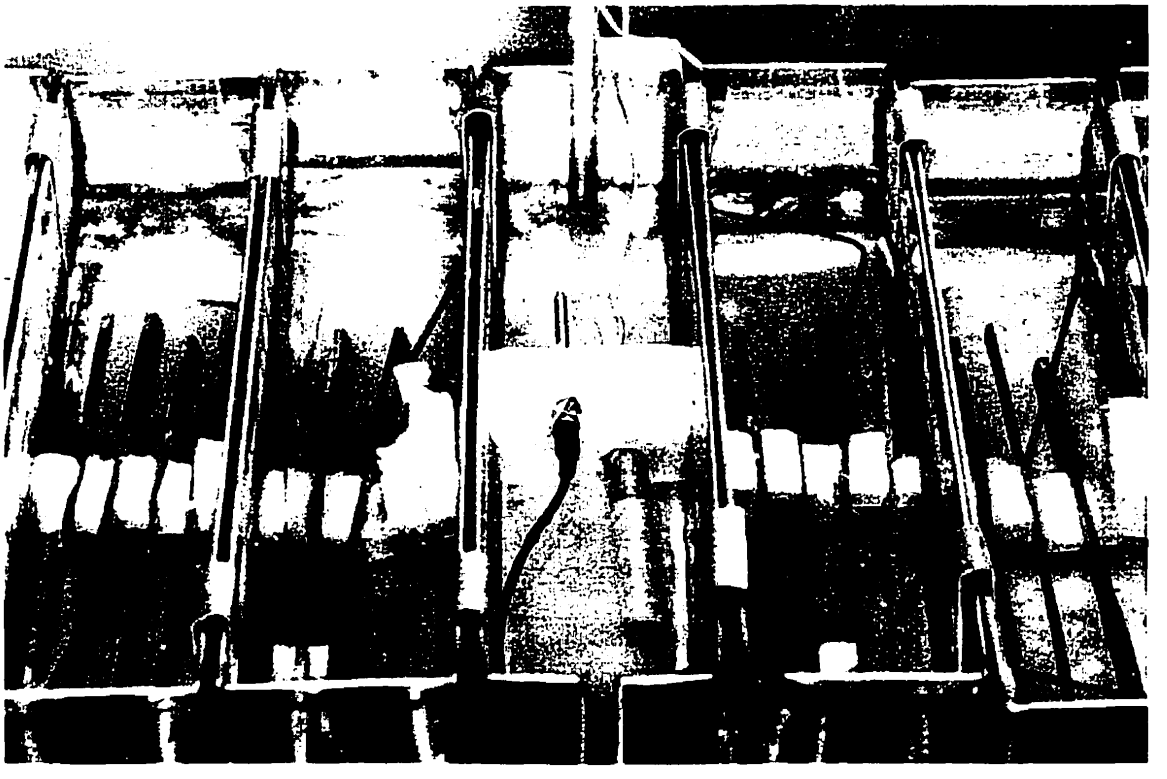

Figure 4.8 Freeze/Thaw Chamber Setup

The freeze/thaw test was performed according to the ASTM Standard C 666, with a freeze/thaw cycle from 4.4°C to -17.8°C followed by a hold at -17.8°C and a ramp up to 4.4°C followed by a hold. The cycle rate was about 2-3 hours per cycle. Since polymeric materials usually have better resistance to freeze/thaw damage than concrete material, the performance evaluation by the tensile test were performed for 310 and 564 cycles. In each test, three specimens were tested and averaged. The samples were also tested wet.

4.8 SPECIMEN DESIGNATION

The specimens were given names according to the exposure conditions and the type of test that was performed.

For the water absorption tests, the specimens have the designation in the form T23F. The first letter refers to the liquid environment: T for tap water, S for salted water and D for distilled water. The middle number refers to the test temperature: 23, 40, 70 or 100°C. The last letter refers to the type of specimen: F for the flange and W for the web. The specimens in the water absorption test under 3-point bending load have an additional "B" at the end. T70WB would denote a web specimen used in tap water at 70°C under 3-point bending. Whenever the small letter "u" is placed at the end of the specimen's name, it refers to an uncoated specimen. Otherwise, they are all edge-coated by epoxy.

Chapter 5

Absorption Theory

5.1 THEORY

Moisture absorption of a polymeric material is described as the process of the diffusion that involves migration of the small water molecules into the pre-existing or dynamically formed spaces between polymer chains. [Crank 1975]. This process is governed by Fick's second law of diffusion (Equation 5.1).

$$\frac{\partial c}{\partial t} = D_z \frac{\partial^2 c}{\partial z^2} \tag{5.1}$$

where

c = moisture concentration in composite

t = time

D_z = mass diffusivity along z direction

The distribution of moisture through the thickness of a thin composite plate, which is exposed to an environment of moisture concentration c_a, is shown in Figure 5.1

Equation 5.1 is solved subject to the following initial and boundary conditions:

$$c = c_i \qquad 0 < z < h \qquad t \leq 0$$

$$c = c_m \qquad z = 0 \; ; \; z = h \qquad t > 0$$

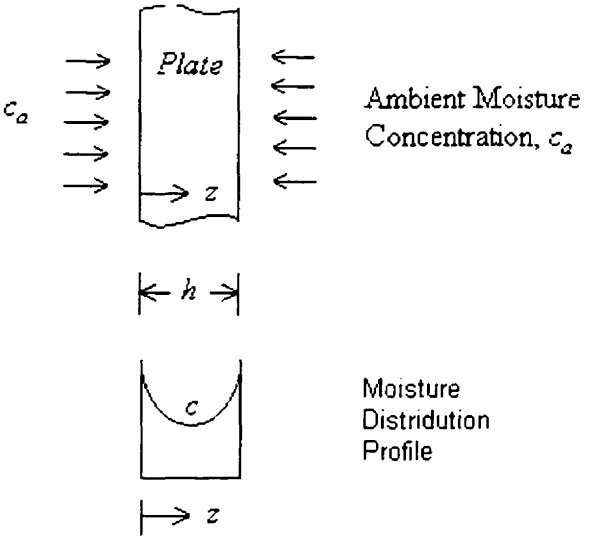

Figure 5.1 Moisture Distribution through a Plate.

The solution to the differential equation is given by equation 5.2 [Gibson 1994, Cai et al., 1994, Shen et al., 1976].

$$\frac{c - c_i}{c_m - c_i} = 1 - \frac{4}{\pi}\sum_{j=0}^{r}\frac{1}{(2j+1)}\sin\frac{(2j+1)\pi z}{h}\exp\left[-\frac{(2j+1)^2\pi^2 D_z t}{h^2}\right] \qquad \textbf{(5.2)}$$

where

c_i = the initial moisture concentration

c_m = the maximum moisture concentration at the surface of the material. (c_m is related to moisture content of the environment, c_a (Figure 5.1))

h = normal thickness, in the direction of diffusion

The total moisture concentration averaged over the thickness, $\bar{c}$, is given by:

$$\bar{c} = \frac{1}{h}\int_0^h c(z,t)dz = (c_m - c_i)\left[1 - \frac{8}{\pi^2}\sum_{j=0}^{r}\frac{\exp\left[-(2j+1)^2\pi^2(D_z t/h^2)\right]}{(2j+1)^2}\right] + c_i \qquad \textbf{(5.3)}$$

Since the weight percentage of moisture absorbed, $\%M$, is the quantity that is normally measured, and the average concentration, c, is linearly related to $\%M$, equation 5.3 can be written as:

$$G = \frac{\%M - \%M_i}{\%M_m - \%M_i} = 1 - \frac{8}{\pi^2}\sum_{j=0}^{\infty}\frac{\exp\left[-(2j+1)^2\pi^2(D_z t/h^2)\right]}{(2j+1)^2} \qquad \textbf{(5.4)}$$

where

$\%M$ = weight percentage of moisture absorbed, %

$\%M_m$ = maximum weight percentage of moisture absorbed (at saturation), %

$\%M_i$ = initial weight percentage of moisture in the material, %

G = moisture weight gain as a function of time

The diffusion process governed by equation 5.4 is called Fickian diffusion. If the initial weight percentage of moisture in the material is zero ($\%M_i = 0$), i.e. a dry material, equation 5.4 can be written as:

$$\%M_{t,F} = \%M_{\infty,F}\left[1 - \frac{8}{\pi^2}\sum_{n=0}^{\infty}\frac{1}{(2n+1)}\exp\left[-\frac{D_z t}{h^2}\pi^2(2n+1)^2\right]\right] \qquad \textbf{(5.5)}$$

where

$\%M_{t,F}$ = Fickian absorption at time t

$\%M_{\infty,F}$ = maximum Fickian absorption at saturation, %

Equation 5.5 is plotted in Figure 5.2 with percent absorption vs. $(\text{days})^{1/2}$. Obviously, there exists a plateau at which the absorption curve becomes horizontal and saturation is achieved.

In many cases, absorption of material does not follow the Fickian equation. The absorption curves do not have an apparent plateau. Instead, a continuous increase in absorption is observed after the Fickian saturation is reached. This happens especially when the absorbed moisture causes swelling of the polymer [Berens and Hopfenberg, 1977]. Swelling of the polymer involves larger scale segmental motion resulting in an increased distance of separation between the polymer molecules. This process is called relaxation. The relaxation process due to absorption is described by the following differential equation [Berens et al., 1977]:

$$\frac{d\%M_{t,R}}{dt} = k(\%M_{\infty,R} - \%M_{t,R}) \qquad \textbf{(5.6)}$$

where

$\%M_{t,R}$ = absorption due to relaxation at time t, %

k = relaxation rate constant

$\%M_{\infty,R}$ = maximum absorption due to relaxation, %

Integration of the equation 5.6 leads to the following solution:

$$\%M_{t,R} = \%M_{\infty,R}[1 - \exp(-kt)] \qquad \textbf{(5.7)}$$

The plot of equation 5.7 is also shown in Figure 5.2.

Berens and Hopfenberg [1977] proposed an absorption model for glassy polymers as the linear superposition of independent contributions from Fickian diffusion and polymeric relaxation. The total amount of absorption at the time t, $\%M_t$, may be expressed as:

$$\%M_t = \%M_{t,F} + \%M_{t,R} \qquad \textbf{(5.8)}$$

Substituting equations 5.5 and 5.7 into equation 5.8 gives the general equation governing the absorption process involving a combination of Fickian diffusion and polymeric relaxation.

$$\%M_t = \%M_{\infty,F}\left[1 - \frac{8}{\pi^2}\sum_{n=0}^{\infty}\frac{1}{(2n+1)}\exp\left[-\frac{D_F t}{h^2}\pi^2(2n+1)^2\right]\right] + \%M_{\infty,R}\left[1-\exp(-kt)\right] \quad \textbf{(5.9)}$$

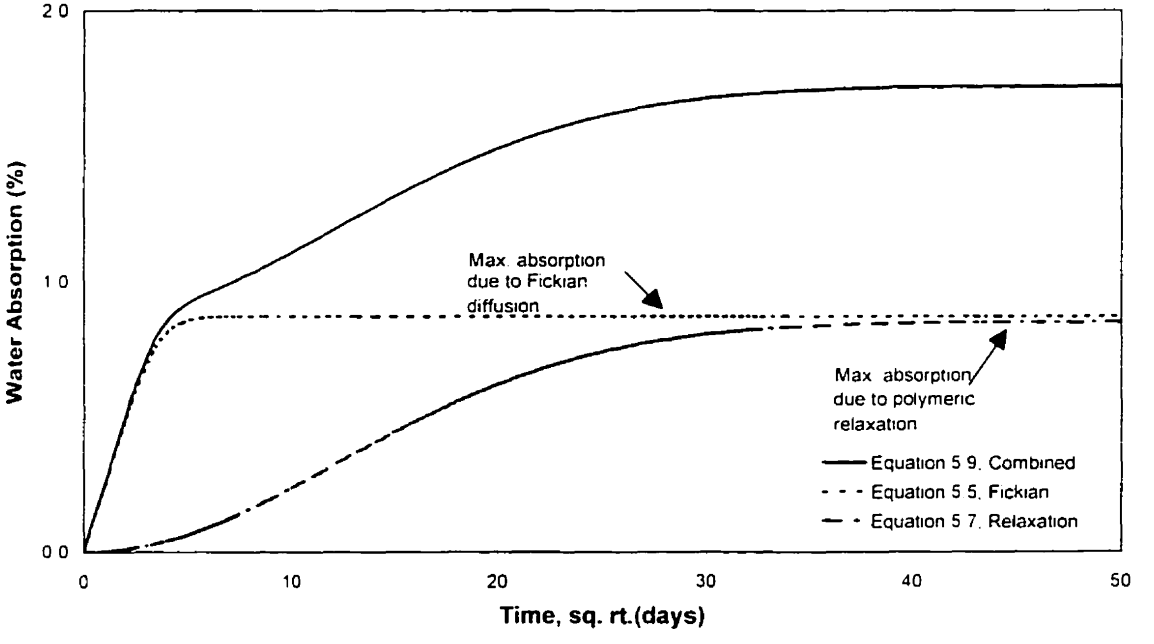

Figure 5.2 Theoretical Absorption Curves Due to Fickian Diffusion and Polymeric Relaxation

Equation 5.9 is plotted in Figure 5.2 as linear superposition of equation 5.5 and 5.7. The linear portion of the total absorption is almost identical to that of Fickian absorption until the Fickian curve starts to bend over, indicating that effect of relaxation on the initial Fickian absorption is not significant. The second part of the combined absorption starts at about the maximum Fickian absorption, when the diffusion rate is substantially decreased and the contribution of the polymeric relaxation to the absorption

is increasing steadily. The final saturation at equilibrium, $\%M_s$ is represented by the sum of the maximum Fickian absorption, $\%M_{s,F}$, and the maximum relaxation absorption, $\%M_{s,R}$.

$$\%M_s = \%M_{s,F} + \%M_{s,R} \tag{5.10}$$

It is noted that the point at which the Fickian diffusion and the relaxation reach their maximum is a characteristic of the material. In Figure 5.2 they happened to be close to each other.

5.2 PREDICTION OF ABSORPTION BY CURVE FITTING

Equation 5.9 is used to perform the curve fitting of the experimental data corrected from the absorption tests. The purpose of the curve fitting is to develop an analytical equation to predict the long-term absorption performance of the composite based on a short-term experiment.

To use equation 5.9, the two parameters, the maximum Fickian absorption, $\%M_{s,F}$, and the maximum absorption due to relaxation, $\%M_{s,R}$, need to be determined first from the absorption tests. Based on the discussion of Figure 5.2, the maximum Fickian absorption is approximated by the linear proportional limit of the absorption data, at which point the curve starts to bend over. The overall water uptake at final saturation of the composite, $\%M_s$, is determined using the accelerated test at 70°C and 100°C. Since absorption at saturation of a composite is a material constant, $\%M_s$ obtained from accelerated tests can be therefore used in equation 5.10 to compute the maximum absorption due to relaxation, $\%M_{s,R}$. With the two parameters, $\%M_{s,F}$ and $\%M_{s,R}$, given, the curve fitting of the experimental data by equation 5.9 will determine the other two parameters, the diffusivity D_z and the relaxation rate, k.

It is noticed that the Fickian diffusion, as given by equation 5.5, is represented by a series. Only the first term of this series was used in the curve fitting. Equation 5.9 is thus simplified to:

$$\%M_t = \%M_{\infty,F}\left(1-\frac{8}{\pi^2}\exp\left(-\frac{D_z t}{h^2}\pi^2\right)\right)+\%M_{\infty,R}\left[1-\exp(-kt)\right], \quad \text{for } \frac{D_z t}{h^2} > 0.05 \quad \textbf{(5.11)}$$

The validity of the approximation is examined by plotting both equations 5.9 and 5.11 in Figure 5.3. With the same four parameters, equation 5.11 with only the first term is identical to equation 5.9 with a Fickian series when $\%M_t/\%M_{\infty,F} > 0.5$. It is equivalent to the condition when $D_z t/h^2 \geq 0.05$. At early age Fickian absorption when $\%M_t/\%M_{\infty,F} < 0.5$ or $D_z t/h^2 < 0.05$, equation 5.11 is different from equation 5.9. Since the curve fitting is to predict long-term absorption behavior, equation 5.11 seems suitable for the purpose, but offers great ease in mathematical operation. Then, Equation 5.9 is used to plot the modeled curves, as the diffusivity and saturation moistures remain constant.

When $\%M_t/\%M_{\infty,F} < 0.5$ or $D_z t/h^2 < 0.05$, the linear portion of the absorption curve can be modeled by the following equation:

$$\%M_{t,F} = 4\%M_{\infty,F}\sqrt{\frac{D_z t}{h^2\pi}} \quad \text{. For } \frac{D_z t}{h^2} < 0.05 \qquad \textbf{(5.12)}$$

Equation 5.12 is also plotted in Figure 5.3 with $\%M_{t,F}$ vs. $(\text{days})^{1/2}$, it is a straight line. By adopting the same parameters, $\%M_{\infty,F}$ and D_z, as used in equation 5.9, the straight line overlaps on the linear portion of the plot of the absorption equation 5.9. This implies that the initial Fickian absorption behavior can be represented by equation 5.12.

As commonly used in Fickian absorption analysis, equation 5.12 can be used to estimate the diffusivity, D_z, of the material. Since the slope of the straight line by equation 5.12 in Figure 5.3 can be measured experimentally. The following equation determines the diffusivity, D_z, of the material in units of $(\text{time})^{-1/2}$:

$$Slope = \frac{\%M_{t,I}}{\sqrt{t}} = 4\%M_{\infty,F}\sqrt{\frac{D_z}{h^2\pi}} \cdot (\text{time})^{-1/2} \qquad \textbf{(5.13)}$$

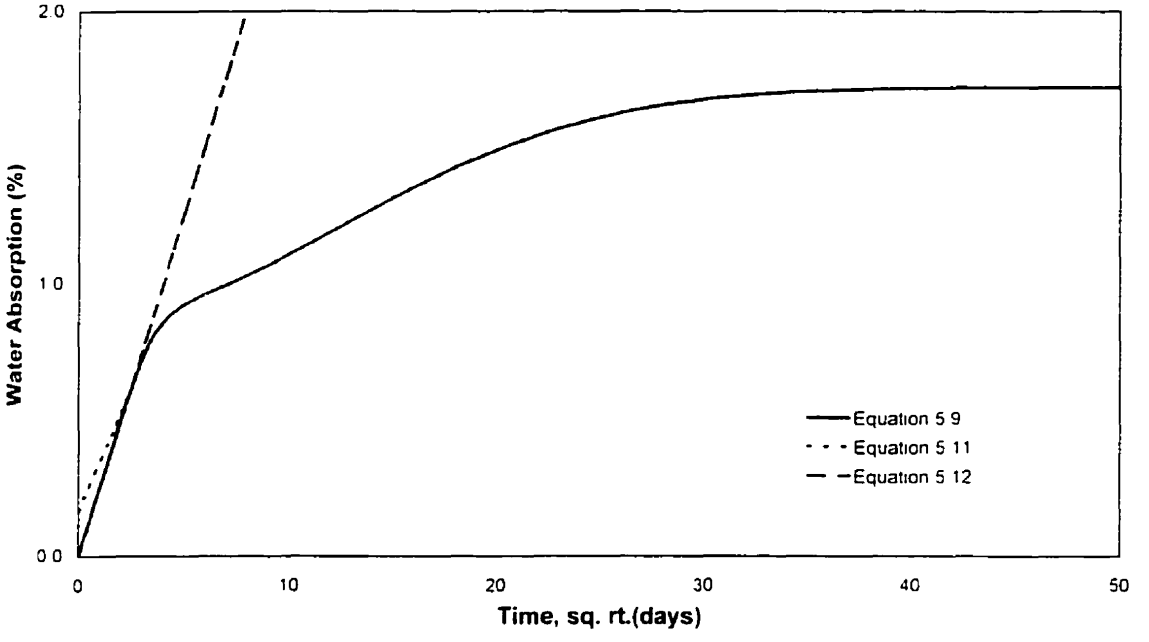

Figure 5.3 Theoretical Curves of Absorption Model

The parameters used to plot the three curves shown in Figure 5.3 are the following:

D_z = 4.2×10^{-6} mm^2/s

h = 4.699 mm

k = 3.8×10^{-8}/s

$\%M_{\infty,F}$ = 0.87 %

$\%M_{\infty,R}$ = 0.85 %

Chapter 6

Experimental Results

6.1 WATER ABSORPTION TESTS

6.1.1 Absorption Test in Tap and Salted Waters at 23°C, 40°C and 70°C

The water absorption tests for the flange and the web were performed at different temperatures in tap water and in salted water. The purpose of this study was to examine the durability of composite in water at ambient temperature by focusing on tap water at the room temperature. High temperature was used to accelerate the absorption process to achieve saturation in a short time period.

The results obtained from the tap and salted water absorption at 23°C are shown in Figure 6.1. The absorption data reported herein are collected up to 260 days, although the tests are still running. Four sets of data are plotted together, with flanges or webs immersed in either tap water (T23F, T23W) or salted water (S23F, S23W). It was observed that percentage absorption in tap water was higher than that in salted water for both flange and web, although the initial absorption rates, represented by the slope of the linear portion, were very close for the same exposure condition. This implies that absorption of composite in low concentration tap water was more severe than that in high concentration salted water. Therefore, the study of absorption in tap water was more representative of the different environments.

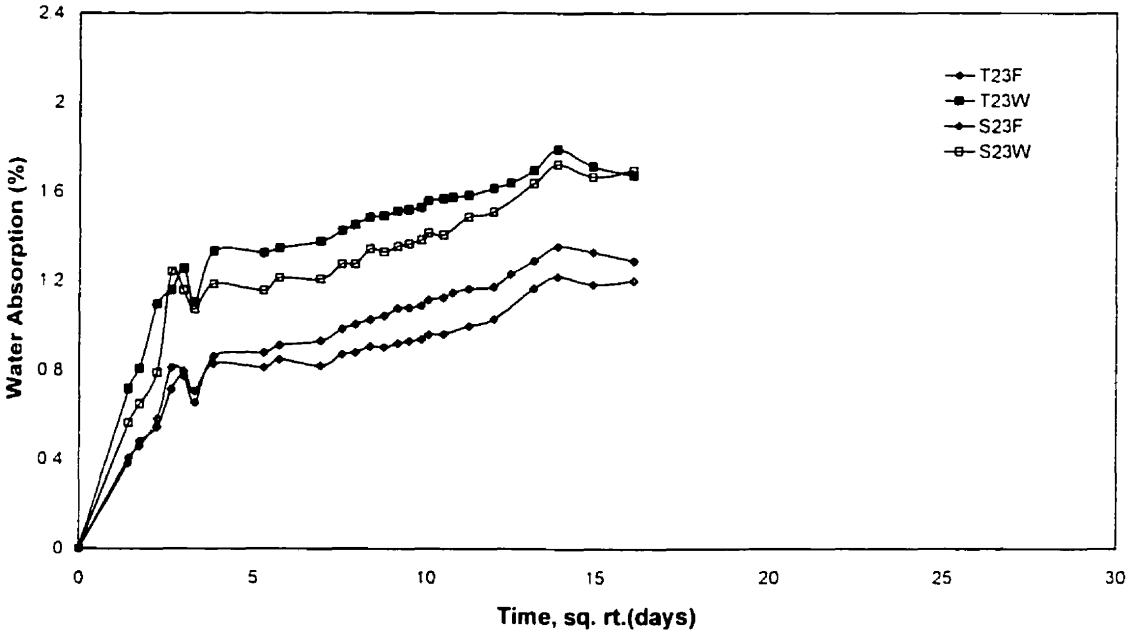

Figure 6.1 Absorption Curves in Tap and Salted Waters at 23°C

It was also observed in Figure 6.1 that the web exhibited higher percentages of water absorption compared with the flange in both tap water and salted water exposure conditions. This could be attributed to two composite parameters, the thickness and the fiber volume ratio. The web had a thickness of 3.2 mm, while the flange had a thickness of 4.7 mm. Thin specimens usually absorbed more water and at a faster rate than the thick ones. This was represented by the steeper slope and the higher percent absorption value for the web (T23W, S23W) in Figure 6.1. The low fiber volume ratio or higher resin ratio in web specimen (see Table 4.3) also contributed to the higher absorption.

It was interesting to notice that, up to 260 days in water at 23°C, the absorption curves were still ascending, and no sign of saturation was observed. The non-Fickian behavior was apparent. The increase of water absorption after the linear proportional limit was likely due to the polymeric relaxation.

Absorption curves for tap water and salted water at 40°C are presented in Figure 6.2. The data were collected up to 137 days. Since a temperature of 40°C is not high enough, the non-Fickian absorption resembled that observed at 23°C.

Similar trends observed at 23°C were seen here. The percentage of water absorbed in tap water was higher than that in salted water. But unlike in the test at 23°C, the trend was maintained from the start of the test. Here again the web displays higher moisture absorption than the flange. Looking at the initial slopes of the absorption curves, the tap water condition presented slightly higher slopes than the salted water condition.

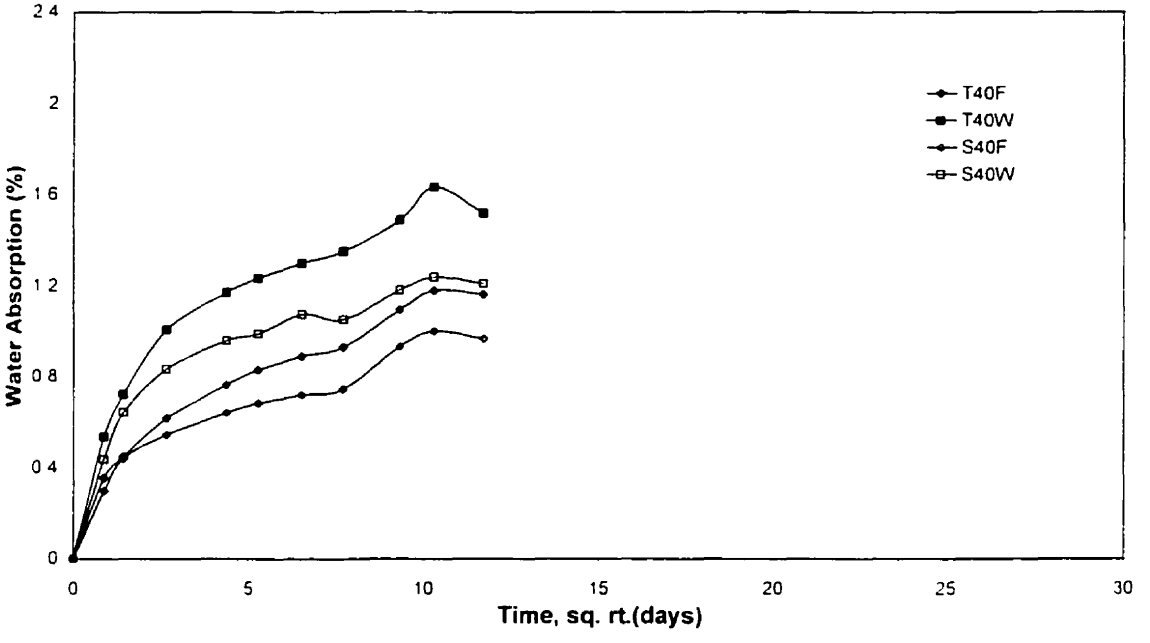

Figure 6.2 Absorption Curves in Tap and Salted Waters at 40°C

The behavior of the absorption of the same composite at 70°C was quite different from what had been observed at 23°C and 40°C. Figure 6.3 shows the absorption curves at 70°C.

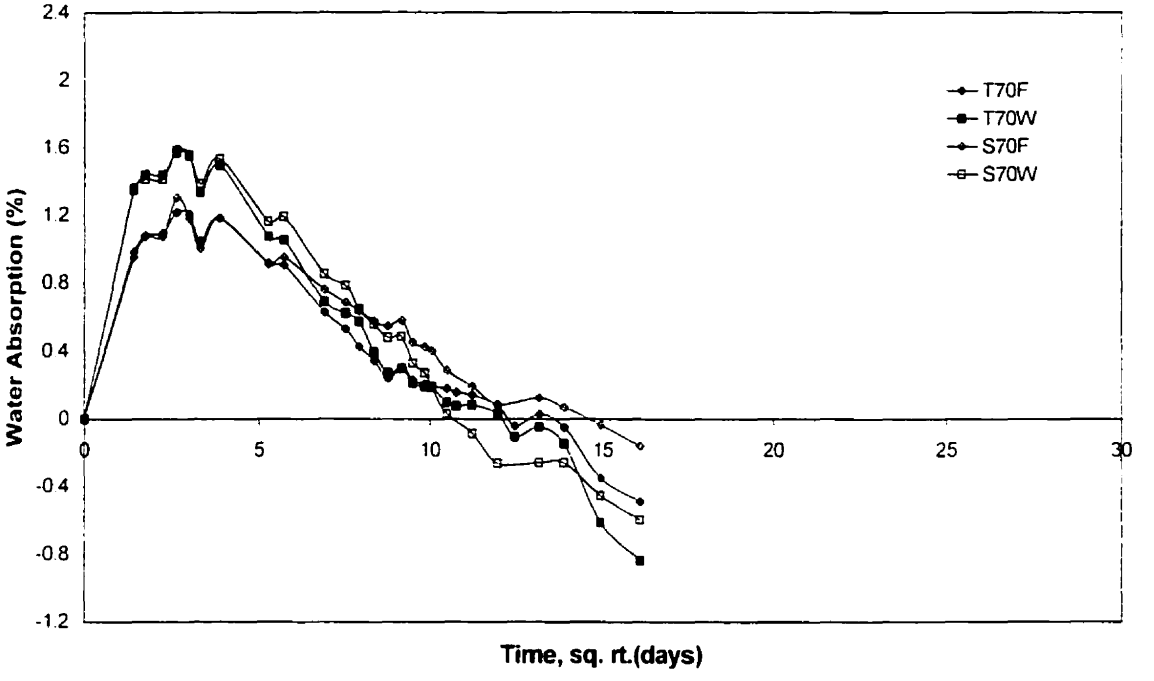

Figure 6.3 Absorption Curves in Tap and Salted Waters at 70°C

The results indicate that there was initially an increase in the calculated percentage water absorbed, followed by a steady decrease in the values. This continued further to a point where the percentage of water absorbed was negative. It indicated that the specimens aged in water at 70°C after a certain time period weighed less than their respective initial conditioned masses. This behavior was observed in both the web and the flange, and in both tap and salted waters (Figure 6.3). For the same type of specimens, either the flange or the web, the curves for tap water and salted water were very close to each other. This suggested that the process that took place was more temperature dependent than solution dependent. It was concluded that significant mass loss occurred in this polyester composite aged in water at 70°C. Similar phenomenon was observed by other researchers with different material systems.

To understand the cause of the mass loss, the effect of epoxy coatings along the specimen edge were first examined by comparing the absorption curves with those

obtained with uncoated specimens. Figure 6.4 shows the absorption curves of the coated versus uncoated web specimens in tap water at 70°C.

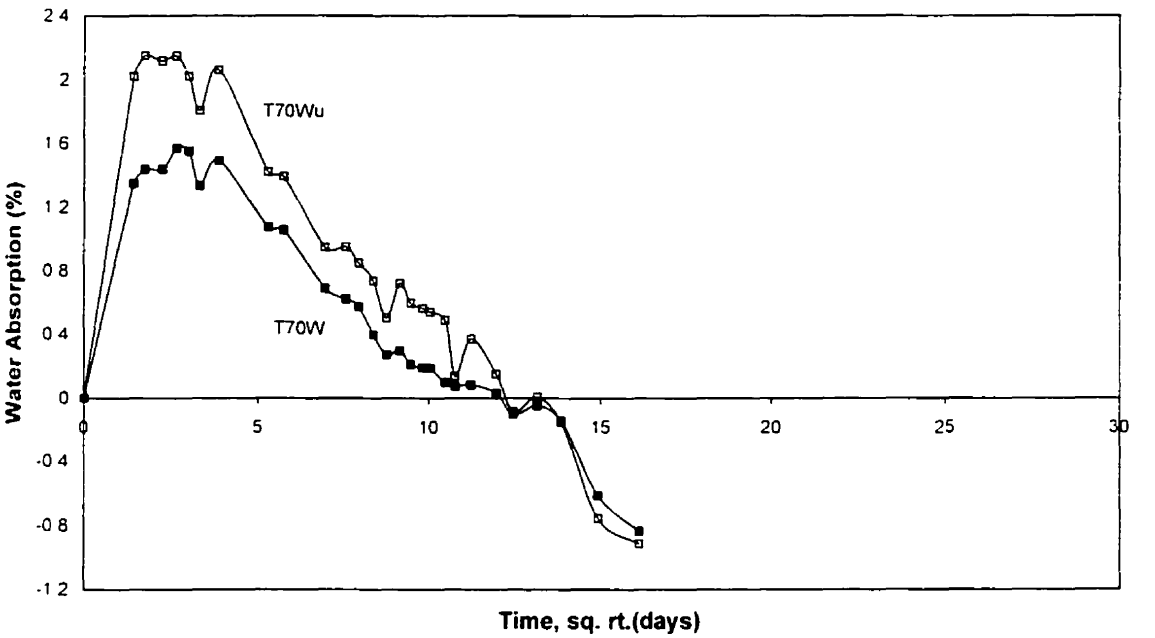

Figure 6.4 Absorption Curves in Tap Water of Coated and Uncoated Web Specimens at 70°C

The uncoated web (T70Wu) also experienced similar mass loss, as did the coated specimen (T70W). The two curves showed the rate of mass loss was very similar in both coated and uncoated specimens with the latter displaying a slightly faster rate. As was expected, the uncoated web specimens had higher percentage of water absorption than the coated web. This discrepancy was probably due to the condition of the edges of the specimens. The uncoated edges allowed for increased moisture ingress at a given time compared to the sealed edges, leading to higher water absorption. This general trend was also observed in tap water at 23°C and 40°C as shown in Figure 6.5 and 6.6. Salted water conditions also exhibited the same trend.

There was no significant mass loss occurring in absorption specimens at 23°C and 40°C. In order to correlate the accelerated tests at 70°C to that at 23°C, it is necessary to correct the mass loss and determine the true water absorption at a certain time.

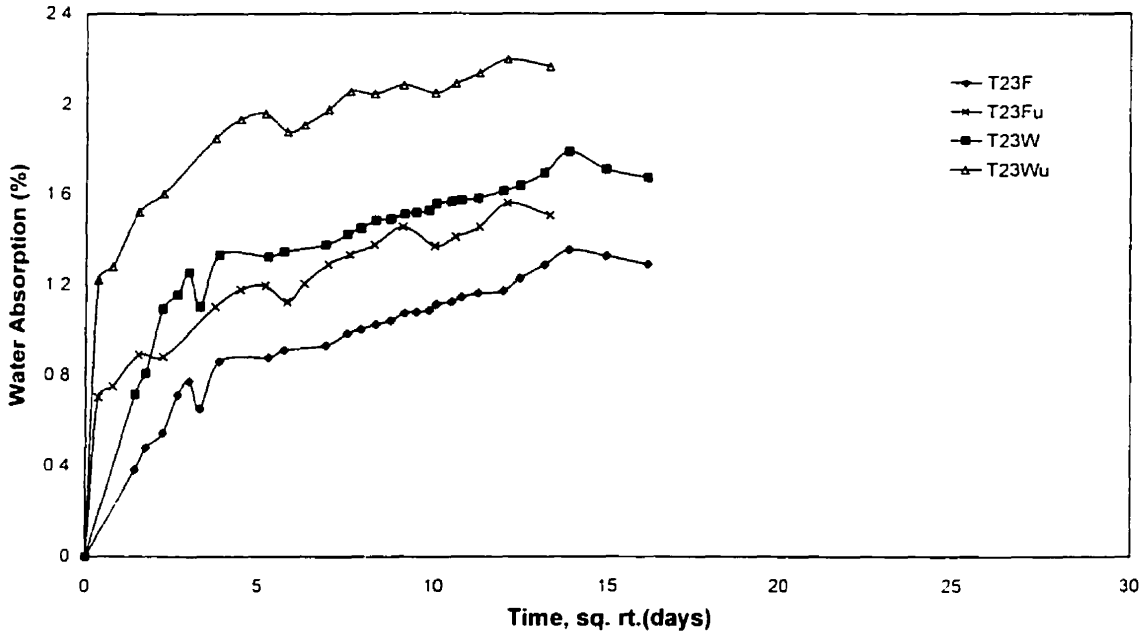

Figure 6.5 Absorption Curves in Tap Water of Coated and Uncoated Specimens at 23°C

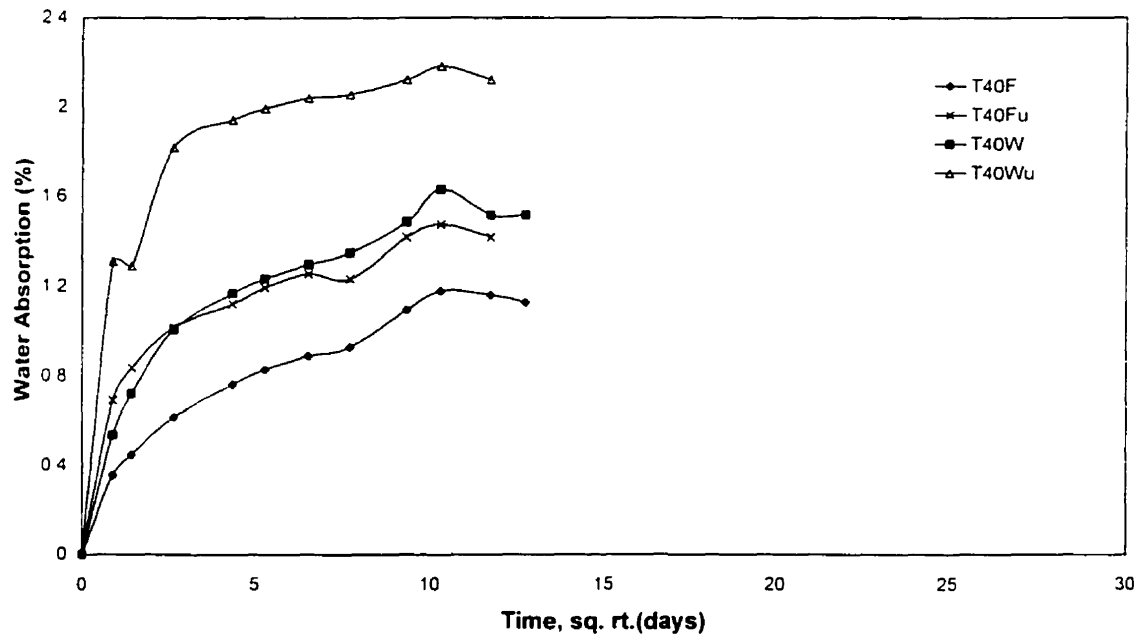

Figure 6.6 Absorption Curves in Tap Water of Coated and Uncoated Specimens at 40°C

6.1.2 Mass Loss Correction of Tap Water absorption at 70°C

Mass loss correction for the composite flange and web aged in tap water at 70°C was carried out only in tap water, because tap water proved to be more aggressive than the salted water in water absorption of the composite. The ASTM Standard D 570 provides a way to adjust the percentage of water absorbed for the mass loss, to determine the true water absorption. It is expressed by equation 4.3. The true absorption is equal to the percentage of absorption minus the percentage of mass loss, if percent mass loss is always negative. Mass loss corrections of specimens for absorption were performed at 28, 107, 192 and 260 days to coincide with the time when tension tests were performed on the aged specimens. In this way, the change in mechanical properties could be correlated to the true percentage of water absorbed. The results obtained from this test are shown in Table 6.1. Each reading was an average of three readings. The mean mass loss at 70°C ($\%M_{Loss}$) and the corrected absorption ($\%M_c$) are also plotted together with the absorption curves at 70°C in Figure 6.7.

Table 6.1 Mass Loss Corrected for Specimens in Water Absorption Test at 70°C

Aged Specimen	$\%M$	$\%M_{Loss}$	$\%M_C$
T70F			
28 Days	0.92	-0.23	1.15
107 Days	0.37	-1.50	1.87
192 Days	-0.08	-1.72	1.64
260 Days	-0.67	-2.33	1.66
T70W			
28 Days	1.15	-0.65	1.80
107 Days	0.30	-2.77	3.07
192 Days	-0.05	-3.16	3.11
260 Days	-0.99	-4.10	3.11

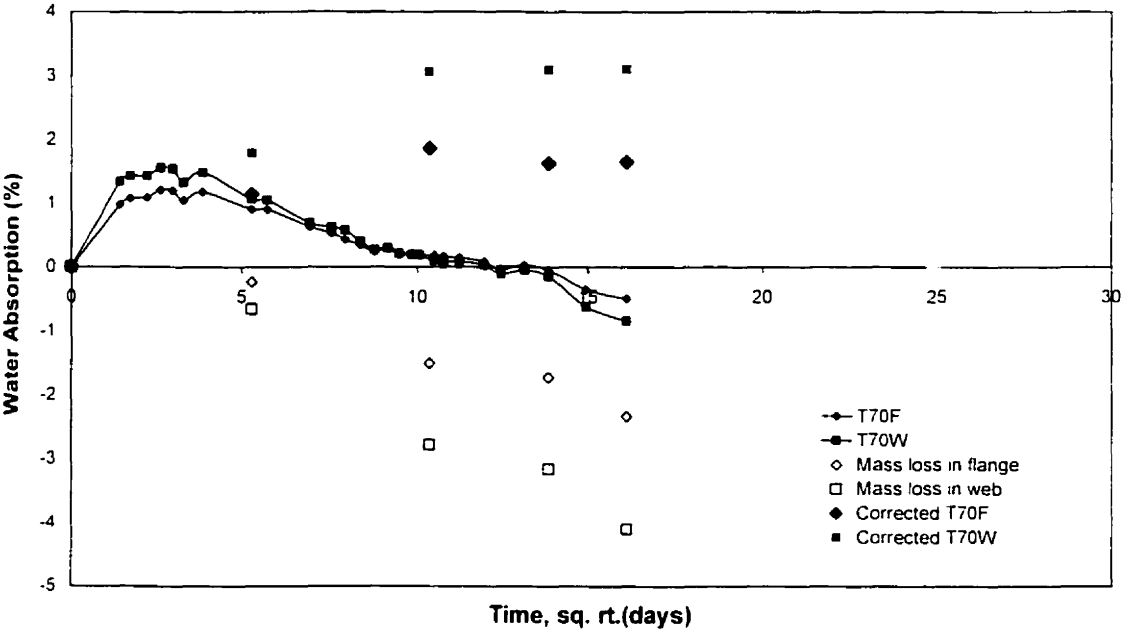

Figure 6.7 Mass Loss Correction for Tap Water Absorption at 70°C

The web still displayed a higher absorption than the flange after the correction. Since the correction was made only at 4 days when the tension tests were scheduled, the points representing the corrected absorption could not be connected to obtain an entirely corrected absorption curve. The purpose of this test was to investigate if the saturation was achieved. Figure 6.7 demonstrates that saturation seems to have been reached at 3.11% for the web and 1.72% for the flange. 1.72% is the average of the absorption readings of the last tension test at 107, 192 and 260 days

In the water absorption tests at 23°C and 40°C, the apparent saturation was not reached. It seems possible to accelerate the test to saturation at 70°C. It is noted that the maximum water absorption at saturation, in a given water environment, is a material property, which is independent of the test temperature [Pritchard et al., 1987]. High temperature can shorten the time to reach saturation and increase the diffusion rate. However, it does not change the maximum absorption at saturation. Therefore, the maximum percentage of water absorbed should be the same for the same material at any test temperature. Evidently, the lower the test temperature the longer it will take to reach the point of saturation.

6.1.3 Boiling Water Absorption Test for Saturation

To further verify the percentage of water absorption at saturation, boiling water tests were conducted. It followed the ASTM Standard D 570 standard for 24-hour boiling water absorption test, with an extension to more than two weeks to examine the point of saturation and the maximum absorption for the given composite material. This would also be used to double check the values obtained from the test at 70°C in tap water. It should be pointed out that the test was done in the most severe environment: boiling distilled water at 100°C, with uncoated cut-edge specimens. Mass loss was observed again and correction was implemented accordingly. The results obtained are presented in Figures 6.8 and 6.9 for the flange and the web respectively. The tabulated results are shown in Appendix C.

The percentage mass loss of the web was higher than that of the flange. The saturation moisture absorption of the web was higher than that of the flange with a value of 1.74% for the former and 3.14% for the latter. These values are slightly different from the ones obtained at 70°C in tap water. The aggressive distilled water used in the test might be the cause for this discrepancy. Tap water and distilled water do not have exactly the same density or viscosity. Distilled water, which has a lower density and viscosity, may be able to penetrate pores of smaller size than tap water. Therefore the moisture saturation by distilled water would be higher than that by tap water and was observed here.

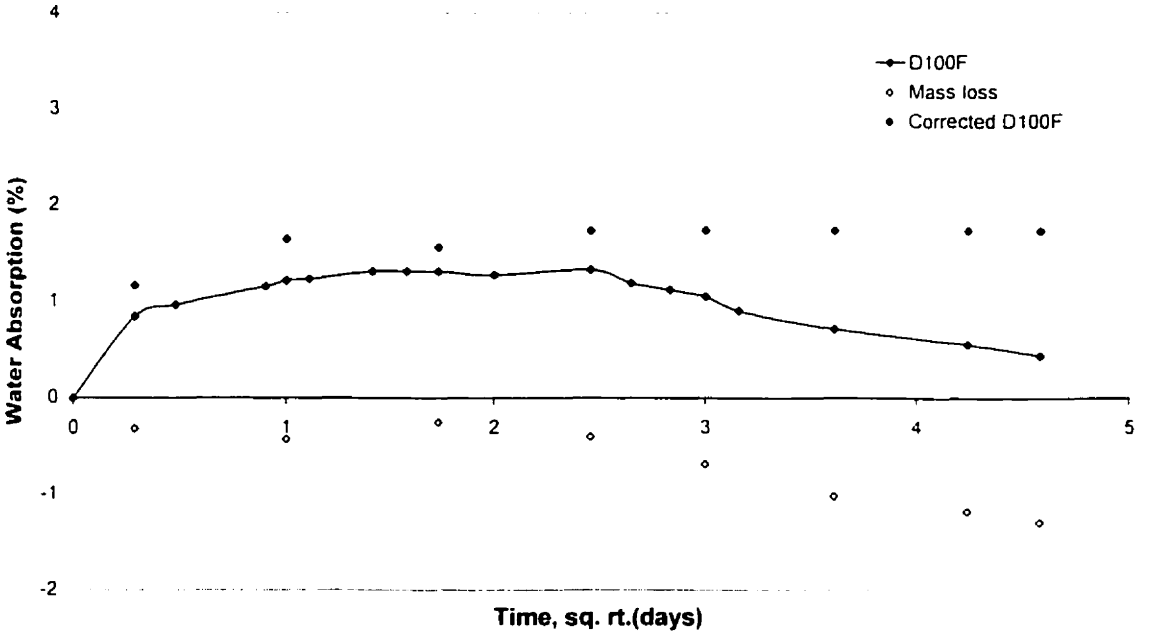

Figure 6.8 Boiling Distilled Water Absorption of Flange

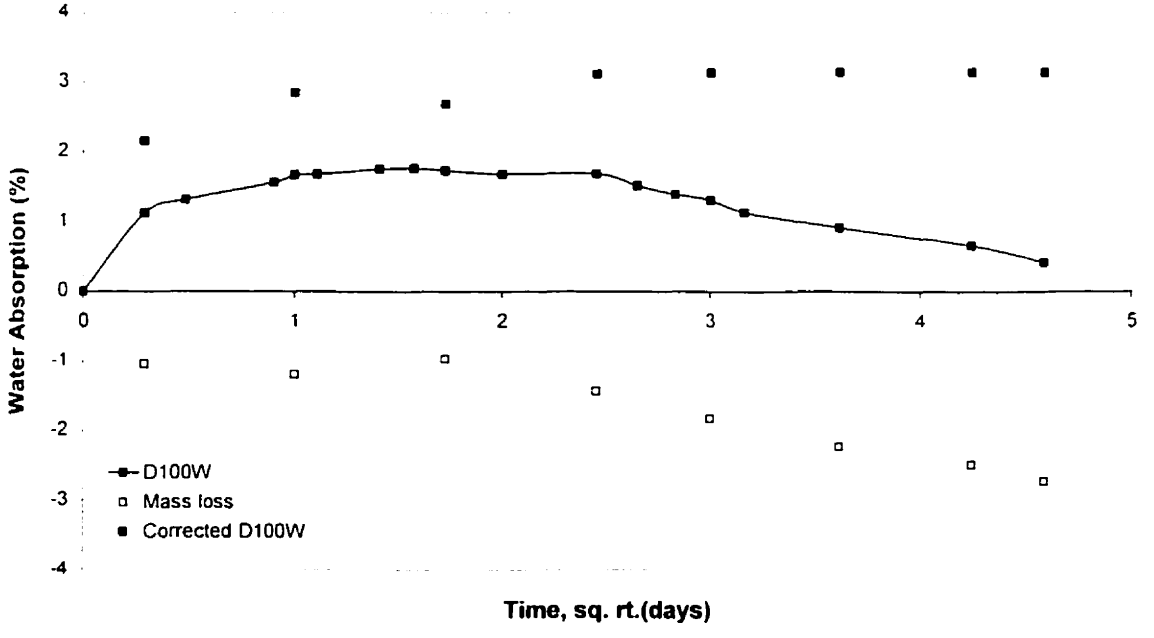

Figure 6.9 Boiling Distilled Water Absorption of Web

6.1.4 Water Absorption under Three-Point Flexural Load

The effect of three-point flexural action on absorption was studied through this test. The test was conducted at 23°C an 70°C in tap water alone. However mass loss correction at the high temperature was not performed, as numerous bending set-ups would have been required. The results obtained from the high temperature loaded absorption test were directly compared to the non-corrected water absorption results at 70°c in the unloaded condition.

A three-point flexural strength test was performed to evaluate the maximum flexural load and determine 25% of this value. Typical load-deflection curves for the flange and the web are shown in Figure 6.10 (See Appendix A for all curves). The load applied for the loaded absorption test was calculated as shown in Table 6.2.

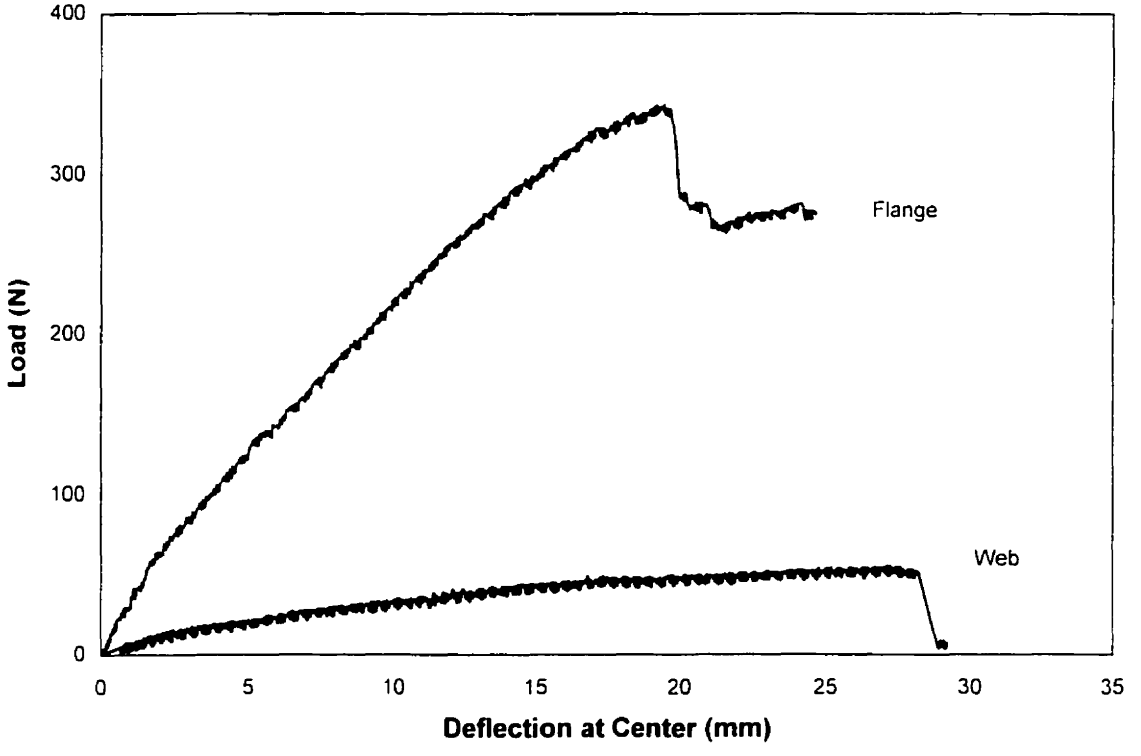

Figure 6.10 Load-Deflection Curves for Dry Composite Beams as Reference

Table 6.2 Loads Used in Loaded Absorption Tests

Specimen	Avg. Maximum Bending Load (kg)	25% Bending Load (kg)	Total Load for 3 Specimens (kg)
Flange	33.0 ± 9	8.2	24.7
Web	5.3 ± 13	1.3	4.0

Each setup used in loaded absorption tests contained 3 specimens of the same type, as was shown in Section 4.5. The load was applied to the specimens through the three loading noses. The weight of the loading plate was taken into account when applying the load. The loading plate in the setup for the web had a weight of 4.0 kg. The setup for the flange had a loading plate that weighed 7.1 kg. External circular weights were added to the loading plate in order to achieve a load of 24.7 kg.

Figures 6.11 and 6.12 show both the water absorption curves with and without the bending loads in tap water at 23°C and 70°C, respectively. For the absorption at 23°C, the specimens under three-point bending load displayed lower absorption than the corresponding unloaded specimens. Here again, the web had higher absorption values than the corresponding values for the flange. Visually, the initial slope of the unloaded specimen was slightly higher than that of the corresponding specimens under load.

At 70°C, the specimens under load did not show the dramatic display of mass loss observed in the unloaded specimens. Indeed, the curves of the water absorption under the load were horizontal at the time the unloaded specimens had undergone about 1% change in water absorption. It seemed that the loaded composites immersed in water did not absorb more than the unloaded. Instead, reduced absorption was observed in this test. It could have been due to the thinning of the pores under bending, in the same manner the surface of an elastic void is reduced when the boundary is stretched along a line.

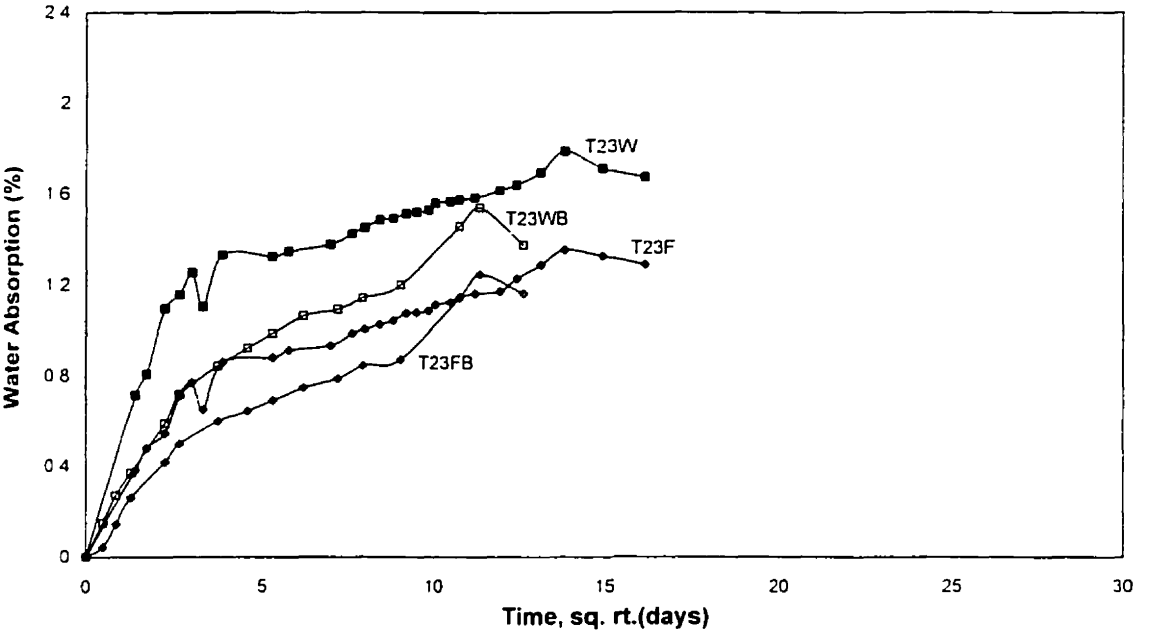

Figure 6.11 Tap Water Absorption under Load at 23°C

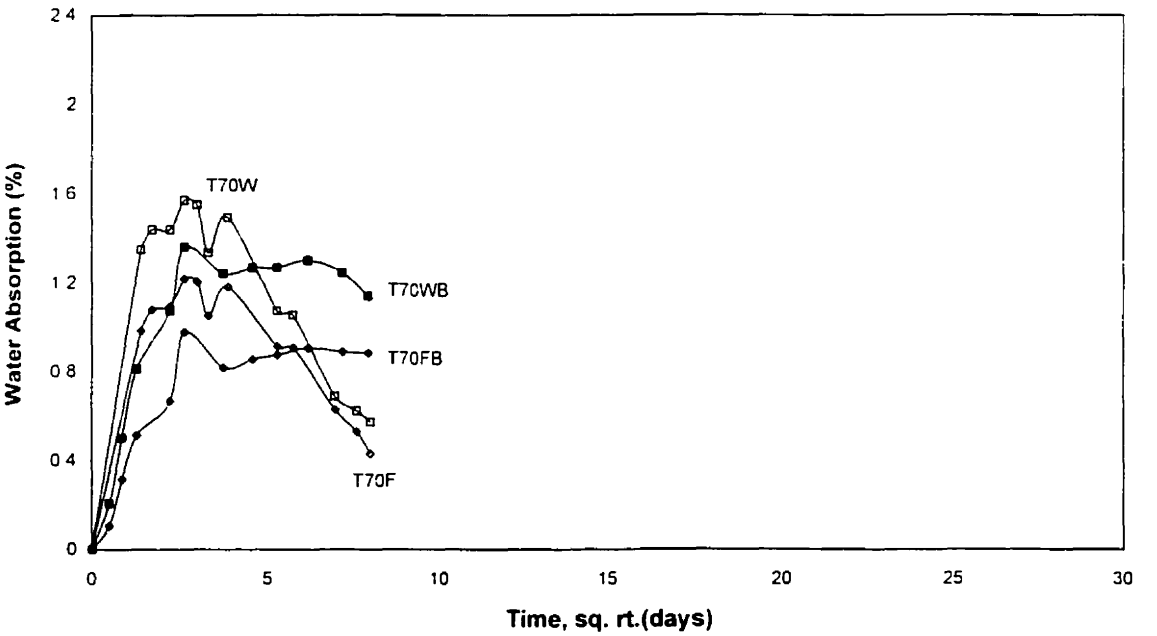

Figure 6.12 Tap Water Absorption under Load at 70°C

6.1.5 Comparison of Water Absorption Rate

The maximum absorption at saturation ($\%M_\infty$) and diffusivity (D_z) characterize the Fickian moisture absorption of a material. D_z reflects the absorption rate. In the solution of basic equation of Fick's law, the initial slope of the absorption curve, when %water absorbed is plotted against $(\text{time})^{1/2}$, follows the relationship given by equation 5.13. The slope calculated has units of $(\text{time})^{-1/2}$. For a given material and a given immersion solution, the values of $M_{\infty,F}$ and h are constants. This is irrespective of temperature. Therefore, the slope is directly proportional to $D_z^{1/2}$. The comparison of initial slope of absorption curves generates the same information on absorption rate as the comparison of diffusion coefficient does.

The flange and the web have different characteristics. The length and width of the flange and web specimens were the same. This means that the surface area of the specimen exposed to water was kept the same in all cases. But the web was thinner with a thickness of 3.176mm compare to the flange, which was 4.699mm-thick. Therefore, the two types of specimen did not have the same weight. Even if they were absorbing the same mass of water every time, the web would still have higher calculated water absorption and a steeper initial slope than the flange. This is because the web is thinner, therefore it has a lower conditioned mass, which reduces the denominator in equation 4.1. Moreover, the lower values of the percentage of water absorbed calculated for the flange would lead to a lower initial slope since the initial straight line passes through the origin. In order for the trend followed in the initial slopes to be representative of that of the diffusivity, the specimens to be compared should be of the same dimensions (length, width, thickness) and weight. Therefore, comparisons can only be made between different test conditions for a given type of specimen. The values of the slopes for the flange cannot be compared against those for the web for the reasons mentioned earlier. Table 6.3 lists the values of the initial slopes obtained for all of the test conditions.

Table 6.3 Initial Slopes of Absorption Curves. (10^{-4} $s^{-1/2}$)

Test Condition	Flange	Standard Deviation	Web	Standard Deviation
Tap water at 23° C Loaded	6.44	0.34	9.33	0.68
Tap water at 70° C Loaded	13.21	0.68	20.91	1.02
Tap water at 23° C	8.99	0.34	15.31	1.36
Tap water at 40° C	11.68	2.4	18.42	2.72
Tap water at 70° C	22.24	1.70	29.95	3.06
Salted water at 23° C	8.98	0.34	13.96	1.70
Salted water at 40° C	10.94	0.68	15.93	1.36
Salted water at 70° C	21.87	1.36	29.74	3.40
Thickness, mm	**4.699**		**3.176**	

In tap water and salted water, the higher the test temperature the steeper the initial slope, indicating a faster absorption. For the same immersion solution and same specimen, the increase in slope implies an increase in diffusion coefficient. For the different immersion solution, the values of the slopes in tap water were very close to those obtained in salted water. However, it does mean the diffusivity is also close, since the $\%M_{\infty,f}$ could be different in tap and salt water. The flexural load had the effect of reducing the initial slopes, therefore reducing the diffusivity. It is obvious that the water absorption by the web is faster than that by the flange, as is also observed that web absorbs more water than flange. This would be attributed to the fact that web is thinner and has higher resin content. A higher moisture diffusion rate does not necessarily imply a higher percent absorption.

6.1.6 ASTM Standard D 570 2-Hour and 24-Hour Water Absorption

Table 6.4 summarizes the results obtained for the 2-hour and 24-hour absorption tests of the specimens in distilled water, at room temperature and in boiling conditions. Often the water absorption of plastics and reinforced plastics are compared using the 2-hour and 24-hour distilled water absorption according to the ASTM Standard D 570. In

Reference, the 24 hr water absorption of isophthalic composites is in the range 0.05%-1.0% at ambient temperature [Peters 1998]

Table 6.4 2-Hour and 24-Hour Distilled Water Absorption

		Flange	Standard Deviation	Web	Standard Deviation
2 Hours, 23°C	$\%M$	**0.14**	0.01	**0.24**	0.01
24 Hours, 23°C	$\%M$	**0.29**	0.02	**0.44**	0.01
2 Hour, boiling	$\%M$	0.85	0.02	1.13	0.00
	$\%M_{Loss}$	-0.32	0.02	-1.03	0.04
	$\%M_c$	**1.12**	0.03	**2.16**	0.04
24 Hour, boiling	$\%M$	1.22	0.07	1.67	0.02
	$\%M_{Loss}$	-0.43	0.01	-1.18	0.05
	$\%M_c$	**1.65**	0.08	**2.85**	0.06

6.2 LOSS OF MECHANICAL PROPERTIES

Tensile tests were performed on specimens to determine the effect of water ageing on the tensile properties of the composite. Tests were performed only on samples aged in tap water at 28, 107, 192 and 260 days, and in boiling distilled water. All tests were performed wet except for the reference test, which was performed dry. The reference test was conducted on the dry material without ageing and in the as received condition. Figure 6.13 shows typical curves for the reference tensile test conducted on the flange and the web. The flange had a higher tensile strength with an average of 433 MPa. The web showed a low average tensile strength at 187 MPa. For the tensile modulus of elasticity, the flange had twice the value of the web with 29.9 GPa and 11.7 GPa, respectively. The results are summarized in Table 6.5 with deviation. Nevertheless, the specimens had more or less the same values of maximum tensile strain at failure (Figure

6.13). When the tensile curve displayed significant curvature, the modulus was calculated finding the slope of the linear fit to the first 60 % of the data points.

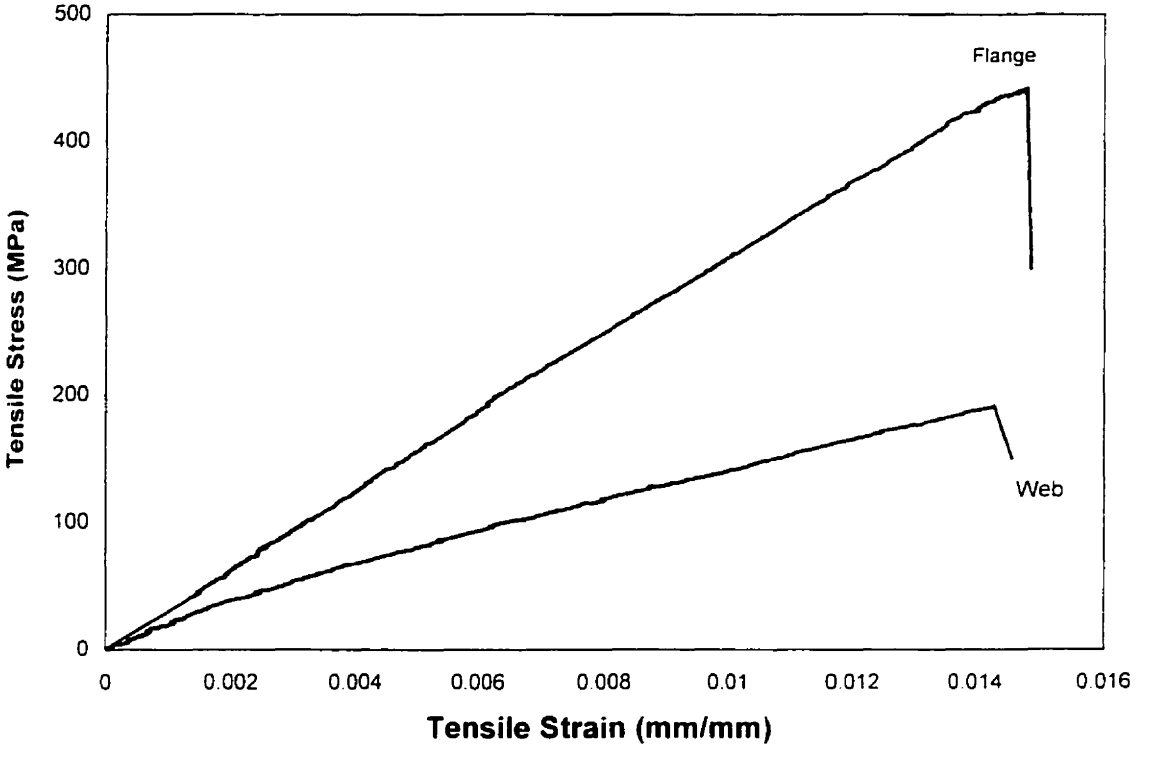

Figure 6.13 Tensile Stress-Strain Curves for Reference Dry Composite

Figures 6.14 and 6.15 show typical curves of the tension tests conducted on the flange and web specimens after immersed in tap water for certain periods of time. All the curves for the tension tests are in Appendix B. Figure 6.14, for the flange specimen, shows that there was a decrease in the maximum tensile strength over time. This process was more accelerated in the higher temperature condition. Despite that, the tensile modulus of elasticity was not affected, as all the curves are almost parallel. Similar trend was also observed for tensile tests performed on the web specimens (Figure 6.15).

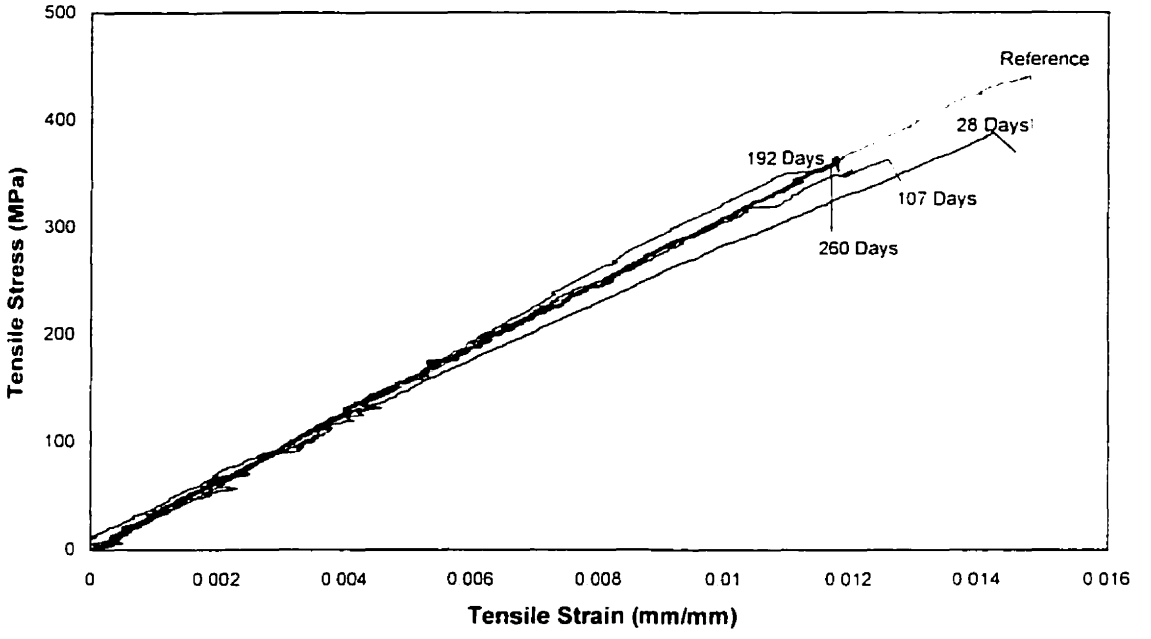

(a) 23°C

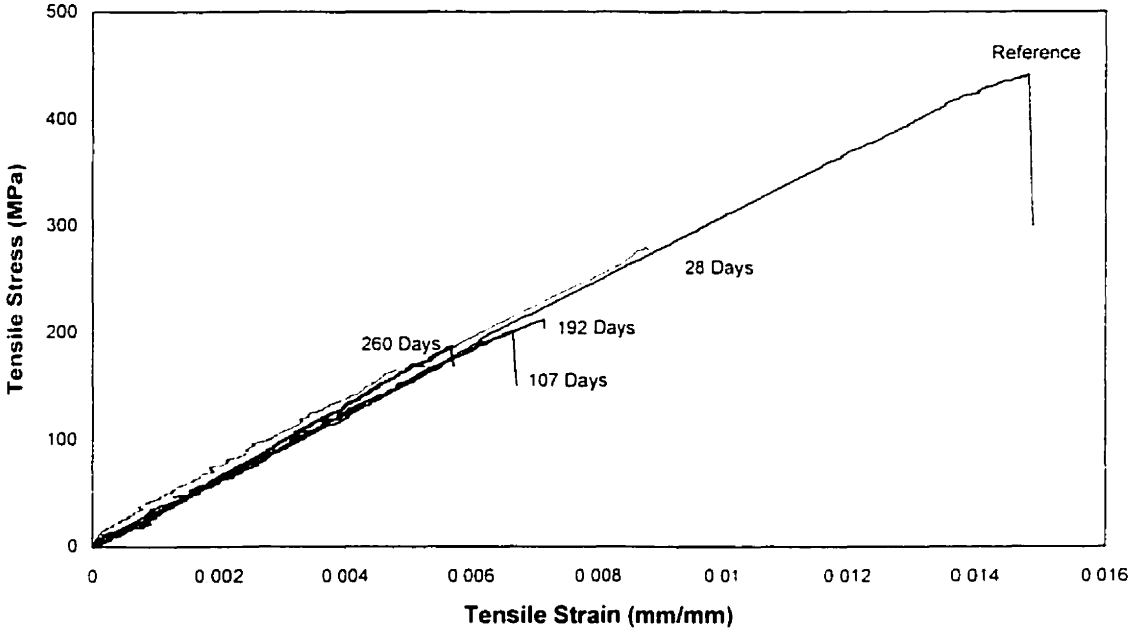

(b) 70°C

Figure 6.14 Tensile Stress-Strain Curves of Tap Water-Aged Flange

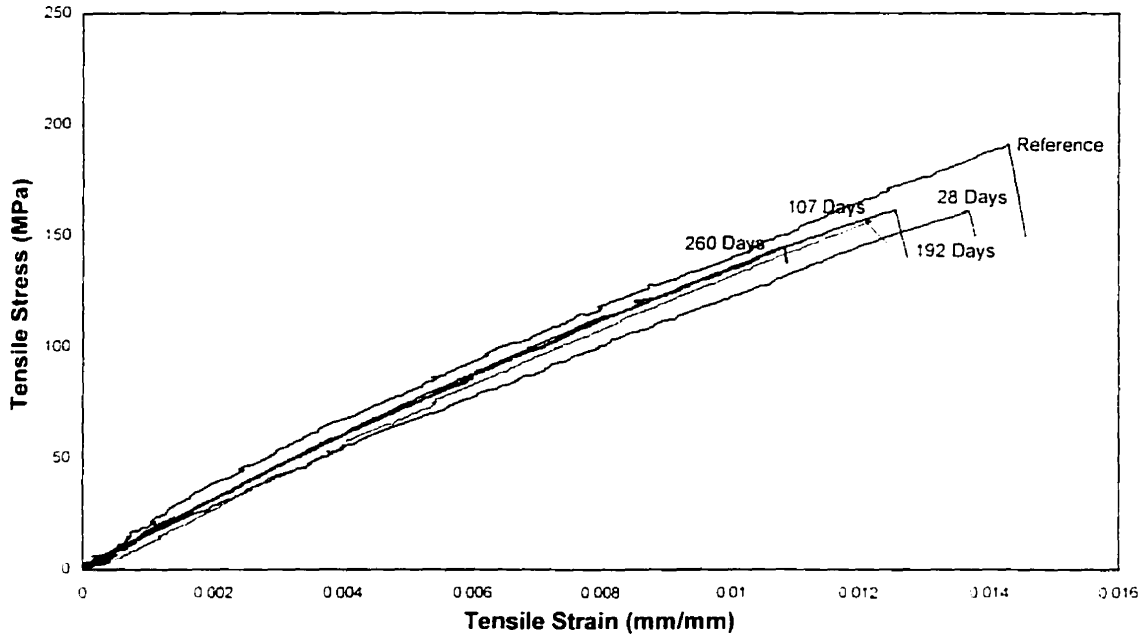

(a) 23°C

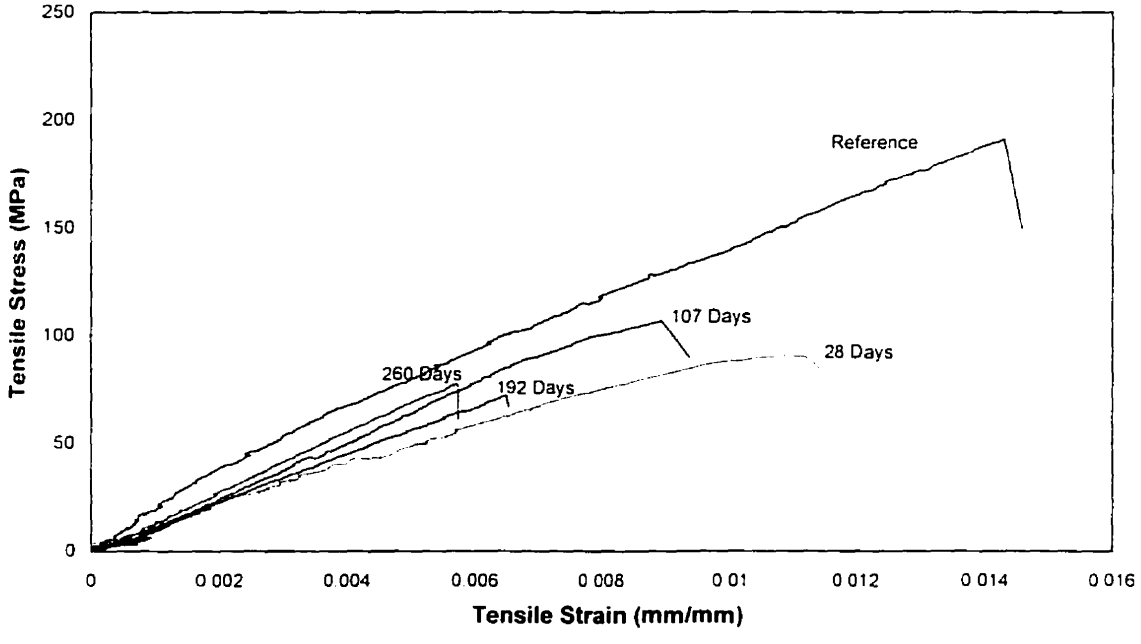

(b) 70°C

Figure 6.15 Tensile Stress-Strain of Tap Water-Aged Web

The dog-bone coupons aged in boiling distilled water for 21 days, at which time the specimens were tested, were aged in tap water at 70°C for 180 days prior to being transferred to boiling conditions. The specimens were saturated before the transfer. But for convenience, the specimens are considered to have aged for 201 days, while still keeping the name D100F for the flange specimen or D100W for the web specimen. Tensile tests performed on specimens in boiling water would give an indication as to whether the loss of mechanical property depends on absorption and not temperature, since distilled water is a more aggressive and the boiling temperature is too high. Typical curves for the flange and web are shown in Figure 6.16 (See Appendix B for all curves).

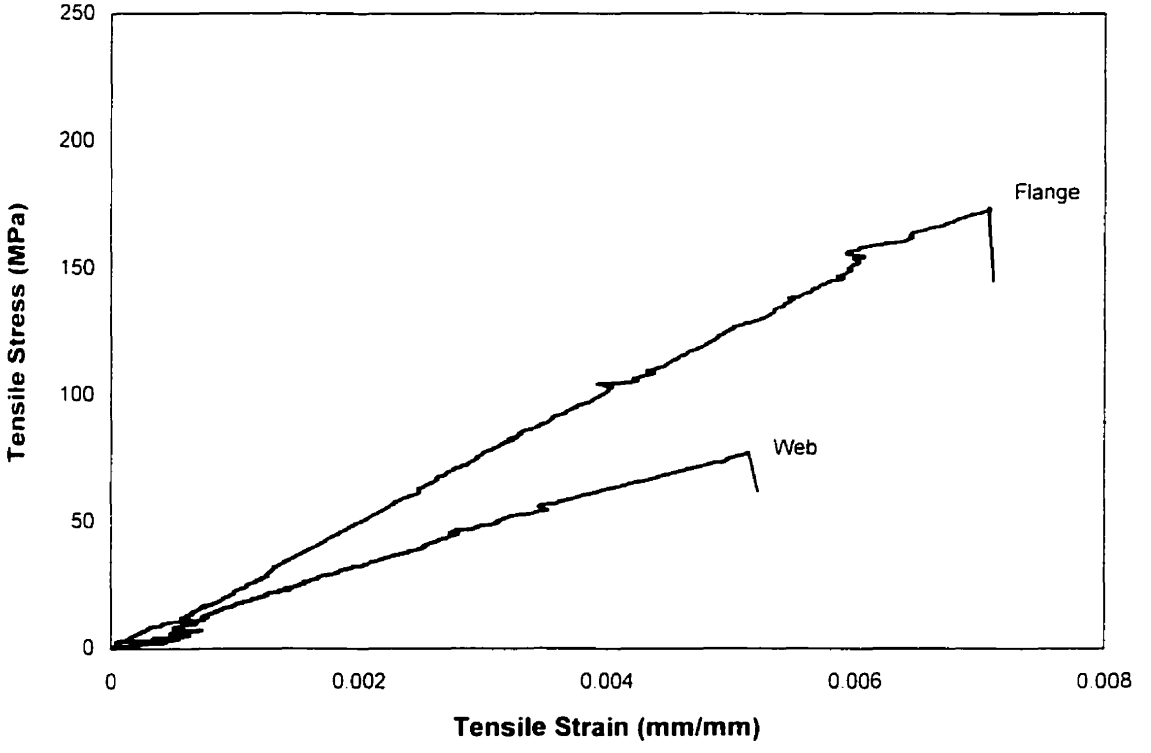

Figure 6.16 Tensile Stress-Strain Curves of Flange and Web Aged in Boiling Water

The results of all the tensile tests are summarized in Table 6.5. Each test result represented the average of at least three specimens.

Table 6.5 Water Absorption Tensile Test

Ageing Period		Avg. Tensile Strength (MPa)	Standard Deviation	Avg. Tensile Modulus (GPa)	Standard Deviation
Reference	Flange	433	15	29.9	1.7
Dry	Web	187	36	11.7	1.7
28	T23F	390	9	28.3	2.1
Days	T23W	161	25	13.2	1.8
	T70F	278	9	28.3	1.1
	T70W	91	6	10.0	1.0
107	T23F	365	13	29.4	2.7
Days	T23W	164	25	15.3	3.0
	T70F	204	2	30.7	1.9
	T70W	86	19	13.7	0.9
192	T23F	359	27	30.5	0.3
Days	T23W	151	41	11.9	3.9
	T70F	213	6	28.5	1.0
	T70W	69	16	10.3	1.2
260	T23F	357	4	32.3	0.9
Days	T23W	162	32	15.8	2.0
	T70F	189	4	32.8	1.3
	T70W	74	5	14.3	2.7
201	D100F	176	3	27.2	1.9
Days	D100W	74	4	13.8	1.4

The tensile strength of both flange and web specimens clearly show the trend of decreasing strength with time. The data from web specimens demonstrated more fluctuation than from the flange. This is attested by the large standard deviation displayed by the web specimen tests. Indeed, looking at the collection of the tension test curves in Appendix B, it is seen that there is a great variation among the web specimens

aged under the same conditions. The flange specimens, within the same batch, showed more consistent values of tensile strength and modulus with smaller variation.

The tensile modulus obtained from the flange specimens was always higher than that of the web specimens at any time. Overall, the tensile moduli of aged composites after different time periods were fluctuating around the reference values of tensile modulus tested for dry flange and web specimens. This was irrespective of the test temperature, 23°C, 70°C or 100°C. Again, the data for the web specimens involved larger standard deviation. It was likely that the tensile moduli of the composites were not substantially affected by the water absorption, even at a high temperature.

6.3 EFFECT OF FREEZE/THAW CYCLING ON TENSILE PROPERTIES

Freeze/thaw tests were conducted on specimens that were originally saturated at 70°C. Tensile tests were performed after 310 and 564 freeze/thaw cycles. The effect of freeze/thaw cycling in tap water on the tensile properties of the saturated composite material was investigated through the comparison with the specimens having the same absorption age but undergoing no cycles.

6.3.1 Effect of Ageing Path

The effect of ageing path was examined after 260 days of ageing period with two sets of specimens. On set of specimens underwent only tap water ageing at 70°C up to 260 days. The other set went through 192 days of tap water ageing at 70°C to reach saturation and then placed in freeze/thaw chamber for 310 cycles, which also added up to 260 days. The comparison between these two sets of specimens was made to study the ageing path effect. A summary of the results is presented Table 6.6 with the plots shown in Figure 6.17. It is clear that different ageing path has no significant effect on the mechanical properties.

Table 6.6 Effect of Freeze/Thaw Cycling and Ageing Path

	Tensile Strength (MPa)		**Tensile Modulus (MPa)**		
	Flange	**Web**	**Flange**	**Web**	**Ageing History**
Dry Reference	433 ± 15	187 ± 36	29.9 ± 1.7	11.7 ± 1.7	As received material. No ageing
Uncycled	189 ± 4	74 ± 5	32.8 ± 1.3	14.3 ± 2.7	260 days in 70°C
310 Cycles	201 ± 6	66 ± 3	32.6 ± 1.3	12.6 ± 0.6	192 days in 70°C + 310 cycles

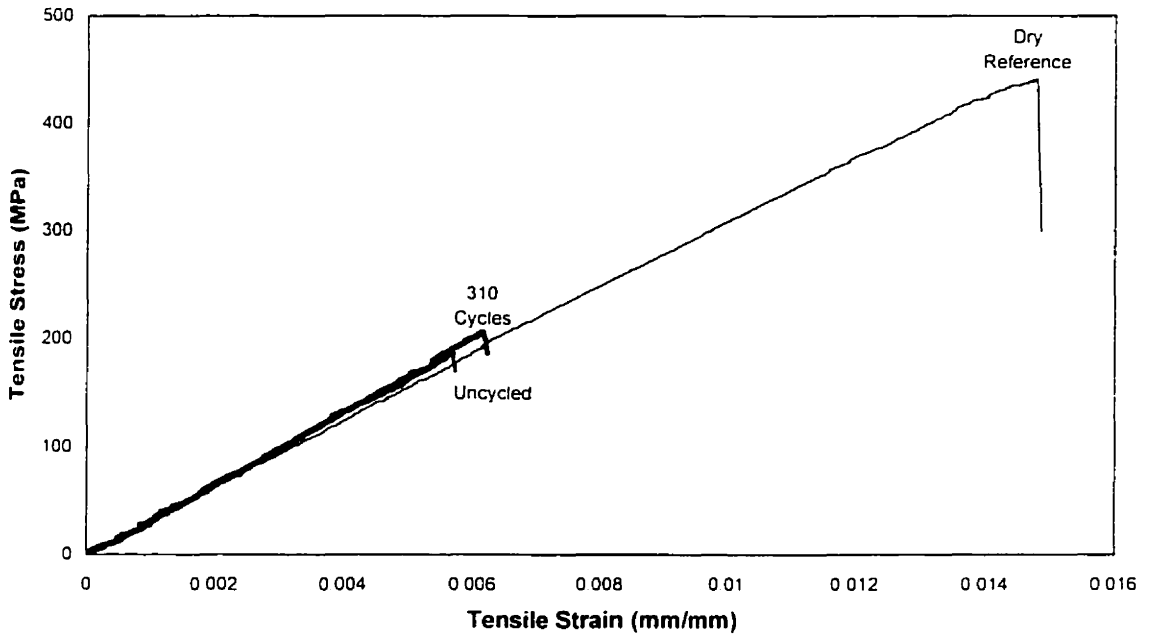

(a) Flange

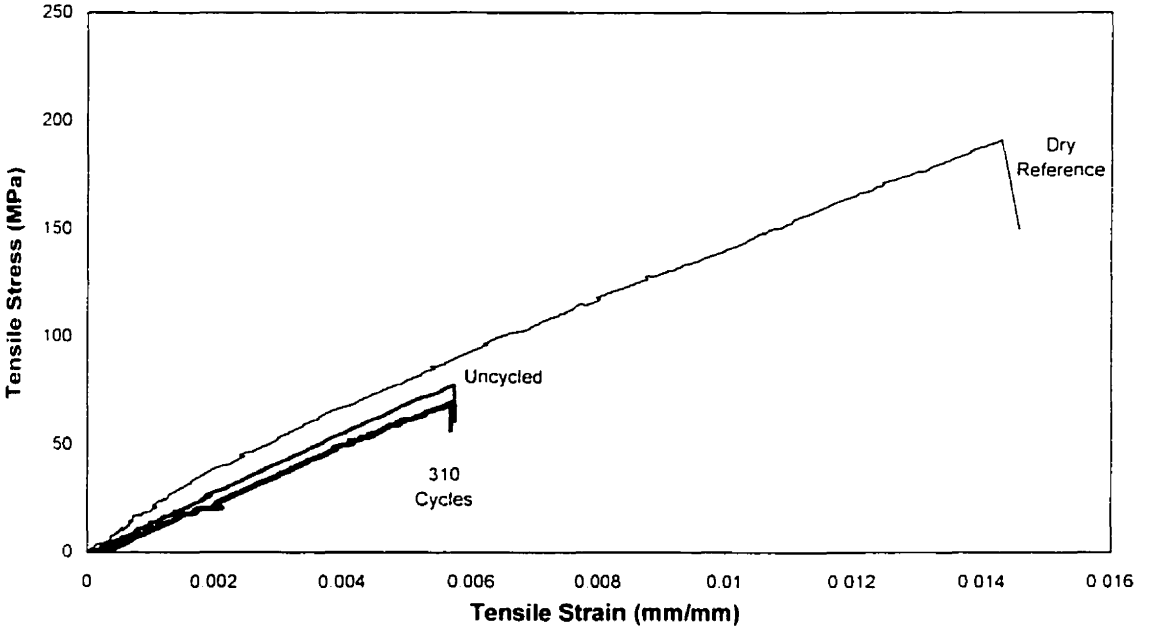

(b) Web

Figure 6.17 Effect of Ageing Path on Tensile Properties

6.3.2 Effect of Freeze/Thaw Cycling

Tensile tests were performed on the specimens cycled between –17°C and +4°C at 0, 310 and 564 cycles. The tensile coupon specimens were initially all aged in water at 70°C until 192 days when saturation was reached. Samples tested at 192 days served as control to study freeze/thaw cycling effect. Six specimens for each flange and web were placed in the freeze/thaw chamber and tested at 310 and 564 cycles. The results are presented in Table 6.7. Figure 6.18 shows the typical curves for the flange and the web.

The results revealed that there was no significant change in the maximum tensile strength of the flange and the web specimens after 564 cycles. The variation that may appear in the case of the web specimens is associated with the variation that has so far been observed in testing web specimens in tension. Table 6.7 demonstrates that the tensile strength and tensile modulus remained the same within the standard deviation of the values measured.

Table 6.7 Effect of Freeze/Thaw Cycling

	Tensile Strength (MPa)		**Tensile Modulus (MPa)**	
	Flange	**Web**	**Flange**	**Web**
Dry Reference	433 ± 15	187 ± 36	29.9 ± 1.7	11.7 ± 1.7
0 Cycles	213 ± 6	69 ± 16	28.5 ± 1.0	10.3 ± 1.2
310 Cycles	201 ± 6	66 ± 3	32.6 ± 1.3	12.6 ± 0.6
564 Cycles	202 ± 12	75 ± 15	29.3 ± 1.5	11.2 ± 2.8

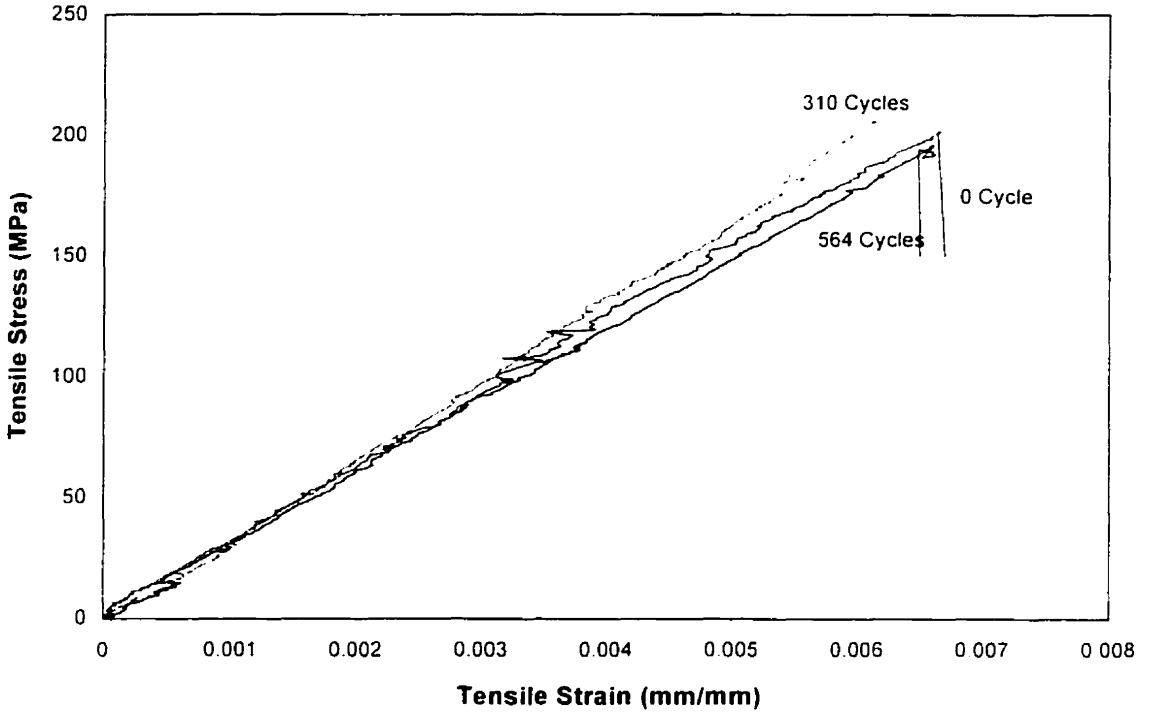

(a) Flange

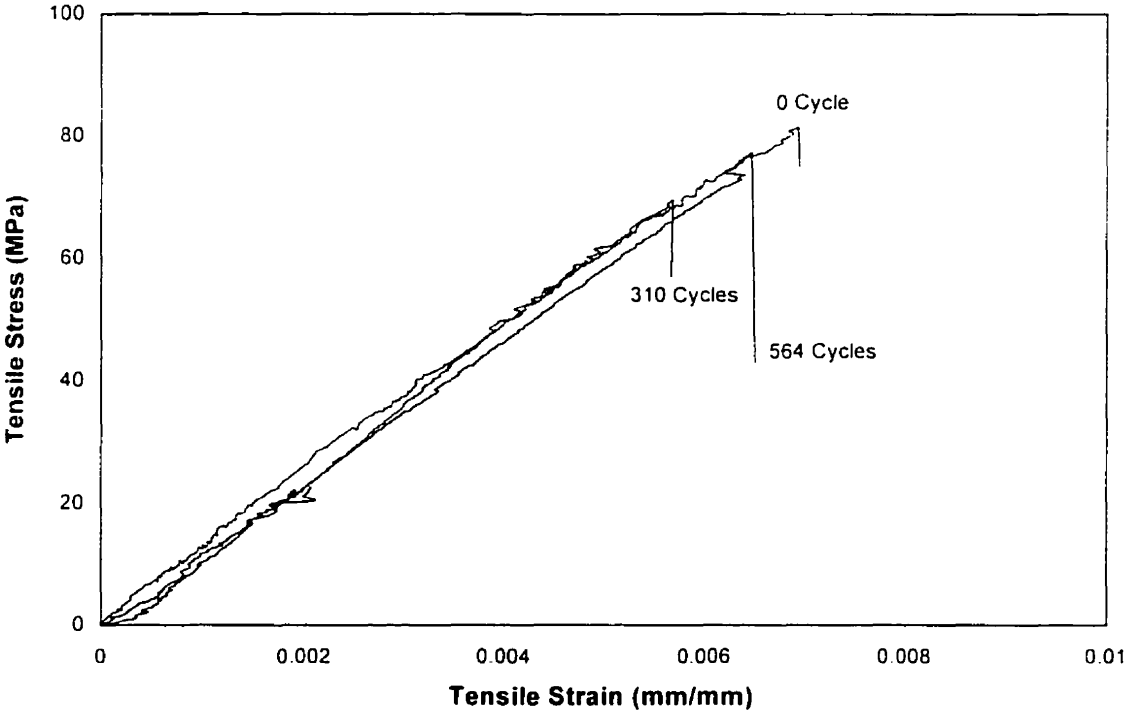

(b) Web

Figure 6.18 Effect of Freeze/Thaw Cycling on Tensile Properties

Chapter 7

Prediction of Water Absorption and Mechanical Properties

This part of the research program aims to predict the maximum water absorption of the composite at ambient temperature as a function of time. The long-term effect of absorption on the mechanical properties of the material will also be determined. This mainly involves two parameters, which are the tensile strength and the tensile modulus of elasticity. The prediction analysis was centered on tap water absorption condition.

7.1 WATER ABSORPTION MODELING

The values of maximum water absorption, $\%M_{\infty}$, at 70°C have been verified by the boiling water absorption test. The curve fitting of the room temperature water absorption test results in tap water was performed. Following the procedure laid out in Chapter 5 the absorption data for T23F and T23W were fitted. The value of $\%M_{\infty,F}$ was read off the graph of the absorption data (Figure 6.1) as the point where there was the first inflection in the curve after the initial linear portion. The maximum moisture absorbed, $\%M_{\infty}$, was determined from the water absorption at 70°C after the correction for mass loss was performed. The maximum moisture absorbed due to relaxation, $\%M_{\infty,R}$, was calculated using equation 5.10. The values of the diffusion coefficient D_z and the relaxation rate constant k were determined by performing the curve fitting of the absorption data for T23F and T23W specimens using equation 5.11. The values obtained are shown in the Table 7.1.

Table 7.1 Parameters for Curve Fitting of Tap Water Absorption with Time

	T23F	T23W
$\%M_{\infty}$, %	1.72	3.11
$\%M_{\infty,F}$, %	0.87	1.33
$\%M_{\infty,R}$, %	0.85	1.78
D_z, 10^{-6} mm^2/s	4.2	3.0
k, 10^{-8} s^{-1}	3.8	1.4
Thickness, mm	4.699	3.176

Using equation 5.9 with 16 terms, the curves of absorption models were plotted as shown in Figure 7.1. The time to 99.9% saturation is 1700 days for flange and 2600 days for web by equation 5.11. Although the initial slope of the flange was apparently lower than that of the web, the former had a higher diffusion coefficient than the web along with also a higher relaxation-rate constant (Table 7.1). In the flange the Fickian diffusion and the polymeric relaxation contributed almost equally to the overall absorption of the material. In the web the polymeric relaxation was more dominant than the Fickian process as the former contributed about 57% to the maximum moisture absorbed.

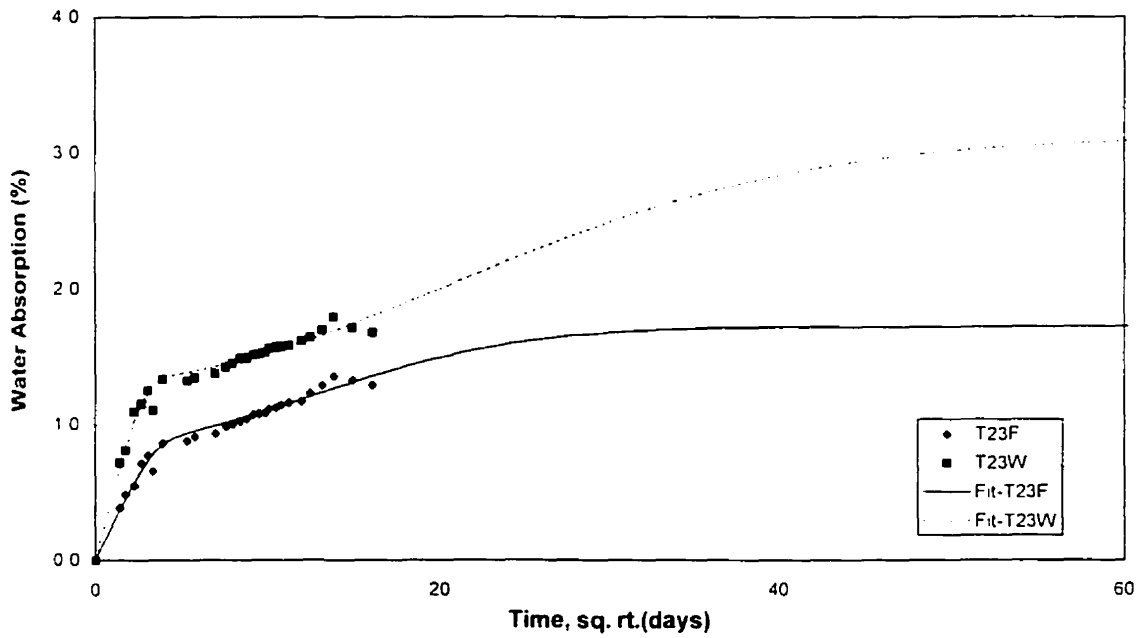

Figure 7.1 Absorption Modeling of T23F and T23W

There were two ways of finding the diffusion coefficient. One method was by curve fitting the absorption data with equation 5.11. The second method discussed in Chapter 5 was by finding the initial slope of the plotted absorption data and using equation 5.13 to calculate D_z. The comparison of the two methods for T23F and T23W test data are shown in Table 7.2.

Table 7.2 Comparison of D_z Values from Different Methods

			Slope Method			**Curve Fitting Method**
	h mm	$M_{w,F}$ %	Slope $(\text{days})^{-1/2}$	Slope $(10^{-4}\ s^{-1/2})$	D_z $(10^{-6}\ mm^2/s)$	D_z $(10^{-6}\ mm^2/s)$
T23F	4.699	0.87	0.26	8.99	4.6	4.2
T23W	3.176	1.33	0.45	15.31	2.6	3.0

The values of the diffusion coefficient calculated using different methods differed by an average of 11%. This difference could be attributed to the fact that finding the initial slope of the plot of the absorption data points could not be precise, as it depended on the points that were chosen to be part of the linear portion of the plot. The maximum Fickian absorption, $\%M_{w,F}$, determined from the linear proportion limit of the absorption curves also demonstrated variation.

7.2 PREDICTION OF MECHANICAL PROPERTIES

7.2.1 Tensile Strength

It was observed that tensile strength was decreased as the absorption in water increased. This reduction however likely stopped when saturation was reached (Table 6.5). The absorption experiments conducted by other researches with laminates had also shown that there was no further mechanical property degradation after the moisture

saturation was reached [Geller et al., 1999, Pritchard et al., 1987]. Figure 7.2 and 7.3 show the plots of tensile strength versus percentage of water absorbed for the flange and the web. The testing dates provided on the two plots were to show how the variation in the percentage moisture absorption followed the absorption curves of the specimens aged in tap water shown in Section 7.1. For example, in Figure 7.2, the test at 107 days had a slightly higher absorption than the test at 192 days for the flange specimens at 70°C. This was directly related to the fluctuation of the absorption curve of the flange at these temperatures. But overall there is a decrease in the tensile strength with percentage water absorbed. The trend was followed in the flange and the web in tap water, at 70°C.

As mentioned in section 6.2, the specimens denoted D100F and D100W were aged for 180 days in tap water at 70°C, then for 21 days in boiling distilled water or 201 days for the total. In Figure 7.2, the point representing D100F tensile test located among the point for tensile tests of T70F at 107, 193 and 260 days. This reinforces the fact that the tensile strength degradation depends on percent absorption, even if slightly different immersion solution was used. This was also seen for D100W coupons in Figure 7.3.

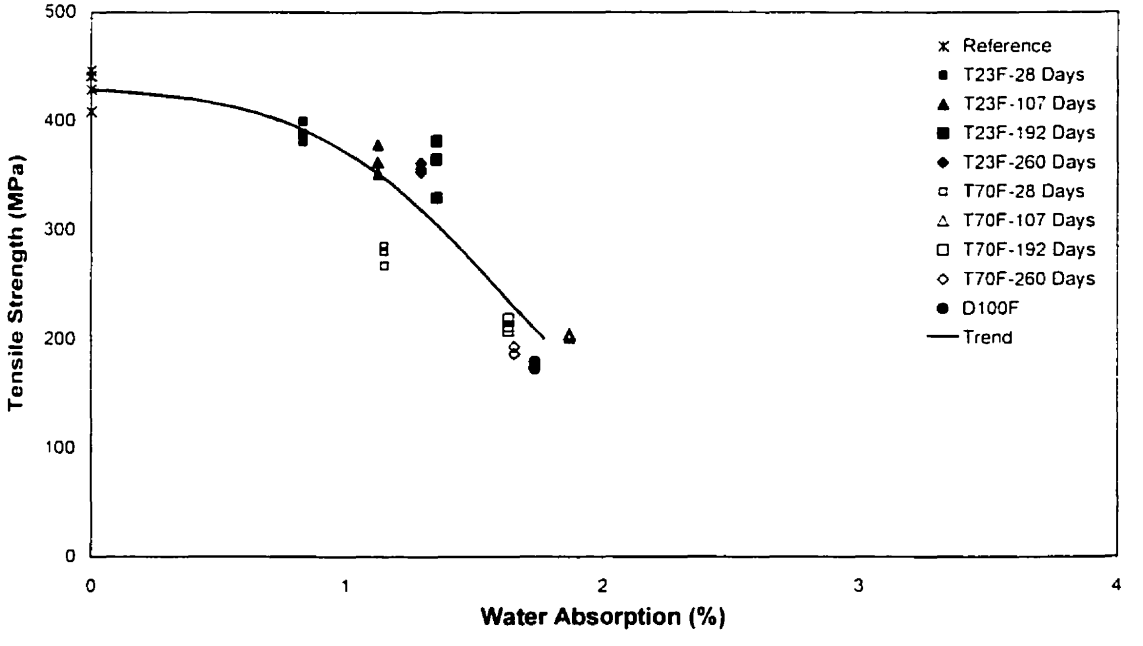

Figure 7.2 Tensile Strength vs. Absorption of Water-Aged Flange

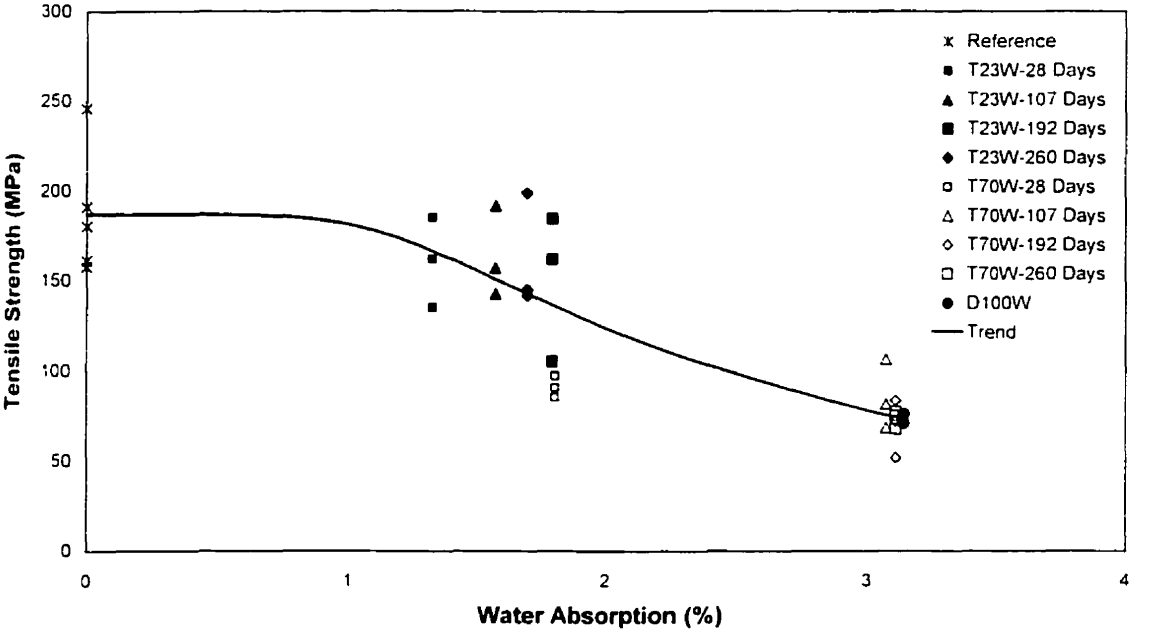

Figure 7.3 Tensile Strength vs. Absorption of Water Aged Web

It needs to be determined whether the degradation of tensile strength had stop with the reach of moisture saturation. From Section 7.1, it was determined that moisture saturation had been reached at 70° C in tap water despite the occurrence of the apparent mass loss. In the plots of tensile strength vs. the percentage of water absorbed, establishing the trend within the T70F and T70W data points needs to be established. Examining the data points for T70F specimens in Figure 7.2, the values of the tensile strength vary around 200 MPa over a period of 153 days (107-day to 260-day). In Section 7.1, the moisture saturation of the flange was evaluated at 1.72%. In Figure 7.2 the absorption at different ages for the specimens T70F varies around this value. From these remarks, it can be concluded that the tensile strength of the flange had been stabilized after moisture saturation had been reached.

In Figure 7.3, the data points for T70W do show a similar trend. With saturation moisture at 3.11%, the tensile strength obtained at 107, 192, 260 day test fluctuated. In order to determine the time, during which the minimum tensile strength would be reached during the service life of the sheet pile, a plot of strength vs. time is needed. The data

points on this plot have to be curve-fitted in order to extrapolate any present trend into the future, with r-values from 0.79 to 0.98.

Since the tensile strength degradation stops with saturation, a limiting plateau should be reached by the tensile strength on the plot of tensile strength vs. time, once the saturation level is reached. After 260 days, saturation was reached at 70°C test condition, in the flange and web specimens. Therefore, the tensile strength at this temperature should have hit a plateau. The absorption test at 23°C did not reach saturation by 260 days. But it has been established earlier that the saturation capacity of the material does not depend on the test temperature. Therefore, the specimens aged at 23°C should eventually have the same saturation moisture as the ones aged at 70° C. Since there is no further tensile strength degradation after saturation, when plotting the tensile strength vs. time, the curve of the test at 23°C should also reach the plateau found at 70°C and follow it. The time at which the two curves will meet is the time at which saturation occurred in the samples at 23°C. For practical purposes, 99.9% moisture absorption is usually referred to as the saturation point instead of 100% saturation. From the curve fitting performed on T23F and T23W specimens in Section 7.1, 99.9% saturation of the flange occurred after 1700 days and 2600 days for the web. Making judicious use of all this information the curve fitting of the tensile strength vs. time was performed and the results are shown in Figures 7.4 and 7.5

The curve fits were obtained using the curve fitting system CurveExpert 1.3, which uses double-precision in a 32-bit package. The best fits for the high temperature data (T70F and T70W) were obtained with equations of the form shown in equation 7.1. In this expression, a represents the value of tensile strength at the plateau. It is the minimum value of tensile strength that could be attained in the future.

$$y = \frac{a}{1 + be^{(-cx)}} \tag{7.1}$$

where

y = Tensile strength, MPa

x = Time, $(\text{days})^{1/2}$

a = Minimum srength, MPa

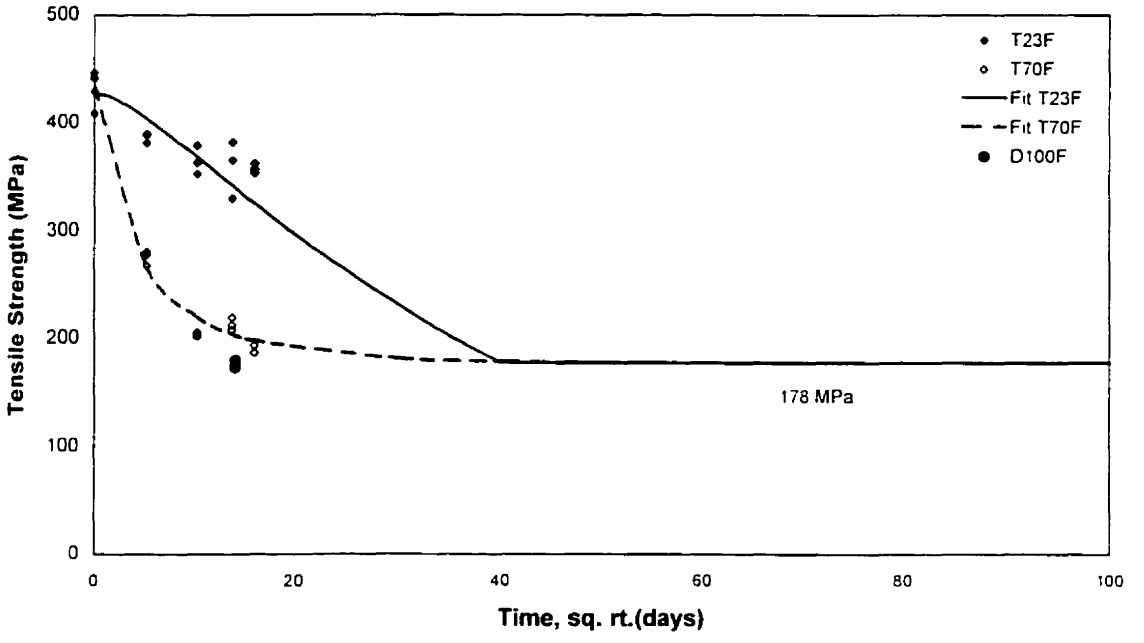

Figure 7.4 Prediction of Tensile Strength of Flange with Time

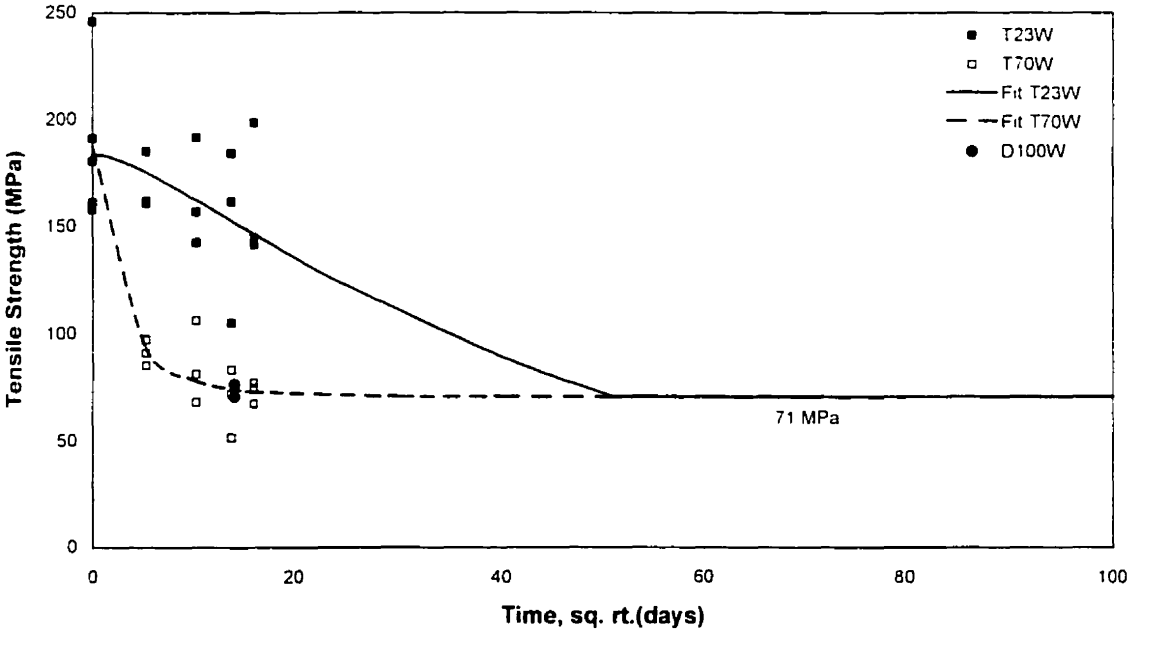

Figure 7.5 Prediction of Tensile Strength of Web with Time

b = Parameter, no unit

c = Parameter, $(\text{days})^{-1/2}$

The room temperature data (specimens T23F and T23W) were fitted with two-piece stepwise functions. In the first step, the data points were fitted with Equation 7.2 from time equal to zero up to the time when 99.9% saturation was expected. After that time, the plot just followed the plateau established earlier at the temperature of 70°C. Here, c represents the value of the tensile strength at time zero, as it is the y-intercept or the tensile strength axis-intercept. It represents the reference tensile strength, without ageing, obtained through the curve fitting.

$$y = a\exp(bx) + cx^{(dx)} \qquad \textbf{(7.2)}$$

where

y = Tensile strength, MPa

x = Time, $(\text{days})^{1/2}$

a = Parameter, MPa

b = Parameter, $(\text{days})^{-1/2}$

c = As-received strength, MPa

d = Parameter, $(\text{days})^{-1/2}$

Use equation 7.2 if: $x \leq 41.2$ days$^{1/2}$ for flange

$x \leq 51$ days$^{1/2}$ for web

y = 178 MPa if: $x > 41.2$ days$^{1/2}$ for flange

y = 71 MPa if: $x > 51$ days$^{1/2}$ for web

The parameters obtained in the curve fittings are given in Table 7.3.

Table 7.3 Parameters from Curve Fitting of Tensile Strength with Time

Equation 7.1			
	a (MPa)	**b**	**c (days$^{1/2}$)**
T70F	178	-5.92E-1	1.08E-1
T70W	71	-6.2E-1	1.79E-1

Equation 7.2				
	a (MPa)	**b (days$^{-1/2}$)**	**c (MPa)**	**d (days$^{-1/2}$)**
T23F	6.07E-5	2.71E-1	426	6.02E-3
T23W	5.69E-5	2.6E-1	183	4.98E-3

The actual values of the tensile strengths obtained for the reference tensile strength tests are 433 MPa for the flange and 187 for the web. These values differ slightly from the values of c in equation 7.2 by 1.6% in the flange and 2.1% in the web.

The results for the prediction of changes in tensile strength with time are summarized in Table 7.4.

Table 7.4 Prediction of Tensile Strength with time

Specimens	$\%M_\infty$	Time to Saturation $\%M_\infty$ (days)	Dry Tensile Strength (MPa)	Saturated Tensile Strength (MPa)	Change in Tensile Strength
Flange	1.72	1700	433	178	-59 %
Web	3.11	2600	187	71	-62 %

7.2.2 Tensile Modulus of Elasticity

The changes in the tensile modulus of elasticity were evaluated with respect to the ageing time and the percentage of water absorbed. Figure 7.6 shows the change in modulus with time. The room temperature and the high temperature of 70°C tensile test results are shown in the Figure 7.6. There were no apparent reduction in modulus occurring within the flange results or within the web results. The standard deviations of the average reference values of tensile modulus and the averages of the values for the rest of the tests are shown in Table 7.5.

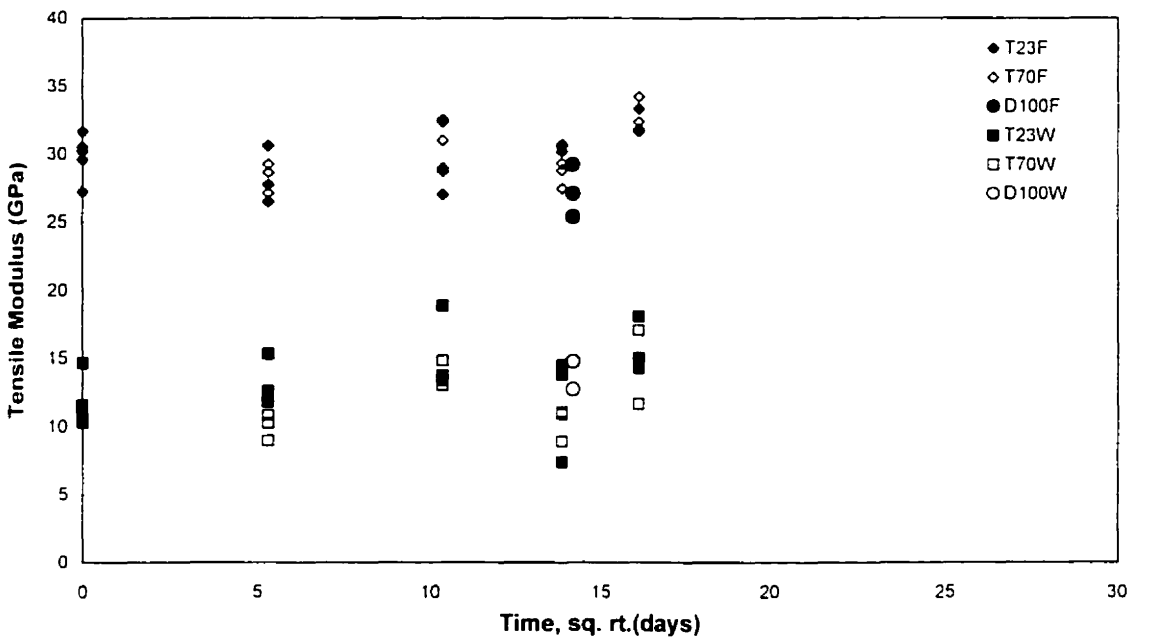

Figure 7.6 Tensile Modulus vs. Time of Water-Aged Specimens

The average reference tensile modulus was the same as the average tensile modulus for all other aged specimen considering the standard deviations of the two values (Table 7.5). This was shown in both the flange and the web. Therefore, there was no significant loss of the tensile modulus with ageing.

Table 7.5 Comparison of the Tensile Modulus of Elasticity

Specimen	Average Tensile Modulus (GPa)	*SD.* Tensile Modulus (GPa)
Dry Reference		
Flange	29.9	1.7
Web	11.7	1.7
Combined tests after ageing		
Flange	30.1	2.1
Web	13.1	2.8

Extrapolating this trend into the future years to follow would seem to be as simple as saying that the tensile modulus of elasticity remains constant with time in a wet environment. The test condition at 70°C was meant to accelerate any degradation that might have taken place. Even then, the values of tensile moduli at 70°C were not different from those at 23°C. Therefore, the tensile modulus of the flange and the web will remain more or less unchanged during the service life of the sheet pile. It is also demonstrated that high temperature acceleration seemed not to generate additional damage to the composites

If the tensile modulus did not change with time, it should not be affected by absorption, even though the percentage absorption changes with time. Indeed, this is what was observed, as Figure 7.7 shows. The values at 70°C were bunched together with respect to absorption in the case of the flange and the web. This is explained by the fact that the specimens were close to saturation by the time the first test was conducted after 28 days of tap water ageing at 70°C.

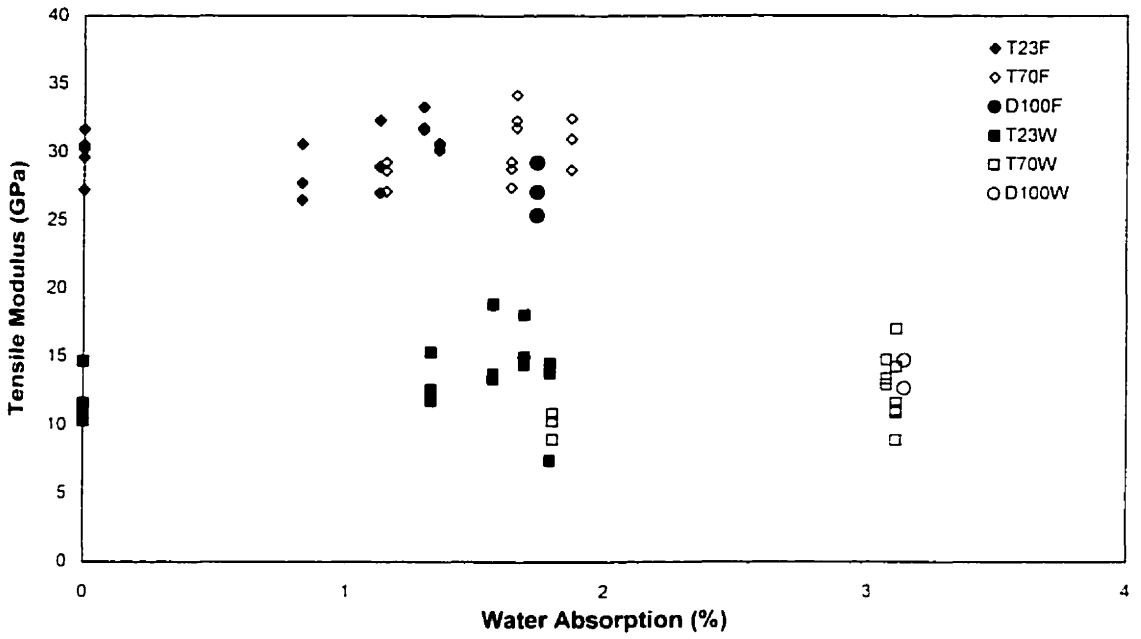

Figure 7.7 Tensile Modulus vs. Absorption of Water-Aged Specimens

Chapter 8

Discussion

8.1 WATER ABSORPTION

Through the water absorption tests, it was noticed that the moisture saturation does not depend on the test temperature. This was confirmed by the moisture saturation in tap water at 70°C and in boiling distilled water being relatively the same. The fact that the distilled water had higher water absorption (0.03% more) compared to tap water is probably due to the lower concentration of the former. This allows the distilled water to penetrate in much smaller microscopic openings that may not be accessible to tap water.

The water absorption tests in salted water conditions presented lower moisture absorption at a given time compared to tap water at the same temperature condition. It seems that since salted water has a higher concentration than tap water, it would migrate into the material less aggressively. Although no salted water absorption test was conducted until saturation, the phenomenon observed between distilled water and tap water absorption suggest that the moisture saturation in salted water would be slightly lower than that in tap water.

In Section 6.1.4, the results of the water absorption under three-point flexural load test showed that the water absorption was reduced under the load action. Two independent studies on composites, conducted by Geller and Turley [1999] and kasturiarachchi et al. [1983] on the effect of loading showed that four-point flexural load action did not change the percent moisture at saturation. Those tests were performed on the various laminates. In this research, since saturation in loaded absorption tests was not reached, it can only be concluded that the water absorption under load is not higher than that of free absorption.

The mass loss was observed during water absorption at 70°C and 100°C, very likely due to the fact that some components of the resin were dissolved in hot water. In independent studies on water absorption of fiberglass-reinforced isophthalic polyester resin, Apicella et al. [1983], Choqueuse et al. [1997] and Pritchard and Speake [1987] also observed similar mass loss phenomenon. Apicella et al. [1983] showed that this behavior was characteristic of the resin. A study conducted by Bonniau and Bunsell [1981] on the water absorption of glass epoxy composites showed the same mass loss behavior. In their study, the loss was attributed to the resin hardener used in the composite. The mechanism of mass loss in pultruded fiberglass polyester sheet pile materials was not studied in this research. Mass loss occurred in isophthalic polyester composites only when materials were immersed in hot water at a temperature of 60°C or higher. Since the sheet pile walls are not designed to serve in that environment, the mass loss is not expected to occur in the field. The ASTM Standard D 570 procedure should be followed to correct the mass loss at high temperature.

Upon visual survey of water-aged specimens, a change of color of the surface of specimens was noticed in the test conditions at 70°C and boiling water, as shown by Figure 8.1. The color became yellowish in specimens after 260 days aging at 70°C. In boiling water, they became pale after 21 days of immersion. This phenomenon was noticed in both the web and flange specimens in tap and salted water. There was no apparent difference in the extent of discoloration between the specimens aged at the same temperature for the same period of time in tap or salted water. High temperature and long immersion period are most likely to be the agents causing this change of color. It was also found that the specimens that lost surface color also had a rough surface, indicating a loss of cover on top of the reinforcement. There was more discoloration of specimens with more mass loss and aged at temperature of 70°C compared to those aged at 23°C. No noticeable color change was observed in the water absorption at 23°C and 40°C. Therefore, this phenomenon is not expected to occur when the composite sheet pile wall is used at ambient temperature of 23°C.

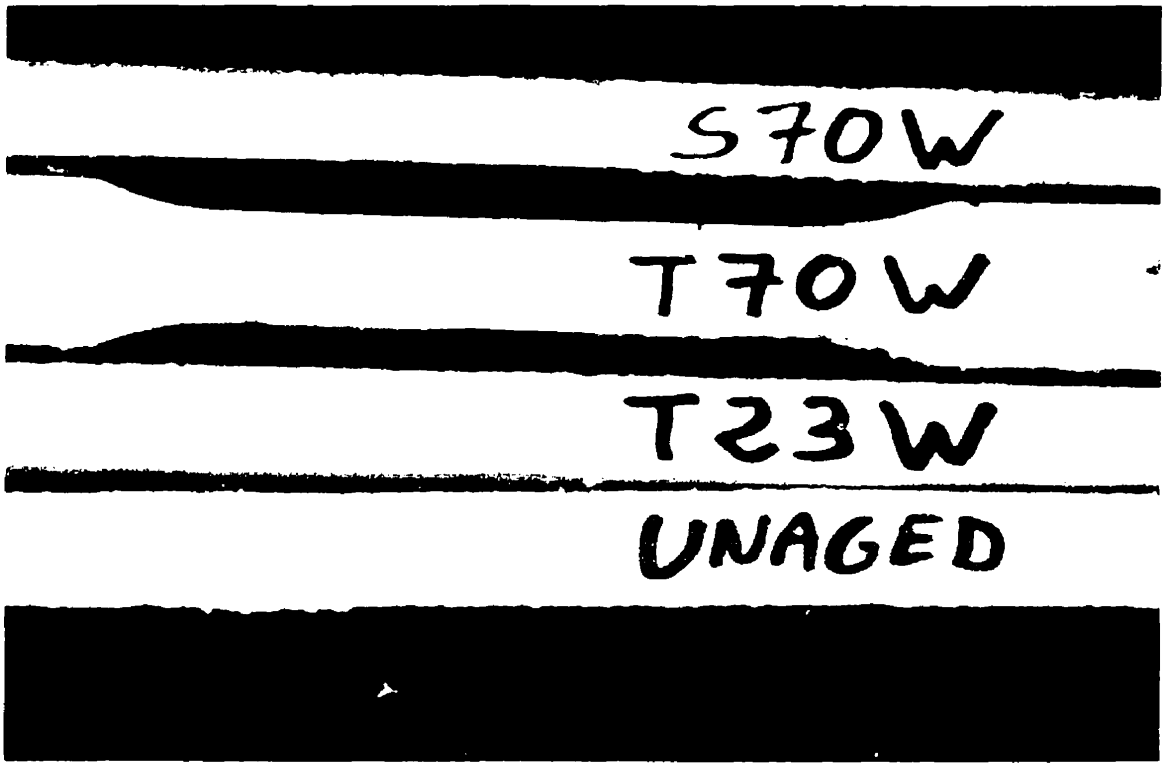

Figure 8.1 Color Change of Specimens in Different Ageing Conditions

The diffusion coefficients obtained during water absorption modeling were 4.2 x 10^{-6} mm^2/s for the flange specimens and 3.0 x 10^{-6} mm^2/s for the web specimens in tap water at 23°C. In their study on the water absorption kinetic of laminate, Pritchard and Speake [1987] found the diffusion coefficient of a fiberglass-reinforced isophthalic polyester composite to be 0.81 x 10^{-6} mm^2/s in water at 30°C, without edge coating. The composite was a 10° unidirectional woven roving laminate fabricated by hand lay-up. The glass reinforcement was 48% by weight of the laminate. On the other hand, Geller and Turley [1999] evaluated the diffusion coefficient of a glass-reinforced isophthalic polyester resin laminate at 2.5 x 10^{-6} mm^2/s. The laminate studied was composed of alternating plies of glass woven roving and chopped strand mat with chopped strand mat with the woven roving as both outer layers. The resin content was 45 ± 1% by weight. The comparison shows that although different material systems may have very close similarities in their matrices and fibers, factors such as the fiber content, the

manufacturing process, and the test condition may well influence the water absorption characteristics of the composite. The results suggest that the pultruded composites absorbed water faster than laminates. Both Grant and Bradley [1994] and Geller and Turley [1999] suggested that the absorption by fiber/resin interface might be more significant than the absorption by the resin itself. Therefore any factors that will directly affect the structure of that interface will also affect the absorption characteristics of the composite.

8.2 TENSILE PROPERTIES

When tensile tests were conducted on the aged web and flange two different failure modes were observed in the specimens. Figure 8.2 shows a web and flange dog-bone coupon after they have been tested in tension. These failure modes were also observed in the specimens tested after freeze/thaw cycling.

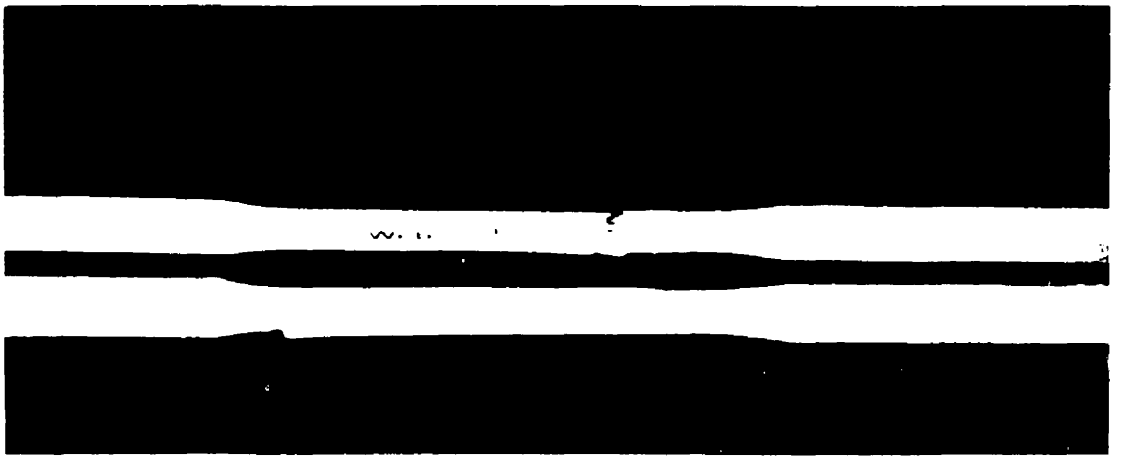

Figure 8.2 Web and Flange Dog-bone Coupons after Tensile Tests

The failed flange coupons had delaminations along two planes parallel to the longitudinal direction and over the entire length of the narrow section on the dog-bone

shaped coupons and sometimes beyond that. These planes went through the rovings, which are located in the middle of the cross-section. There was also a transverse fracture through the layers of random chopped mat and transverse fibers on either side of the rovings. Figure 8.3 shows a detailed schematic diagram of the fractured flange coupon. On the other hand, the web coupons always fractured through the cross-section of the specimen with needle-like fibers sticking out from both cross-sections of the half specimens as shown in Figure 8.4. These needles are mainly from the rovings and the continuous filament mat.

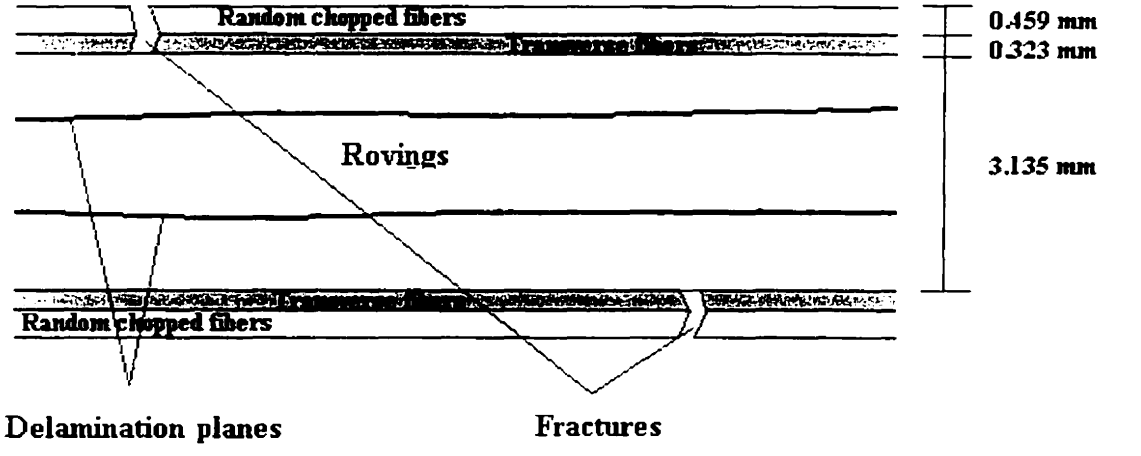

Figure 8.3 Schematic Diagram of Failed Flange Coupon

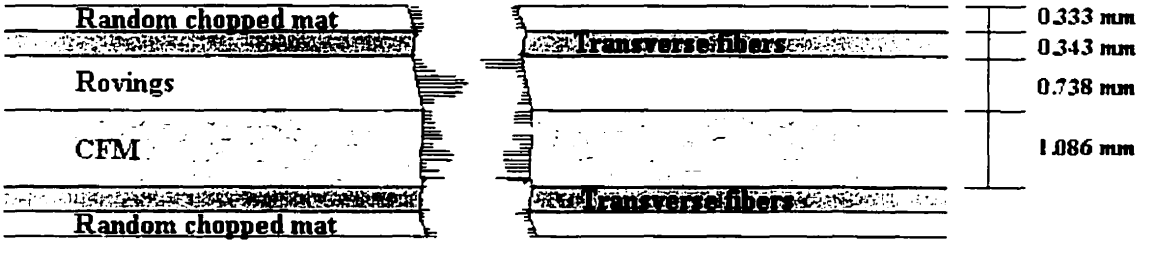

Figure 8.4 Schematic Diagram of Failed Web Coupon

The layer of rovings seems to be the factor governing the failure mode. In the flange, the thickness of that layer makes up 67% of the entire thickness of the flange

while that value is only 23% in the web. Measurements showed that the thickness of the layer of rovings in the flange is about 4 times that found in the web. The parallel nature of rovings in the longitudinal direction establishes a preferential direction of weakness for delamination to propagate when a tensile force is applied. The bundle nature of rovings does not allow the resin to efficiently penetrate between each strand of fiber. As a result, the fibers are not well bonded together and become very susceptible to delamination. The other layers in the flange can be considered as being layers of randomly oriented fibers that may not be subjected to such actions. In the case of the layer of transverse fibers, the direction of weakness with respect to delamination is the one perpendicular to the direction of tensile load being applied. But the layers of random chopped mat and transverse fibers are weaker and much thinner than the rovings with all the fibers aligned in the direction of the load being applied. This is why the outside layers fractured in the flange while the roving stayed in one piece. The reason why delamination did not occur between two adjacent layers is because the thickness of the layer of rovings was large in comparison to other layers, therefore increasing that zone of weakness embedded in that layer.

In the web, although the layer of rovings may be the strongest in tension it is not the thickest layer and there are no large differences in thickness between layers. The roving layer is 23% of the total thickness, with an overall-roving ratio of 11%. These factors and the fact that the web is thinner allowed for a fracture through the entire cross-section of the dog-bone coupon.

The tensile properties of the flange and the web were not significantly altered after 564 temperature cycles between 4.4°C and −17.8°C. The resistance of a composite to freeze/thaw cycling depends on the ability of water to freeze in micro-pores. If these pores are too small, water will be unable to freeze just at −17°C. There will not be any expansion of the pores, limiting the damages due to the freeze/thaw. Verghese et al. [1999] found that the pore size in the unreinforced polyester resin was on the order of about 6 -20 Å. As a reference, water in the concrete can only freeze at −40°C in pores less than 100 Å. It is expected that water will not freeze inside the pores of the resin. Since the resin is not susceptible to freeze/thaw damage, and fiberglass does absorb water, water can only condense in the fiber/matrix interface where microcracks are likely

to form and propagate. Probably in the material used in the present study, the microcracks were not large enough to allow the water to freeze. Therefore, the damage due to the freeze/thaw cycling was greatly limited. The flange and the web are likely to retain most of their strengths and moduli after freeze/thaw cycling.

Chapter 9

Conclusion

A study was carried out to characterize the absorption behavior of pultruded composite sheet piles immersed in water at ambient temperature. High temperature at 70°C was used to accelerate the absorption tests. The correlation of the results between the ambient temperature and high temperature was established to predict long-term performance based on short-term experiment data.

It was found that the maximum moisture content of the composite at saturation was not temperature-dependent. Therefore, the accelerated tests at high temperatures can be used to obtain the maximum percentage of absorption at saturation. However, the temperature has an effect on the diffusivity of the composite. The higher the temperature used, the higher is the diffusion coefficient, indicating a faster absorption. Of all the immersion solutions, tap water proved to be more aggressive than salted water. Although salted water tests were not corrected for mass loss to establish the moisture saturation, the results obtained indicate that the percentage of saturation will not be higher than that obtained in tap water. Therefore, the results obtained from the tap water tests can be used to evaluate the salted water condition, which is a less aggressive environment as far as the moisture diffusion is concerned.

The water absorption under the action of a three-point bending load was not higher than the free absorption. It would be beneficial for the composite to be used in retaining structures.

Significant mass loss of the composite was observed in water absorption tests at 70°C and 100°C. This was likely due to the leaching of non-bound substances in the resin. The factors affecting this loss were the temperature and the time of immersion. The higher the temperature and longer the immersion time, the higher the mass loss is. However, there was no significant difference between the mass loss in tap water and

salted water at 70°C. The ASTM Standard D 570 procedure should be followed to correct the loss to obtain the true water absorption.

The U.S. Army Corp of Engineers established a performance specification for composites to be used in sheet piling system [USACRL 123 1998]. The water absorption for composite was limited to 5%. The composite sheet pile wall panel studied in this research demonstrated a maximum absorption at saturation of 1.72% for the flange and 3.11% for the web. Saturation will be reached in 4.5 years for the flange and 7 years for the latter. These values obtained are well within the limits of the moisture absorption prescribed by the U.S Army Corp of Engineers. The process by which moisture diffusion took place was non-Fickian. It was a combination of Fickian moisture diffusion and polymeric relaxation of the composite. In the web, polymeric relaxation contributed more to moisture absorption than the Fickian process. In the flange the contribution from both processes was equal.

The first parameter of the tensile properties of the composite investigated was the tensile modulus of elasticity. There was virtually no change of tensile modulus of elasticity with water-ageing. This was demonstrated at both room and high temperatures. As a result, the section modulus, EI, should also remain constant over the service life of the structure. The U.S. Army Corp of Engineers specified that the decrease in the composite EI for sheet pile wall should not exceed 10% [USACRL 123 1998]. This requirement is expected to be met during the service life of the sheet pile wall made from the composites studied in this research.

The second tensile property investigated was the tensile strength of the material. There will be a decrease in the tensile strength of the composite over the service life of the structure. The change was estimated at about 60% for both the web and the flange. This will occur after 4.5 years in the flange and 7 years in the web, when the saturation is reached. The design load in the current sheet pile wall design is 25% of the ultimate load. There was a 60% loss of the tensile strength as compared with the strengths of the as received composites (433 MPa for the flange and 187 MPa for the web). The 40% residual strengths were 178 MPa for the flange and 71 MPa for the web. This may be acceptable since the design values at 25% are much lower than that.

The freeze/thaw resistance of the saturated composites proved to be excellent. 564 freeze/thaw cycles, from 4.4°C to −17.2°C, had very little effect on the tensile properties of the material. There was no further degradation in the tensile strength and the modulus of elasticity, after moisture saturation had been reached.

This research program established that the material is not suitable for high temperature water applications. Since the material was not designed for these particular applications, the composite was expected to perform adequately in the field.

RECOMMENDATIONS FOR FUTURE WORK

The results obtained from this research prompted further investigations that would compliment the first step undertaken here. The proposed recommendations for future work are the following:

- To determine the nature of the mass loss by independently investigating the effect of the resin hardener, catalyst, filler, isophthalic acid, in a high temperature water absorption test; By varying one of theses factors at the time, comparison of mass loss can be made with the original material.
- To perform a salted water absorption test at high temperature to evaluate the moisture saturation in this condition.
- To perform an accelerated loaded absorption test under 3-point bending, with mass loss correction, to determine that the moisture saturation.
- To perform a creep test on a sheet pile panel to determine the long term effect of static load with respect to deflection and strain.

REFERENCES

Abeysinghe, H.P. et al. (1982), "Degradation of Crosslinked Resins in Water and Electrolyte Solutions", Polymer, vol. 23, November, pp. 1785-1790.

Apicella, A. et al. (1983), "The water Ageing of Unsaturated Polyester-based Composites: Influence of Resin Chemical Structure", *Composites*, vol. 14, No. 4, October, pp. 387-390.

Berens, A.R. and H.B. Hopfenberg (1977), "Diffusion and Relaxation in Glassy Polymer Powders: 2. Separation of Diffusion and Relaxation Parameters", Polymer, vol. 19, May, pp. 489-491.

Bonniau P. and A.R. Bunsell (1981), "A Comparative Study of Water Absorption Theories Applied to Glass Epoxy Composites", *Journal of Composite Materials*, vol. 15, May, pp. 273-278

Cai, L.-W. and Y. Weitsman (1994), "Non-Fickian Moisture Diffusion in Polymeric Composites", *Journal of Composite Materials*, vol. 28, No. 2, pp. 130-151

Cardon, A.H. Ed., (1996), "Application of Composites in a Marine Environment: Status and Problems", Durability Analysis of Structural Composite systems, ... pp. 34-43.

Choqueuse, D. et al. (1997), "Aging of Composites in Water: Comparison of Five Materials in Terms of Absorption Kinetics and Evolution of Mechanical Properties", *High Temperature effects on Polymeric Composites*, vol. 2, ASTM STP 1302, T.S. Gates and A. Zureick, Eds., ASTM, pp-73-96, used pp-74, 79.

Crank, J. (1975), "The Mathematics of Diffusion", Clarendon Press, Oxford

Davies, P. (1996), "Application of Composites in a Marine Environment: Status and Problems", *Durability analysis of Structural Composite Systems*, Cardon, A.H., Ed.

Dutta et al. (1991), "Thermal Cycling studies of a Cross-plied P100 Graphite Fiber Reinforced 6061 Aluminum Composite Laminate", *Journal of Materials Science*, pp. 26

Gellert, E.P. and D.M. Turley (1999), "Seawater Immersion Ageing of Glass-fiber Reinforced Polymer Laminates for Marine Applications", *Composites*, Part A, May, pp. 1260-1264.

Gibson, R.F. (1994), Principles of Composite Material Mechanics, McGraw-Hill, New York, U.S.

Gomez, J.P. and B. Casto, (1996), "Freeze-Thaw Durability of Composite Materials", *Virginia Transportation Research Council.*

Grant, T.S. and W.L. Bradley (1995), "In-situ Observations in SEM of Degradation of Graphite/Epoxy Composite Materials Due to Seawater Immersion", *Journal of Composite Materials*, vol. 29, No. 7, pp. 853

Gutierrez, J., Le Lay, F., and Hoarau, P., (1992), "A study of Ageing of Glass Fibre-Resin Composite in a Marine environment", *Nautical Construction with Composite Materials*, P. Davies and L. Lemoine, Eds., IGREMER, France, pp. 338-346

Haramis, J. (2000), "Characterization of Freeze-Thaw Damage Mechanisms in Composites for Civil Infrastructure", *Advanced Composite Materials in Bridges and Structures*, 3rd Conference, J. Humar and A.G. Razaqpur, Eds., August, pp. 663-668.

Iskander, M.G. (1998), "State of the Practice Review in FRP Composite Piling", *ASCE Journal of Composites for Construction*, vol. 2, No. 3, August, pp. 116.

Kasturiarachchi, K.A. and G. Pritchard (1983), "Water Absorption of Glass/epoxy Laminates under Bending Stresses", *Composites*, vol. 14, No. 3, July, pp. 247-248.

Peters, S.T., Ed. (1998), Handbook of Composites, 2nd ed., Chapman & Hall, Tonbridge, England, pp. 35, 134-135, 498.

Pritchard, G. and S.D. Speake (1987), "The Use of Water Absorption Kinetic Data to Predict Laminate Property Changes", *Composites*, vol. 18, No. 3, July, 227-231.

Shen, C.-H. and G.S. Springer (1976), "Moisture Absorption and Desorption of Composite Materials", *Journal of Composite Materials*, vol. 10, January, pp. 2-9.

Tomlinson, M.J. (1994), Pile Design and Construction Practice, 4th Edition, E & FN Spon, London, UK, pp. 361-368.

USACRL 123 (1998), "Development and Demonstration of FRP Composite Fender, Loadbearing, and Sheet Piling Systems", UACERL Technical Report, 123, September 1998, pp. 7-9, B15

Verghese, N., Haramis, J., Morrell, M.R., Horne, M.R. and Lesko, J.J (1999), "Freeze-Thaw Durability of Polymer Matrix Composites in Infrastructures", *Duracosys*.

Appendix A

Reference 3-Point Flexural Strength Curves

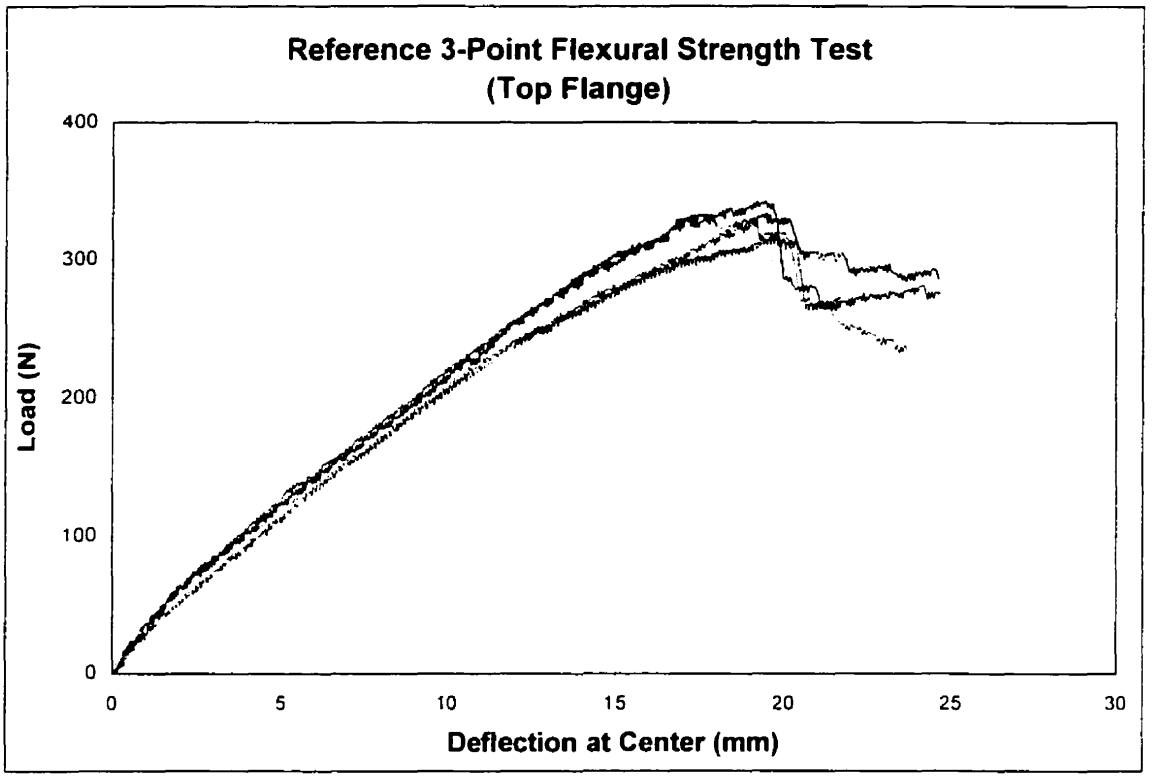
Reference 3-Point Flexural Strength Test
(Top Flange)
Load (N)
400
300
200
100
0
0
5
10
15
20
25
30
Deflection at Center (mm)

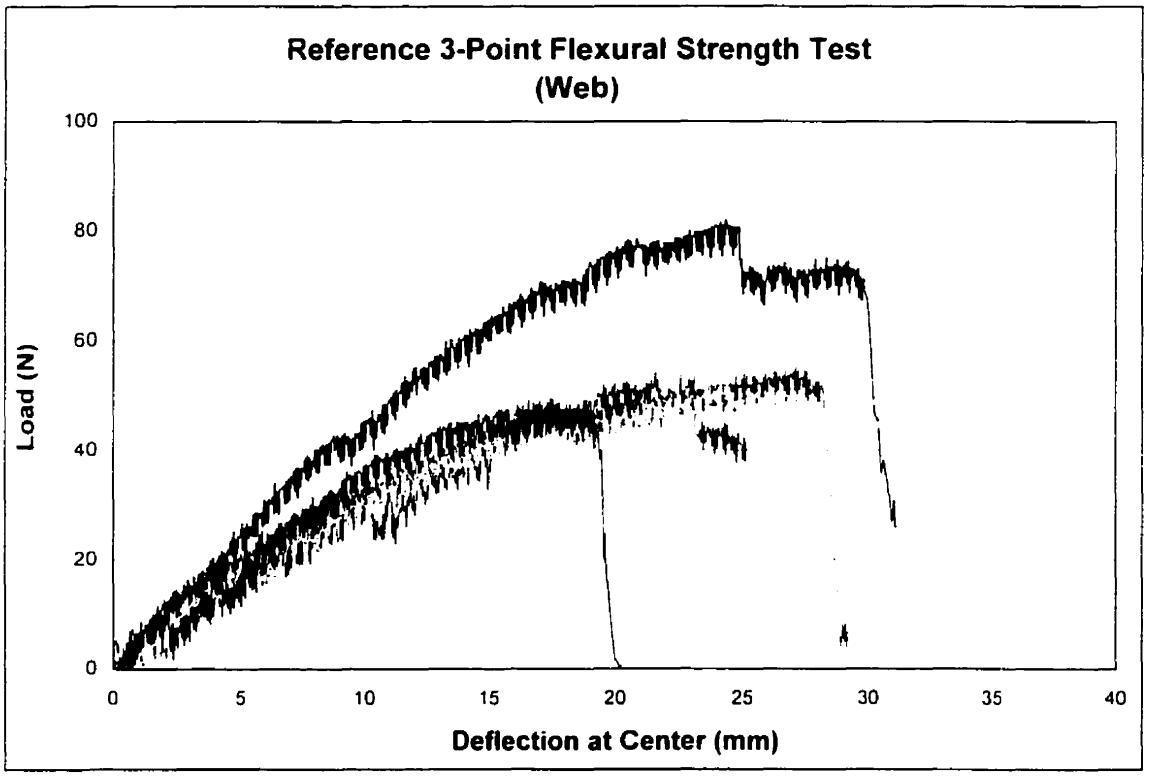
Reference 3-Point Flexural Strength Test
(Web)
Load (N)
100
80
60
40
20
0
0
5
10
15
20
25
30
35
40
Deflection at Center (mm)

Appendix B

All Tensile Strength Curves

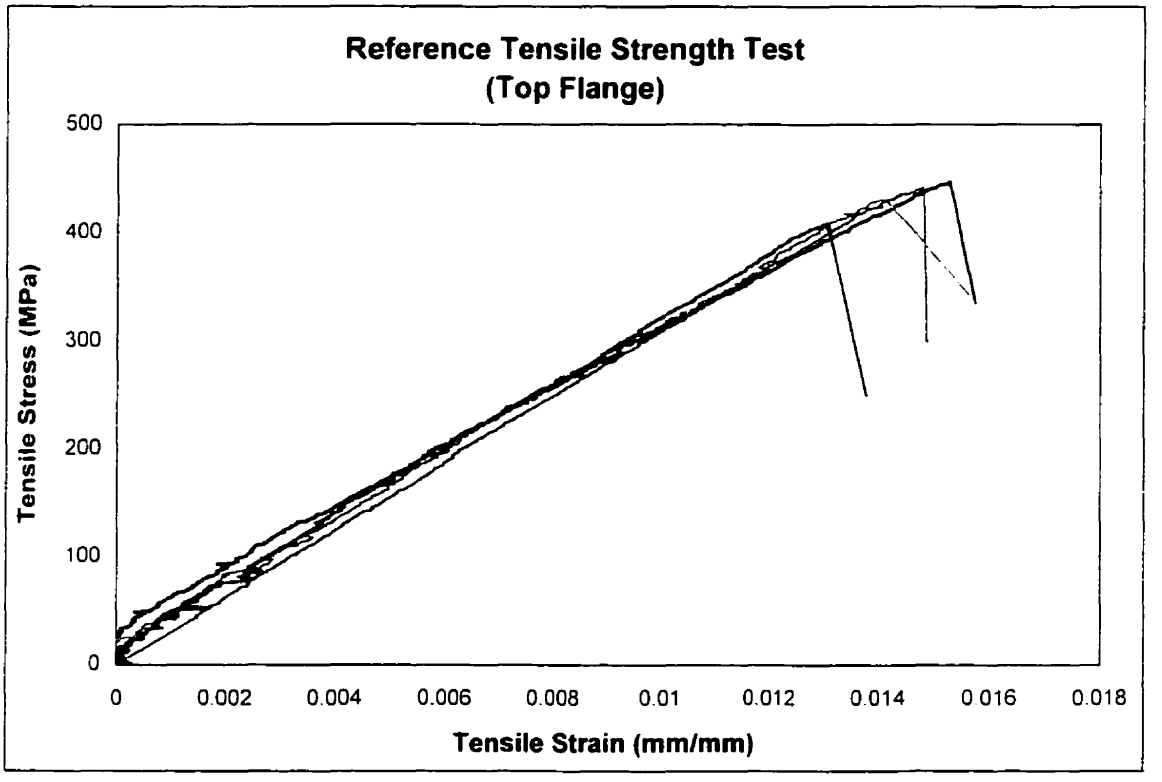
Reference Tensile Strength Test
(Top Flange)
Tensile Stress (MPa)
500
400
300
200
100
0
0
0.002
0.004
0.006
0.008
0.01
0.012
0.014
0.016
0.018
Tensile Strain (mm/mm)

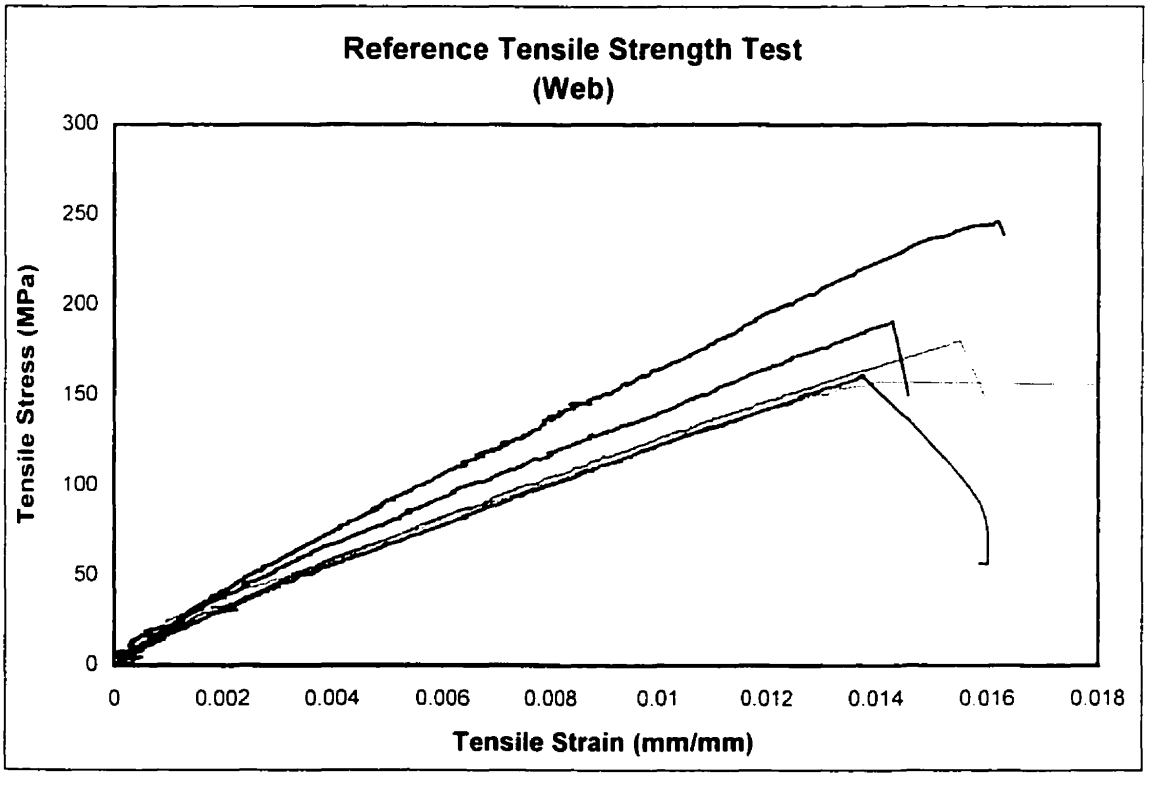
Reference Tensile Strength Test
(Web)
Tensile Stress (MPa)
300
250
200
150
100
50
0
0
0.002
0.004
0.006
0.008
0.01
0.012
0.014
0.016
0.018
Tensile Strain (mm/mm)

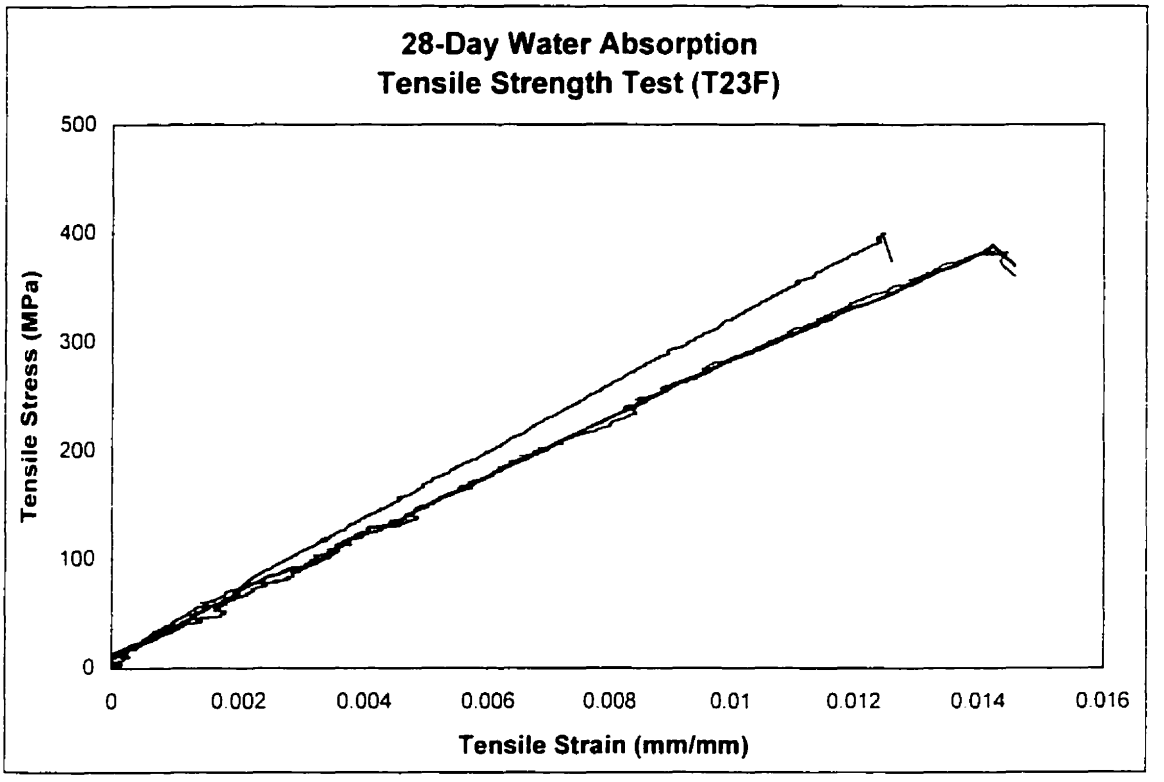
28-Day Water Absorption
Tensile Strength Test (T23F)
Tensile Stress (MPa)
500
400
300
200
100
0
0
0.002
0.004
0.006
0.008
0.01
0.012
0.014
0.016
Tensile Strain (mm/mm)

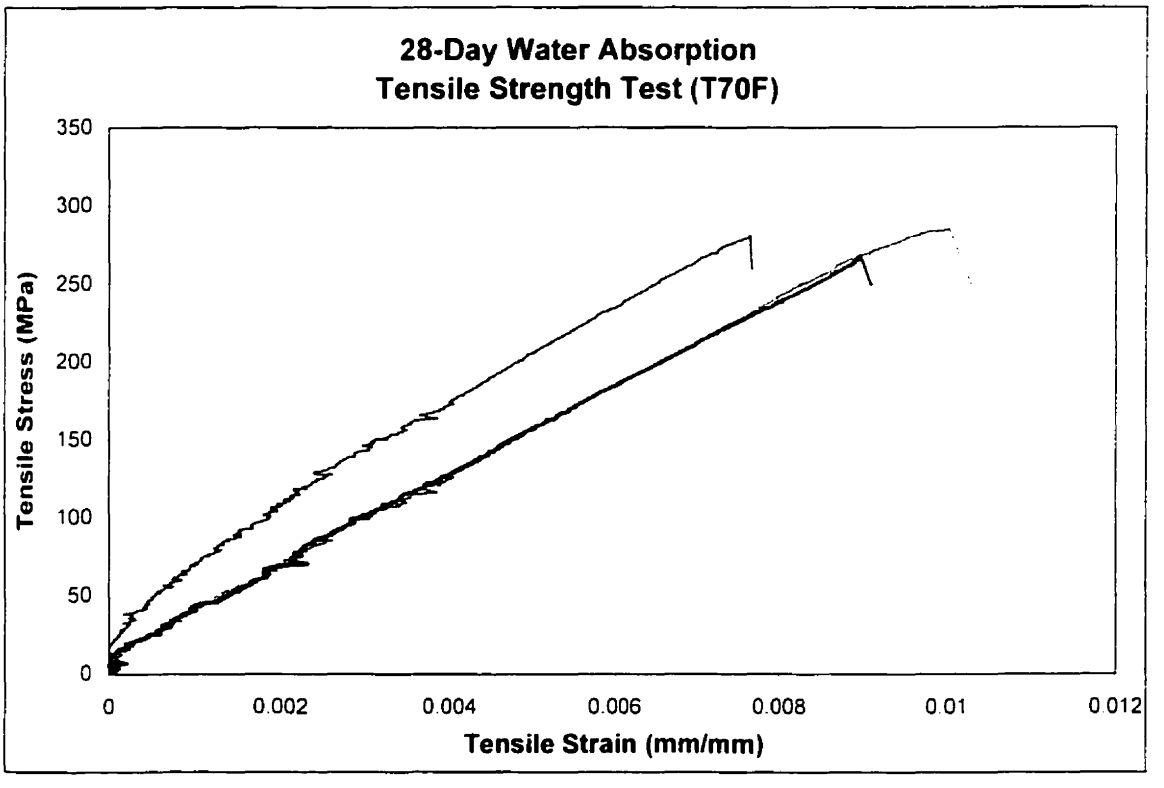
28-Day Water Absorption
Tensile Strength Test (T70F)
Tensile Stress (MPa)
350
300
250
200
150
100
50
0
0
0.002
0.004
0.006
0.008
0.01
0.012
Tensile Strain (mm/mm)

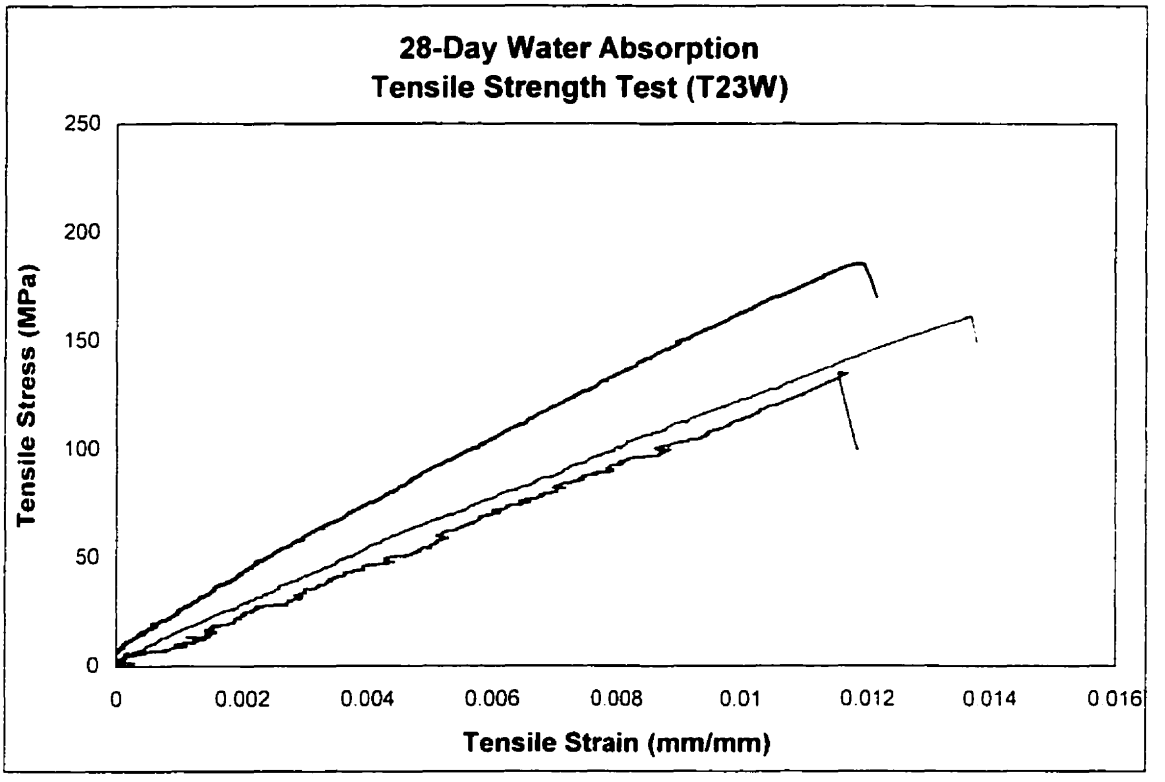
28-Day Water Absorption
Tensile Strength Test (T23W)
Tensile Stress (MPa)
250
200
150
100
50
0
0
0.002
0.004
0.006
0.008
0.01
0.012
0.014
0.016
Tensile Strain (mm/mm)

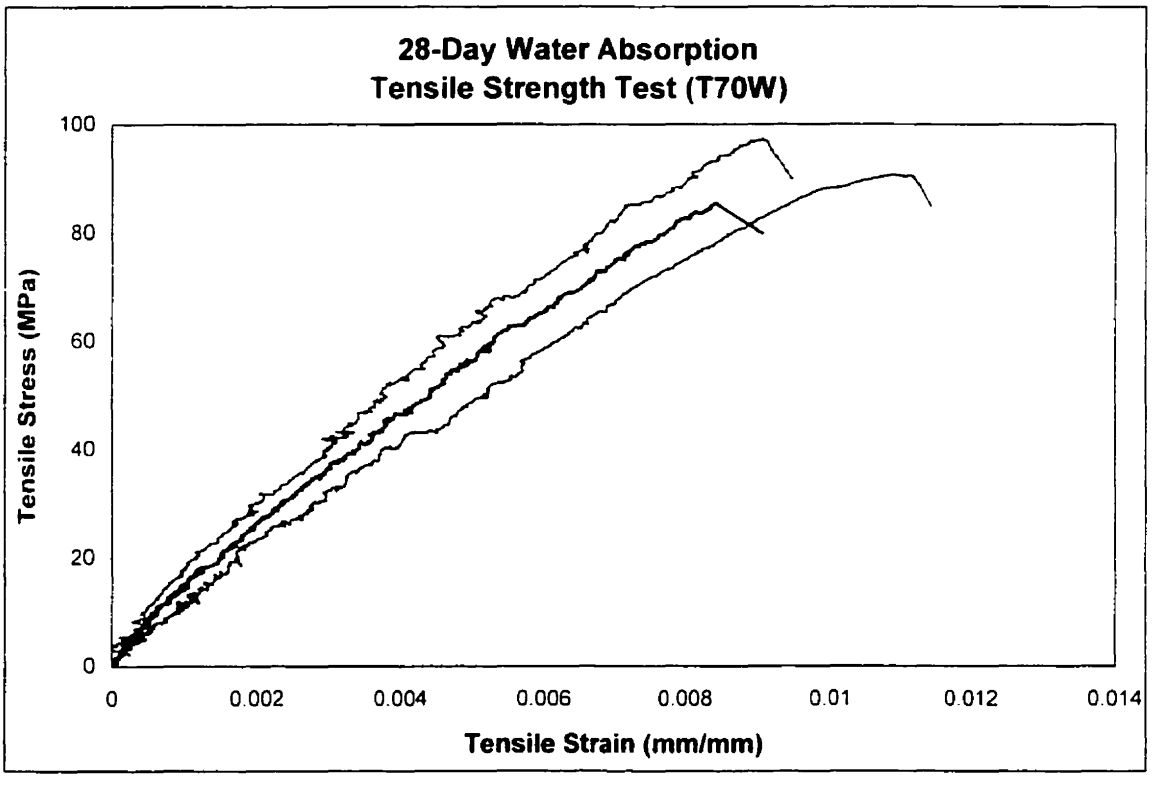
28-Day Water Absorption
Tensile Strength Test (T70W)
Tensile Stress (MPa)
100
80
60
40
20
0
0
0.002
0.004
0.006
0.008
0.01
0.012
0.014
Tensile Strain (mm/mm)

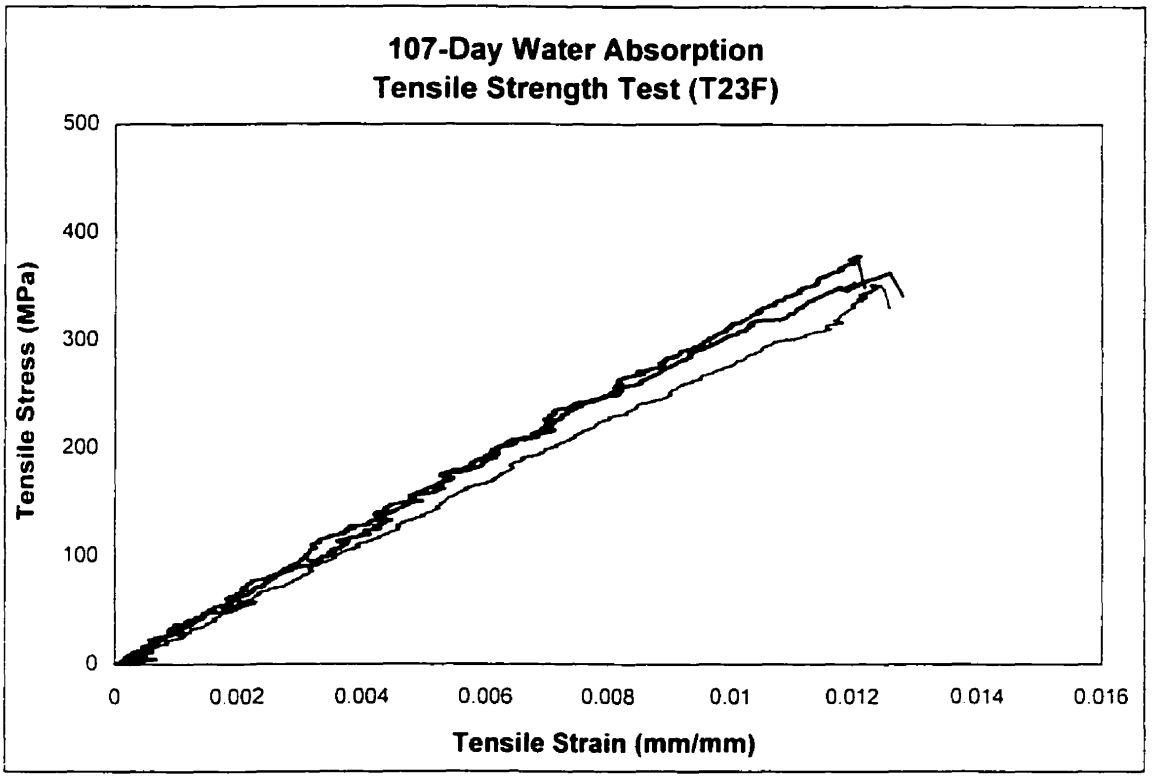
107-Day Water Absorption
Tensile Strength Test (T23F)
Tensile Stress (MPa)
500
400
300
200
100
0
0
0.002
0.004
0.006
0.008
0.01
0.012
0.014
0.016
Tensile Strain (mm/mm)

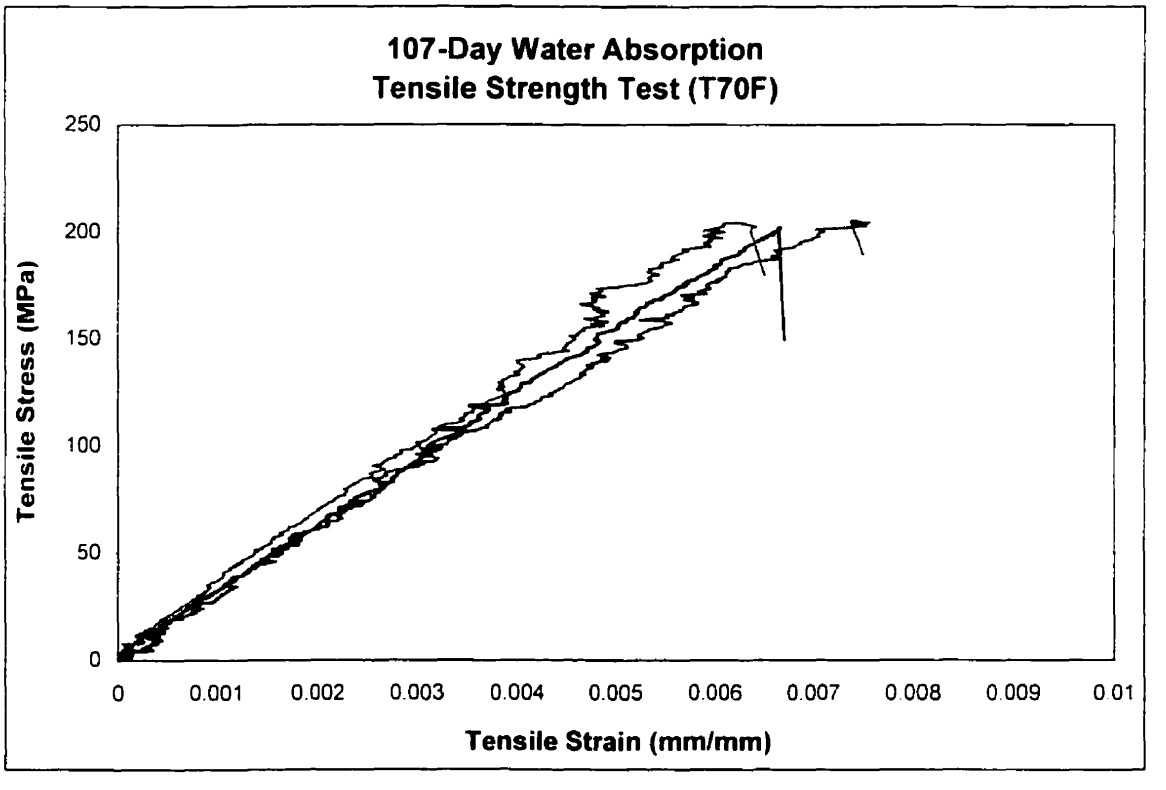
107-Day Water Absorption
Tensile Strength Test (T70F)
Tensile Stress (MPa)
250
200
150
100
50
0
0
0.001
0.002
0.003
0.004
0.005
0.006
0.007
0.008
0.009
0.01
Tensile Strain (mm/mm)

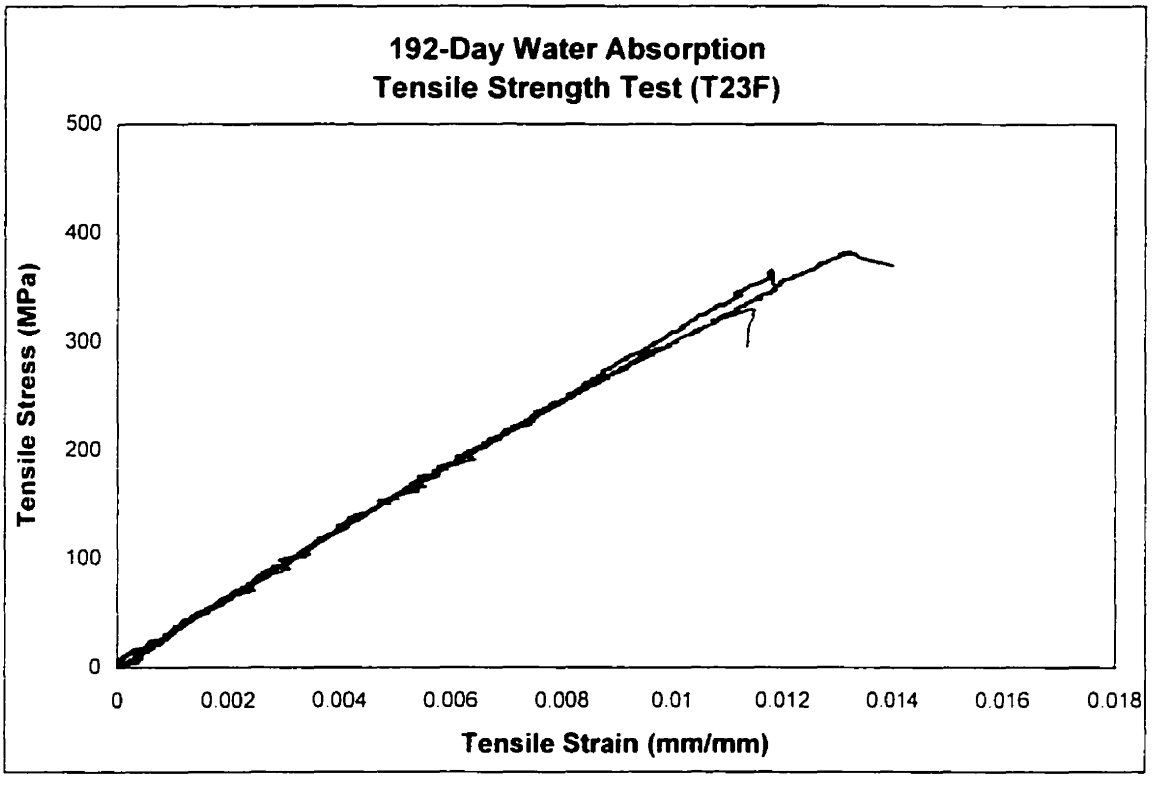
192-Day Water Absorption
Tensile Strength Test (T23F)
Tensile Stress (MPa)
500
400
300
200
100
0
0
0.002
0.004
0.006
0.008
0.01
0.012
0.014
0.016
0.018
Tensile Strain (mm/mm)

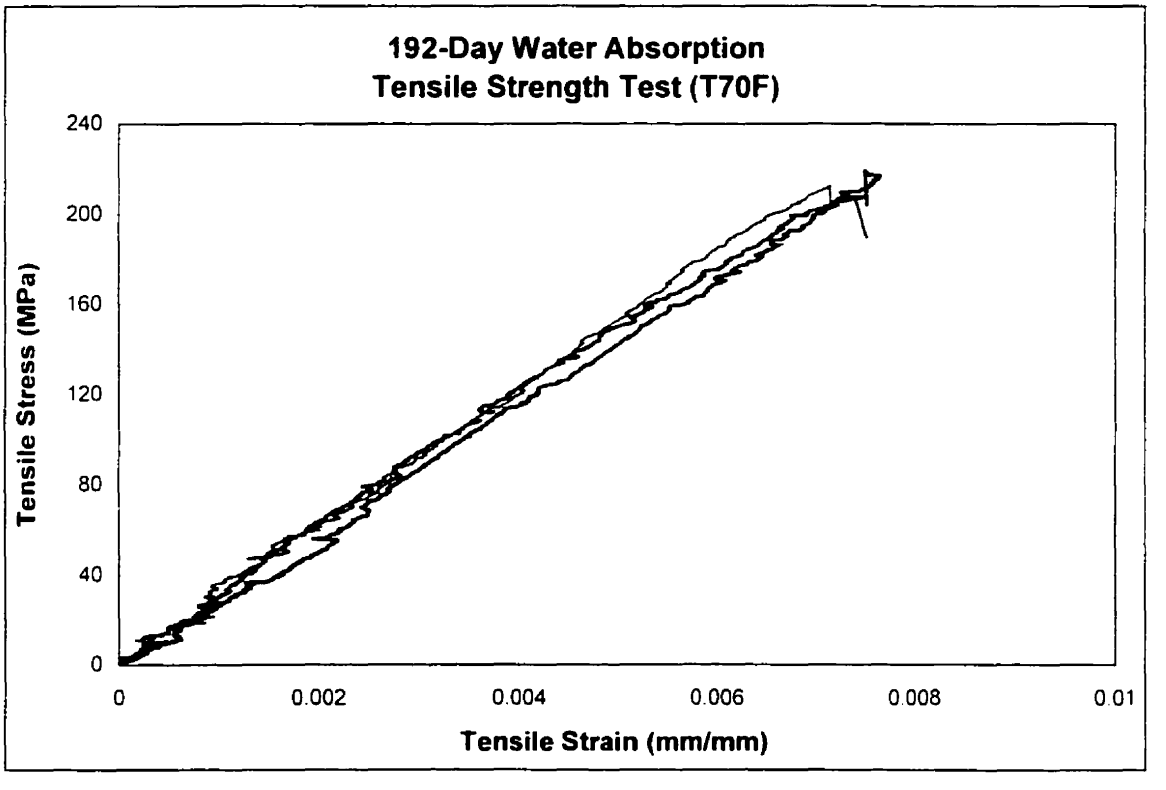
192-Day Water Absorption
Tensile Strength Test (T70F)
Tensile Stress (MPa)
240
200
160
120
80
40
0
0
0.002
0.004
0.006
0.008
0.01
Tensile Strain (mm/mm)

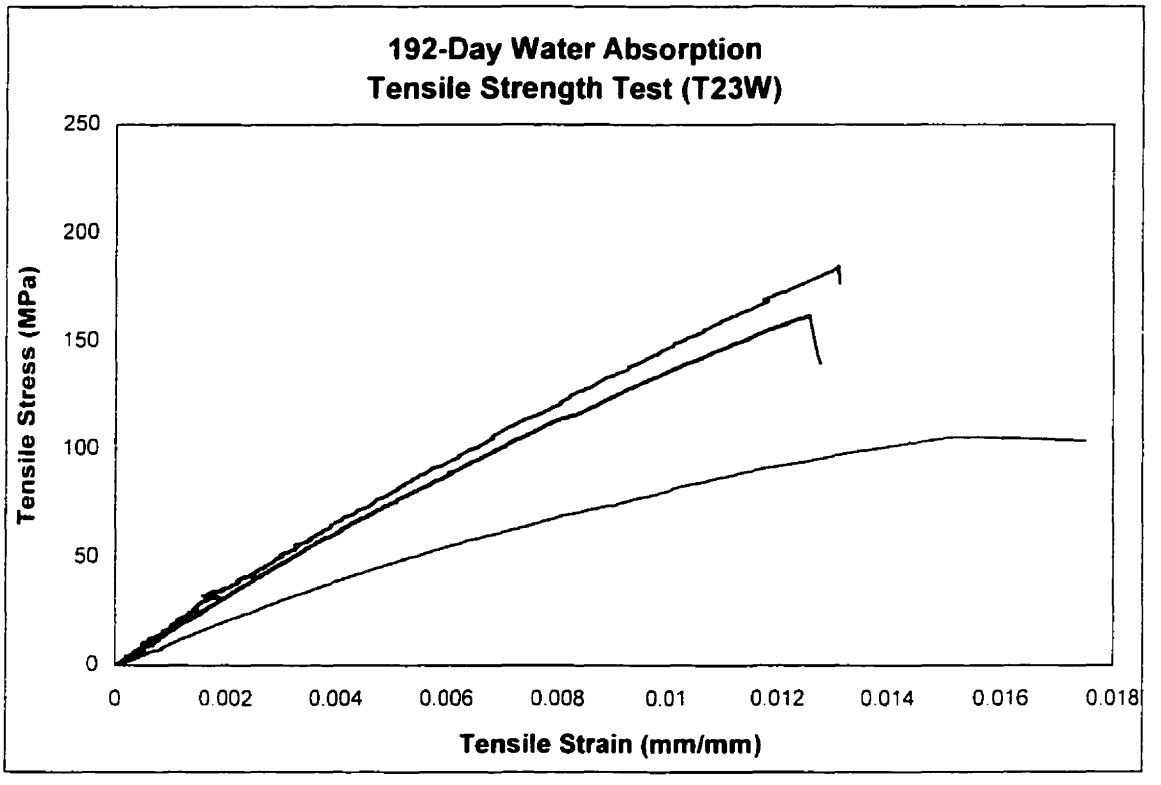
192-Day Water Absorption
Tensile Strength Test (T23W)
Tensile Stress (MPa)
250
200
150
100
50
0
0
0.002
0.004
0.006
0.008
0.01
0.012
0.014
0.016
0.018
Tensile Strain (mm/mm)

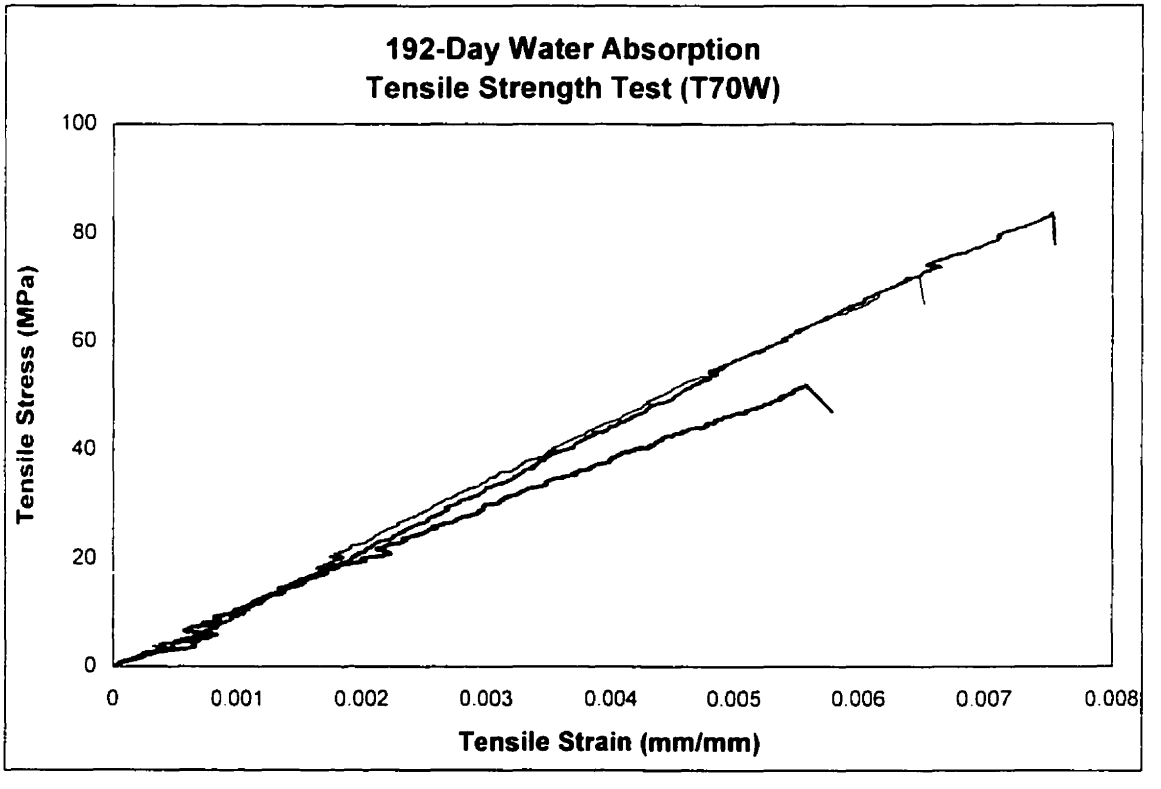
192-Day Water Absorption
Tensile Strength Test (T70W)
Tensile Stress (MPa)
100
80
60
40
20
0
0
0.001
0.002
0.003
0.004
0.005
0.006
0.007
0.008
Tensile Strain (mm/mm)

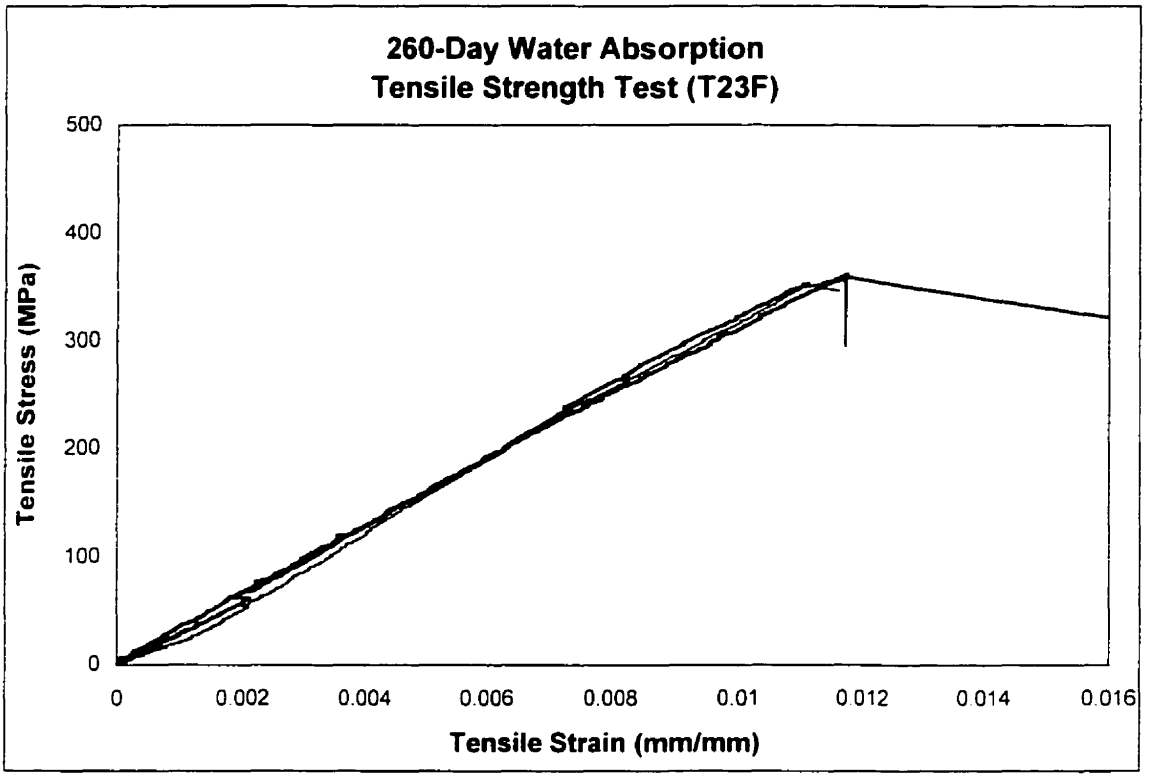
260-Day Water Absorption
Tensile Strength Test (T23F)
Tensile Stress (MPa)
500
400
300
200
100
0
0
0.002
0.004
0.006
0.008
0.01
0.012
0.014
0.016
Tensile Strain (mm/mm)

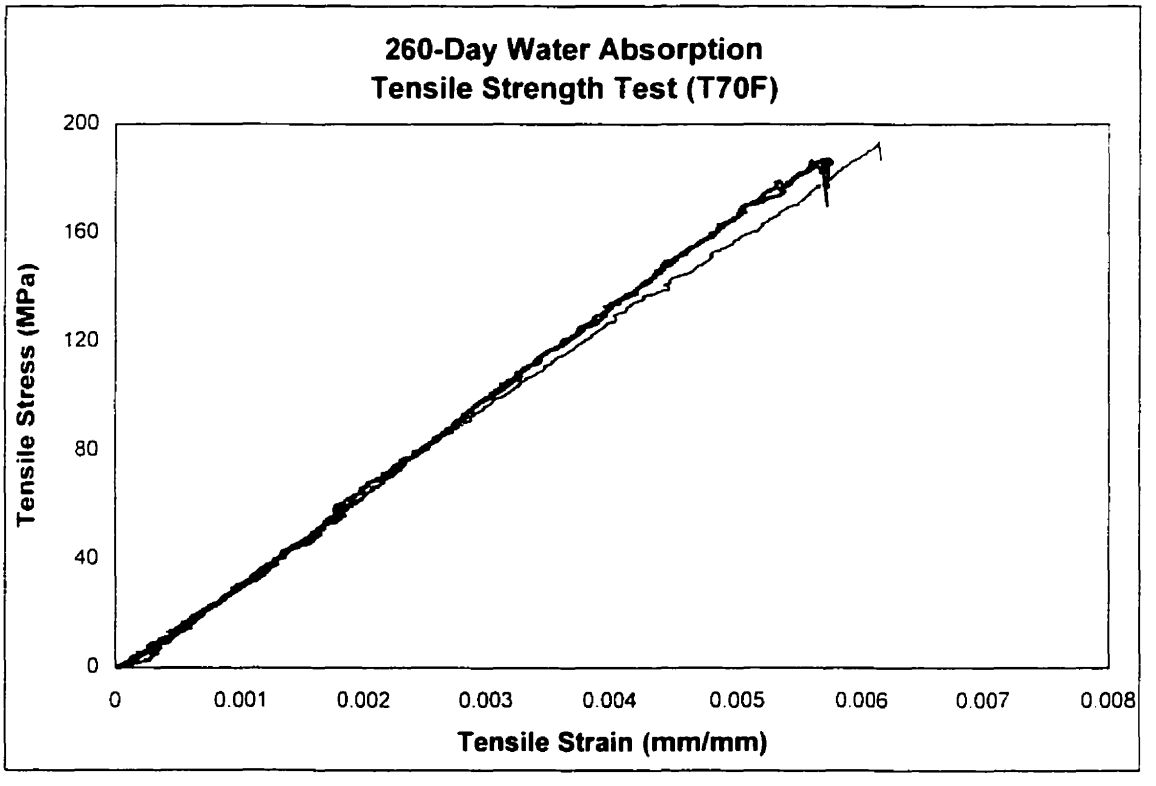
260-Day Water Absorption
Tensile Strength Test (T70F)
Tensile Stress (MPa)
200
160
120
80
40
0
0
0.001
0.002
0.003
0.004
0.005
0.006
0.007
0.008
Tensile Strain (mm/mm)

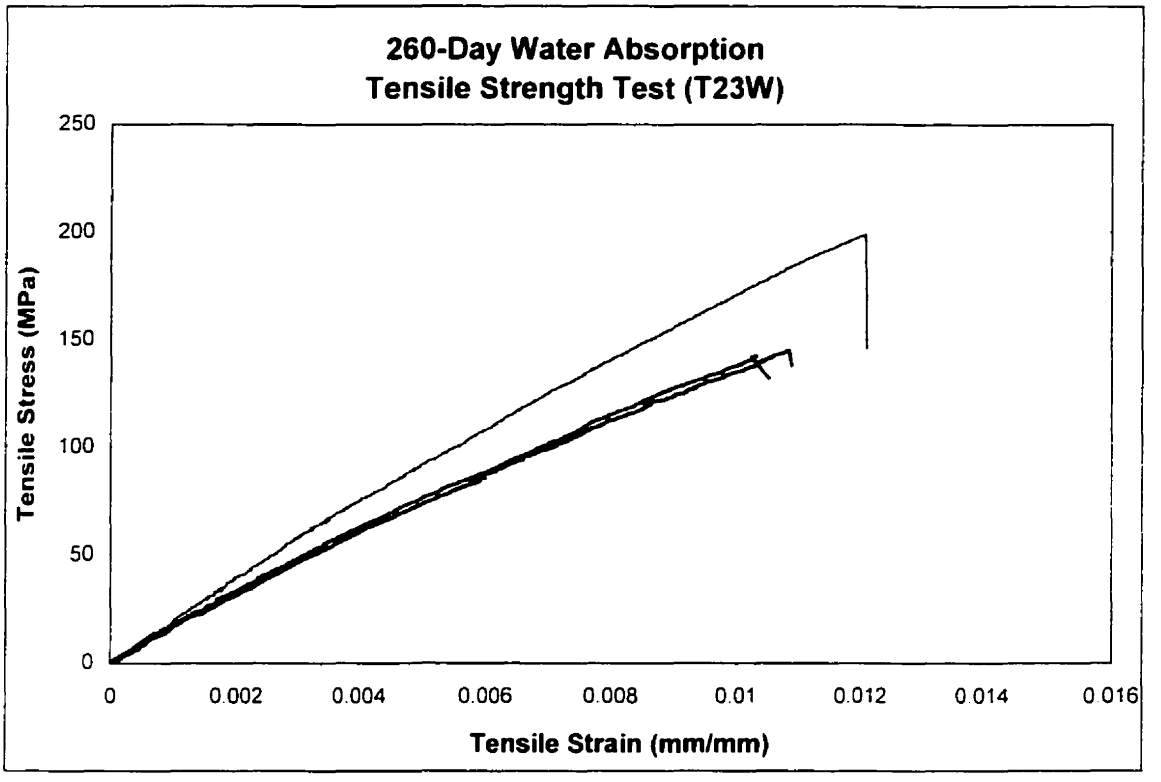
260-Day Water Absorption
Tensile Strength Test (T23W)
Tensile Stress (MPa)
250
200
150
100
50
0
0
0.002
0.004
0.006
0.008
0.01
0.012
0.014
0.016
Tensile Strain (mm/mm)

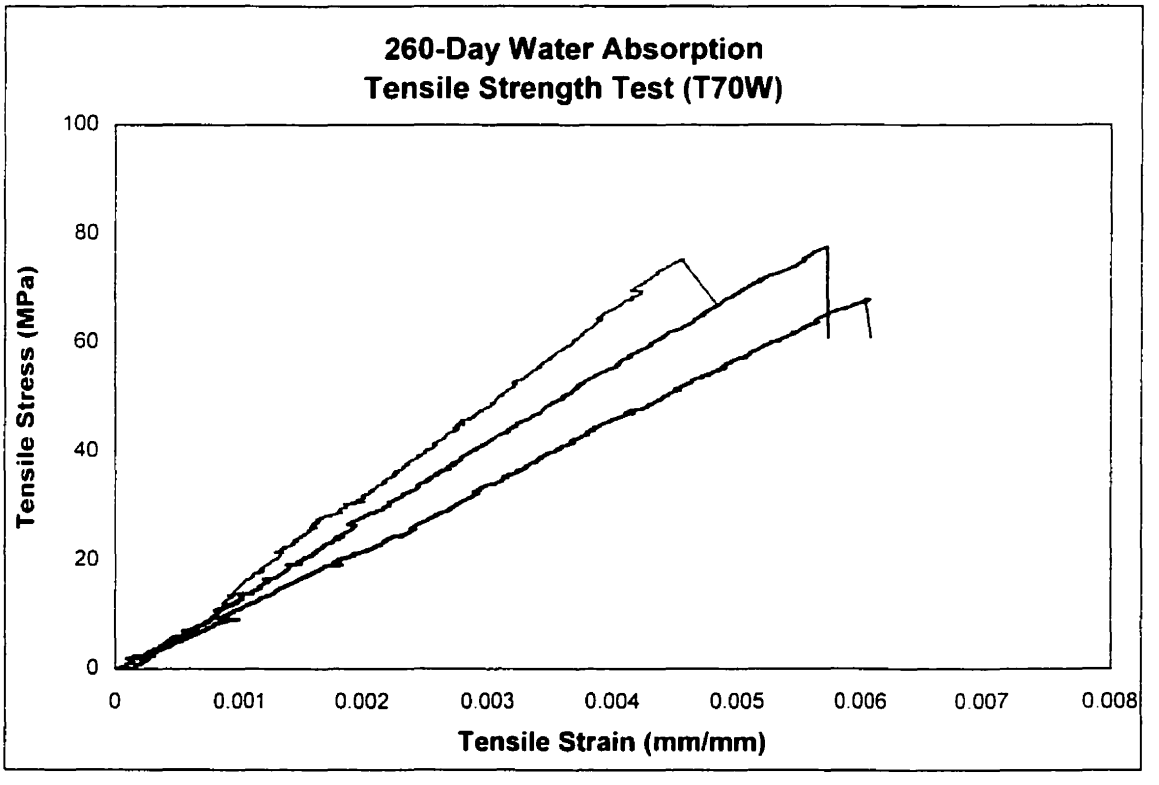
260-Day Water Absorption
Tensile Strength Test (T70W)
Tensile Stress (MPa)
100
80
60
40
20
0
0
0.001
0.002
0.003
0.004
0.005
0.006
0.007
0.008
Tensile Strain (mm/mm)

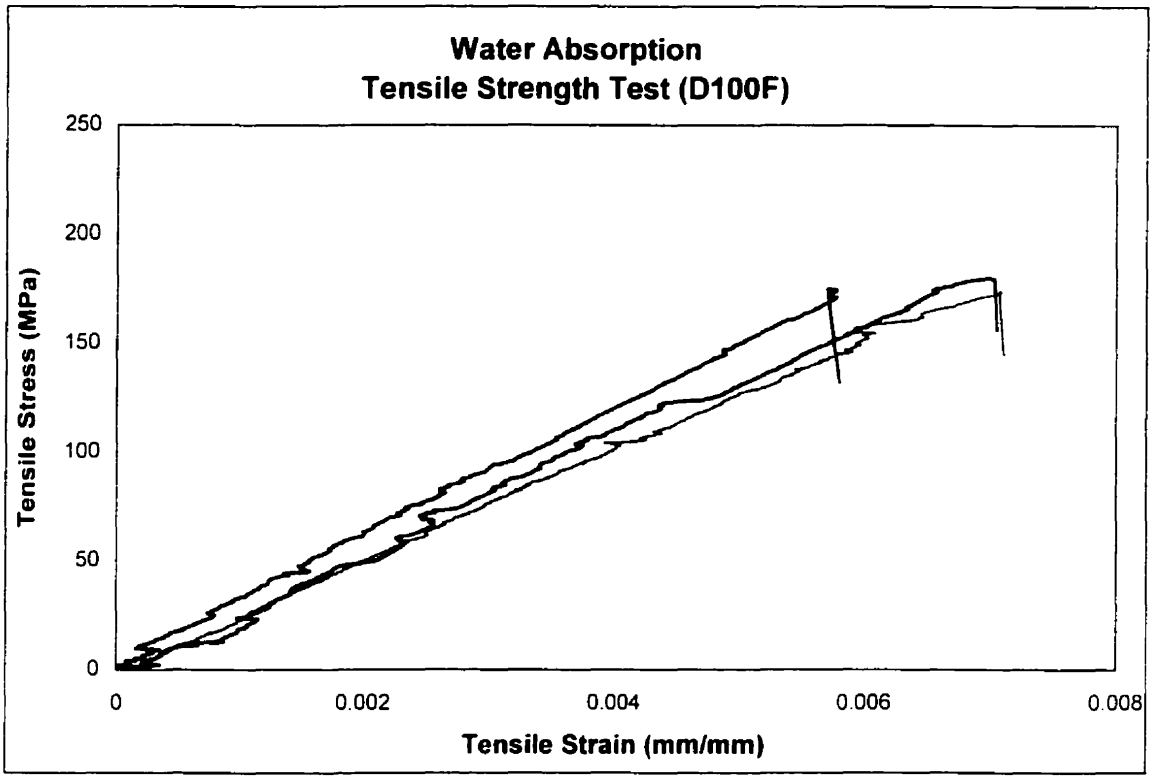
Water Absorption
Tensile Strength Test (D100F)
Tensile Stress (MPa)
250
200
150
100
50
0
0
0.002
0.004
0.006
0.008
Tensile Strain (mm/mm)

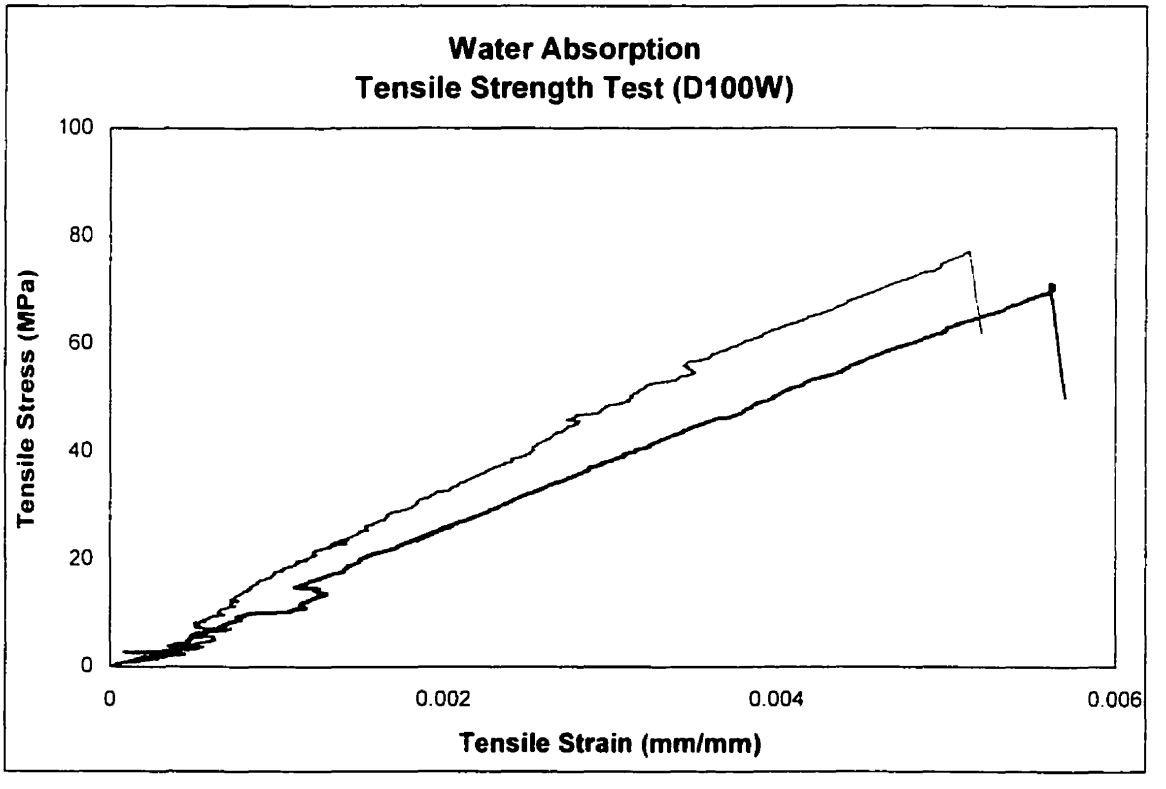
Water Absorption
Tensile Strength Test (D100W)
Tensile Stress (MPa)
100
80
60
40
20
0
0
0.002
0.004
0.006
Tensile Strain (mm/mm)

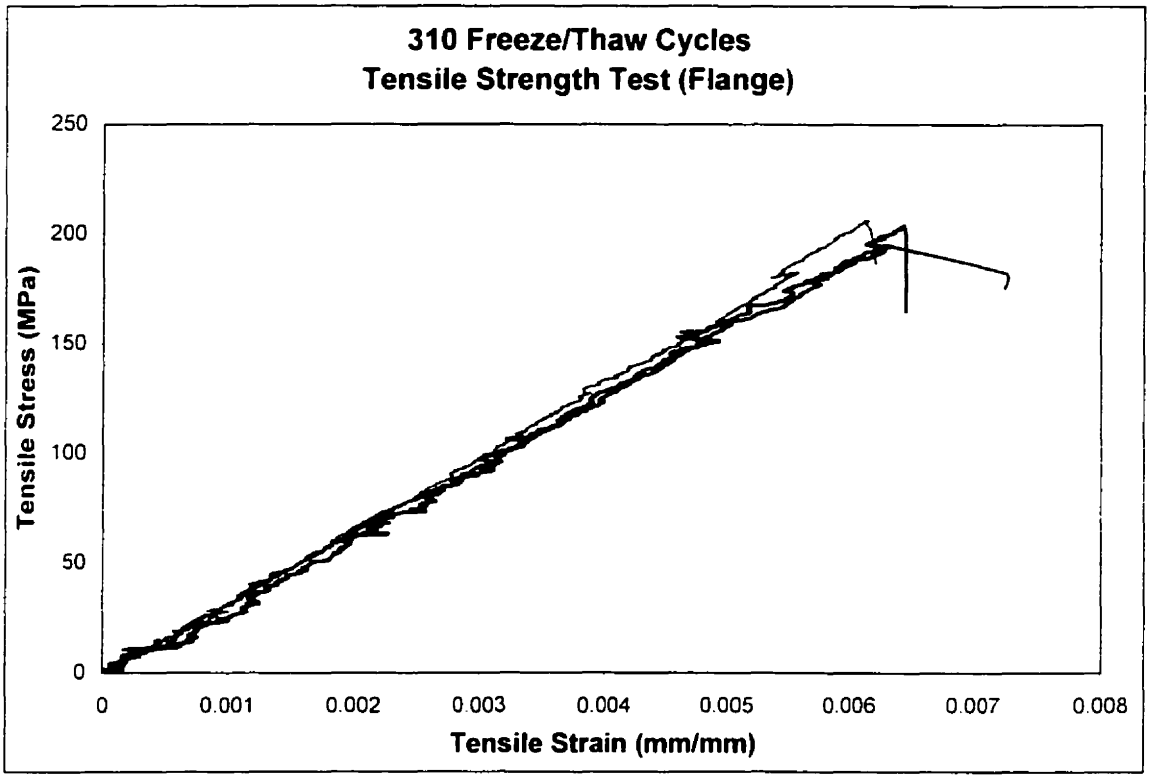
310 Freeze/Thaw Cycles
Tensile Strength Test (Flange)
Tensile Stress (MPa)
250
200
150
100
50
0
0
0.001
0.002
0.003
0.004
0.005
0.006
0.007
0.008
Tensile Strain (mm/mm)

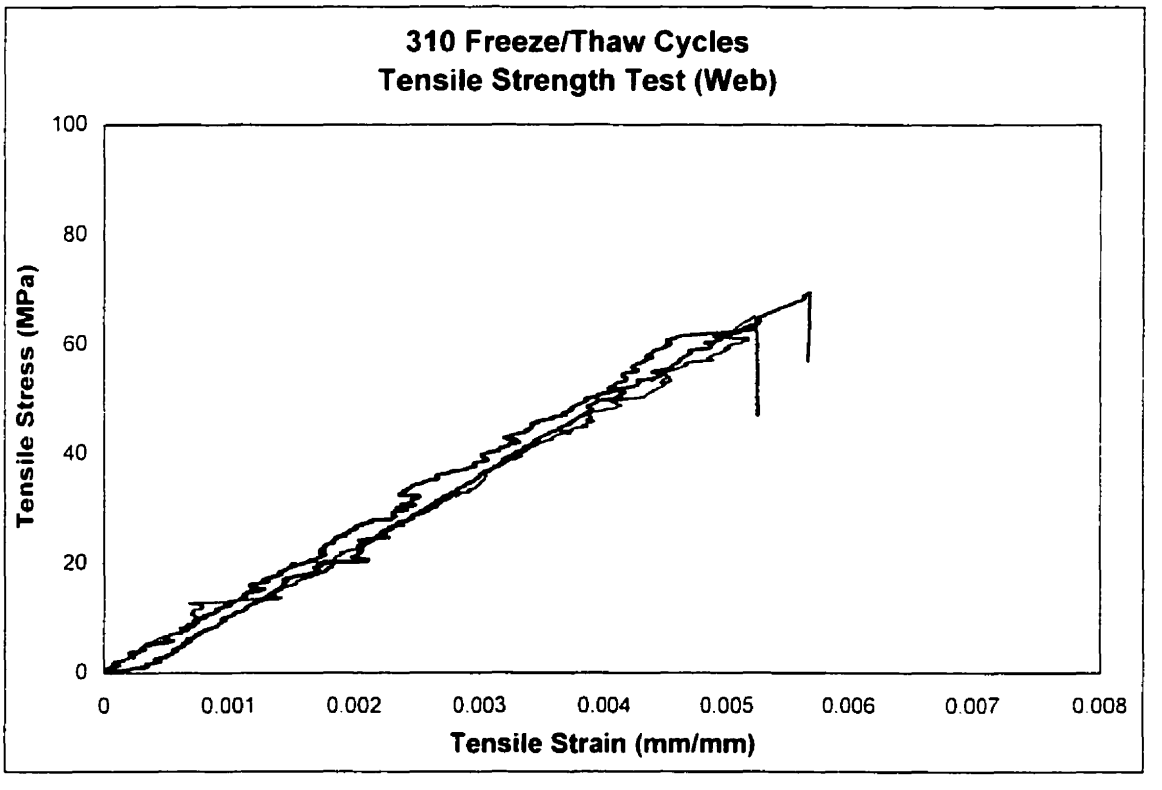
310 Freeze/Thaw Cycles
Tensile Strength Test (Web)
Tensile Stress (MPa)
100
80
60
40
20
0
0
0.001
0.002
0.003
0.004
0.005
0.006
0.007
0.008
Tensile Strain (mm/mm)

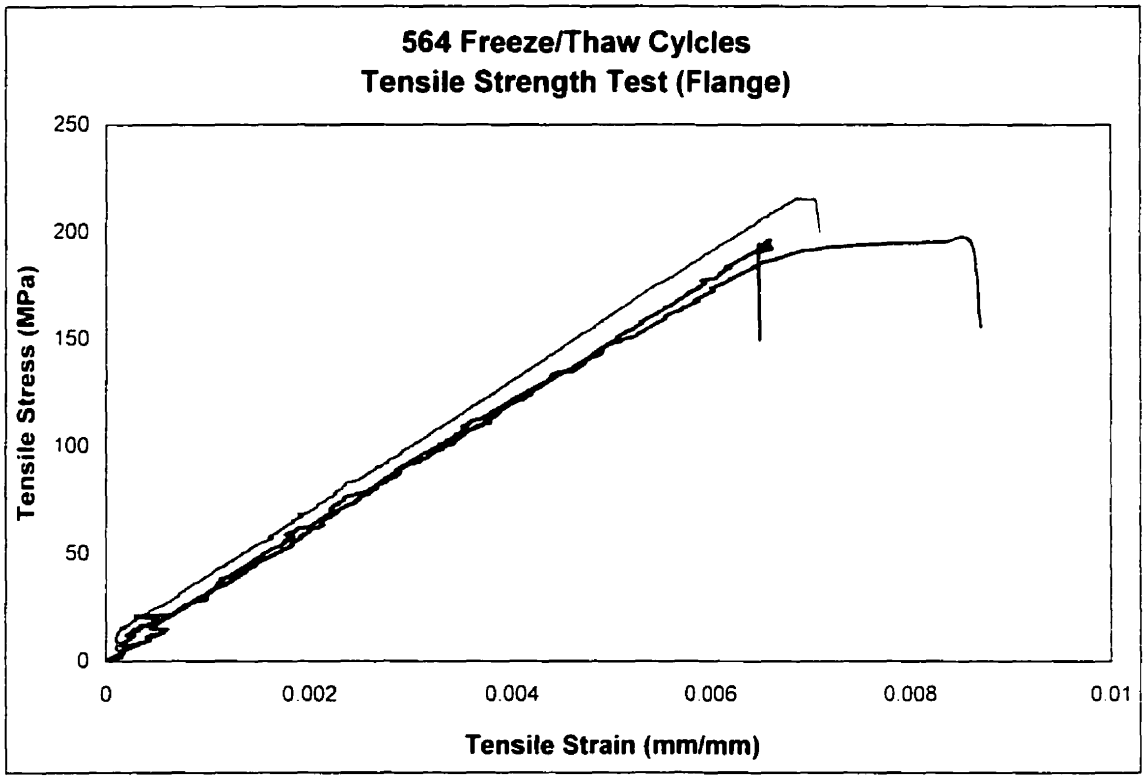
564 Freeze/Thaw Cycles
Tensile Strength Test (Flange)
Tensile Stress (MPa)
250
200
150
100
50
0
0
0.002
0.004
0.006
0.008
0.01
Tensile Strain (mm/mm)

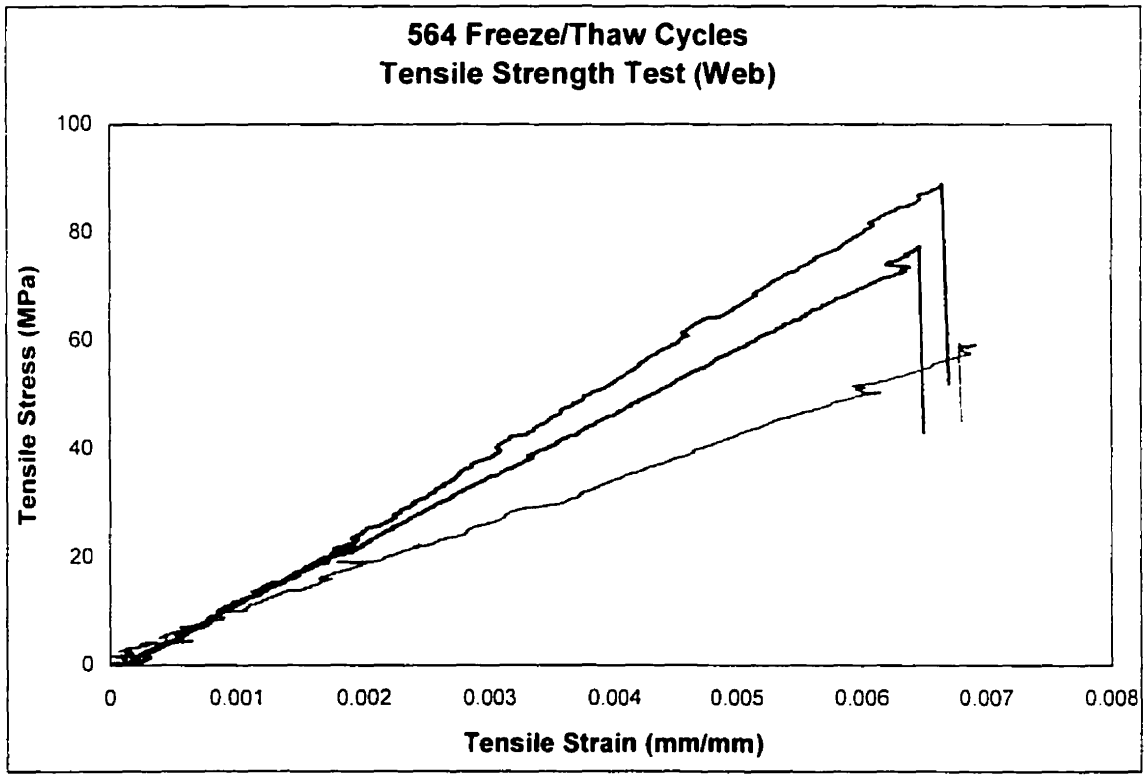
564 Freeze/Thaw Cycles
Tensile Strength Test (Web)
Tensile Stress (MPa)
100
80
60
40
20
0
0
0.001
0.002
0.003
0.004
0.005
0.006
0.007
0.008
Tensile Strain (mm/mm)

Appendix C

Boiling Distilled Water Absorption Data

		Flange	Standard Deviation	Web	Standard Deviation
2 Hours, 23°C	$\%M$	0.14	0.01	0.24	0.01
24 Hours, 23°C	$\%M$	0.29	0.02	0.44	0.01
2 Hour, boiling	$\%M$	0.85	0.02	1.13	0.00
	$\%M_{Loss}$	-0.32	0.02	-1.03	0.04
	$\%M_c$	1.12	0.03	2.16	0.04
24 Hour, boiling	$\%M$	1.22	0.07	1.67	0.02
	$\%M_{Loss}$	-0.43	0.01	-1.18	0.05
	$\%M_c$	1.65	0.08	2.85	0.06
3 Days, boiling	$\%M$	1.31	0.07	1.73	0.04
	$\%M_{Loss}$	-0.25	0.02	-0.96	0.04
	$\%M_c$	1.56	0.09	2.69	0.08
6 Days, boiling	$\%M$	1.33	0.04	1.69	0.12
	$\%M_{Loss}$	-0.40	0.01	-1.43	0.00
	$\%M_c$	1.73	0.05	3.12	0.13
9 Days, boiling	$\%M$	1.05	0.02	1.31	0.08
	$\%M_{Loss}$	-0.69	0.02	-1.82	0.08
	$\%M_c$	1.74	0.04	3.14	0.16
13 Days, boiling	$\%M$	0.72	0.01	0.91	0.05
	$\%M_{Loss}$	-1.02	0.07	-2.23	0.09
	$\%M_c$	1.74	0.09	3.14	0.14
18 Days, boiling	$\%M$	0.56	0.03	0.66	0.06
	$\%M_{Loss}$	-1.18	0.05	-2.48	0.05
	$\%M_c$	1.74	0.08	3.14	0.11
21 Days, boiling	$\%M$	0.44	0.03	0.42	0.09
	$\%M_{Loss}$	-1.3	0.01	-2.72	0.11
	$\%M_c$	1.74	0.04	3.14	0.20